



US Army Corps
of Engineers®

New Lock for Soo Locks and Dam, Sault Ste. Marie, Michigan, St. Mary's River

Hydraulic Model Investigation

John E. Hite, Jr., and Andrew M. Tuthill

September 2005



New Lock for Soo Locks and Dam, Sault Ste. Marie, Michigan, St. Mary's River

Hydraulic Model Investigation

John E. Hite, Jr.

*Coastal and Hydraulics Laboratory
U.S. Army Engineer Research and Development Center
3909 Halls Ferry Road
Vicksburg, MS 39180-6199*

Andrew M. Tuthill

*Cold Regions Research Engineering Laboratory
U.S. Army Engineer Research and Development Center
72 Lyme Road
Hanover, NH 03755-1290*

Final report

Approved for public release; distribution is unlimited

Prepared for U.S. Army Engineer District, Detroit
 477 Michigan Avenue, Detroit, MI 48226
 U.S. Army Engineer District, Huntington
 502 8th Street, Huntington, WV 25701-2070

ABSTRACT: The U.S. Army Engineer District, Detroit (LRE) proposes construction of a new lock at the Soo Locks on the St. Mary's River near Sault Ste. Marie, Michigan. The lock will replace the existing Davis and Sabin locks in the North Canal. Currently, the Poe Lock is the only facility at Soo Locks capable of handling the Great Lakes system's largest vessels. These large vessels account for more than half of the potential carrying capacity of the Great Lakes fleet. A laboratory model study was performed to evaluate the lock filling and emptying system and ice lockage procedures. It is expected that the new lock will have upper approach ice congestion problems similar to those experienced at the existing Soo Locks. A major objective of the ice tests in the physical model was to maximize ice lockage performance. The original design filling and emptying system was modified to achieve acceptable filling and emptying times. The total number of ports was reduced and structural baffles were installed on the upper and lower ports of the system to provide an even distribution of flow into and out of the chamber during filling and emptying. The permissible filling and emptying times based on maximum allowable hawser forces were 13.0 and 12.4 min, respectively. The lower ice valves brought the ice farther into the lock during ice drawing experiments although having the ice in direct contact with the lower miter gates would interfere with their operation. The upper ice valves were about equal to the combined use of filling valves and the manifolds in the upper miter gates in terms of ice flushing performance.

DISCLAIMER: The contents of this report are not to be used for advertising, publication, or promotional purposes. Citation of trade names does not constitute an official endorsement or approval of the use of such commercial products. All product names and trademarks cited are the property of their respective owners. The findings of this report are not to be construed as an official Department of the Army position unless so designated by other authorized documents.

Contents

Conversion Factors, Non-SI to SI Units of Measurement.....	vii
Preface	viii
Executive Summary	ix
1—Introduction	1
Background.....	1
The Prototype.....	1
Purpose and Scope.....	2
2—Physical Model.....	4
Description.....	4
Appurtenances and Instrumentation	4
Similitude Considerations.....	10
Kinematic similitude	10
Dynamic similitude	11
Similitude for lock models	11
Plastic Ice Material and Scaling.....	13
Experimental Procedures	13
3—Model Experiments and Results.....	14
Headloss Measurements.....	14
Loss coefficient	14
Lock coefficient.....	15
Intake Vortex Experiments	16
Plan A intake design.....	16
Type 2 intake design	16
Type 3 intake design	17
Type 4 intake design	17
Type 5 intake design	18
Plan A Design Chamber Performance Without Ship.....	18
Lock filling.....	18
Lock emptying.....	19
Outlet Experiments	19
Plan A Design Chamber Performance with Ship.....	20
Hawser forces during filling.....	20
Hawser forces during emptying	22
Type 2 Chamber Design	22
Hawser forces during filling, type 2 chamber design.....	22

Hawser forces during emptying, type 2 chamber design	23
Plan A and Type 2 Chamber Design Hawser Forces	24
Water-Surface Differential Experiments	25
Type 3 Chamber Design	26
Type 4 Chamber Design	26
Type 5 Chamber Design	26
Types 6-9 Chamber Designs	27
Type 10 Chamber Design	29
Type 11 Chamber Design	29
Type 12 Chamber Design	30
Numerical Model	33
Upper approach flow conditions	33
Lower approach flow conditions	35
Ice Passage Investigations.....	36
Drawing ice into the lock chamber.....	40
Flushing ice from the lock chamber	40
Ice accumulation near culvert intakes	43
Additional Intake and Outlet Experiments	46
Type 6 intake design	47
Type 7 intake design	47
Types 2 and 3 outlet designs	48
Type 4 outlet design	48
4—Conclusions and Recommendations	50
Lock Filling and Emptying System	50
Upper and Lower Approach Flow Conditions.....	52
Ice Investigations	52
Ice drawing	52
Ice flushing	53
Upper approach ice accumulation near intakes during lock filling	53
References	54
Plates 1-69	
SF 298	

List of Figures

Figure 1.	Vicinity map.....	2
Figure 2.	Layout of existing project	3
Figure 3.	1:25-scale model of the filling and emptying system	
	a. Overall view looking downstream.....	5
	b. Overall view looking upstream	6
	c. Close-up view of intakes	6
	d. Ports inside lock chamber.....	7
	e. Close-up of port.....	7

	f. Upper ice valves.....	8
	g. Lower ice valves.....	8
	h. Lower miter gates and culvert transition	9
	i. Outlets and valves	9
Figure 4.	Hawser-pull (force links) measuring device.....	10
Figure 5.	Piece size distribution of plastic ice material compared to field observations	13
Figure 6.	Schematic of flow with original bulkhead sill.....	17
Figure 7.	Test drawing ice from upstream approach into lock chamber viewed from upstream	37
Figure 8.	Test flushing ice from lock chamber viewed from downstream	38
Figure 9.	Upper approach ice accumulation test.....	39
Figure 10.	Surface water velocities for ice drawing tests	40
Figure 11.	Ice edge position while drawing ice into lock.....	41
Figure 12.	Longitudinal section showing use of upper ice valve to increase water currents out of the lock chamber	41
Figure 13.	Manifolds in upper miter gates to create surface currents for ice flushing	42
Figure 14.	Surface water velocities for ice flushing cases.....	42
Figure 15.	Percent ice coverage vs. time for ice flushing cases.....	43
Figure 16.	Upper approach centerline surface water velocity profiles during lock filling.....	44
Figure 17.	Position of upper approach ice edge vs. time during lock filling.....	44
Figure 18.	High-flow air curtain retaining upper approach ice during lock filling.....	45
Figure 19.	Average surface water velocity vs. unit airflow to the bubbler diffuser	46

List of Tables

Table 1.	Loss Coefficients Plan A Design Filling System	14
Table 2.	Outlet Experiments, Plan A Filling and Emptying System, Upper Pool El 601.6, Lower Pool El 580.1	20
Table 3.	Filling Characteristics, Plan A Filling and Emptying System, 21.5-ft Lift, Upper Pool El 601.6, Lower Pool El 580.1	21

Table 4.	Emptying Characteristics, Plan A Filling and Emptying System, 21.5-ft Lift, Upper Pool El 601.6, Lower Pool El 580.1	23
Table 5.	Filling Characteristics, Type 2 Filling and Emptying System, 21.5-ft Lift, Upper Pool El 601.6, Lower Pool El 580.1	24
Table 6.	Filling Characteristics, Type 2 Filling and Emptying System, 21.5-ft Lift, Upper Pool El 601.6, Lower Pool El 580.1	25
Table 7.	Filling Characteristics, Type 5 Filling and Emptying System, 21.5-ft Lift, Upper Pool El 601.6, Lower Pool El 580.1	27
Table 8.	Emptying Characteristics, Type 5 Filling and Emptying System, 21.5-ft Lift, Upper Pool El 601.6, Lower Pool El 580.1	28
Table 9.	Filling Characteristics, Type 11 Filling and Emptying System, 21.5-ft Lift, Upper Pool El 601.6, Lower Pool El 580.1	30
Table 10.	Filling Characteristics, Type 12 Filling and Emptying System, 21.5-ft Lift, Upper Pool El 601.6, Lower Pool El 580.1	31
Table 11.	Comparison of Permissible Filling Times with Different Filling and Emptying Designs.....	32
Table 12.	Emptying Characteristics, Type 12 Filling and Emptying System, 21.5-ft Lift, Upper Pool El 601.6, Lower Pool El 580.1	32
Table 13.	Permissible Emptying Times.....	33
Table 14.	Comparison of Ice Lockage Times.....	46
Table 15.	Comparison of Permissible Filling Times with Different Intake Designs, Upper Pool El 601.6, Lower Pool El 580.1	47
Table 16.	Comparison of Permissible Filling Times, Upper Pool El 601.6, Lower Pool El 580.1.....	48
Table 17.	Permissible Emptying Times, Upper Pool El 601.6, Lower Pool El 580.1.....	48
Table 18.	Outlet Experiments, Type 4 Outlet Design, Upper Pool El 601.6, Lower Pool El 580.1	49

Conversion Factors, Non-SI to SI Units of Measurement

Non-SI units of measurement used in this report can be converted to SI units as follows:

Multiply	By	To Obtain
feet	0.3048	meters
miles	1.609344	kilometers
square feet	0.09290304	square meters
tons (force)	8.896443	kilonewtons
tons (mass)	907.1847	kilograms

Preface

The model investigation reported herein was authorized by the Headquarters, U.S. Army Corps of Engineers, at the request of the U.S. Army Engineer District, Huntington (LRH), in June 2002. The model experiments were performed during the period September 2003 to May 2005 by personnel of the Coastal and Hydraulics Laboratory (CHL) of the U.S. Army Engineer Research and Development Center, ERDC, under the general supervision of Mr. T. W. Richardson, Director of the CHL; Dr. W. D. Martin, Deputy Director of the CHL; Mr. D. C. Wilson, Chief of the Navigation Branch, CHL, and Drs. Knight and Pope, Technical Directors, CHL.

The experimental program was led by Messrs. J. E. Myrick and J. P. Crutchfield under the supervision of Dr. J. E. Hite, Jr., Leader, Locks Group, and Mr. A. M. Tuthill, Cold Regions Research Engineering Laboratory. Model construction was completed by Messrs. J. A. Lyons, C. Hopkins, R. Wrosdick, and K. K. Raner of the Model Shop and Messrs. C. Burr, R. Bufkin, and C. Oliver of the Carpenter Shop, Messrs. O. Duncan, and H. Little of the Electric Shop, Department of Public Works (DPW), ERDC, under the supervision of Mr. J. Schultz, Chief of the Model Shop, Mr. T. M. Beard, Chief of the Carpenter Shop, and Mr. John Murray, Chief of the Electric Shop. Data acquisition and remote-control equipment were installed and maintained by Messrs. S. W. Guy and T. E. Nisley, Information Technology Laboratory (ITL), ERDC. Data acquisition software was developed by Dr. B. W. McCleave, ITL. This report was written by Dr. Hite and Mr. Tuthill. Mr. Mario Sanchez performed a peer review of the report.

During the course of the model study Messrs. S. Smith, T. Hamb, D. Sullivan, and D. White of the U.S. Army Engineer District, Huntington (LRH), and Mr. R. Erwin of the U.S. Army Engineer District, Detroit (LRE), visited ERDC to observe model operation, review experiment results, and discuss model results.

At the time of publication of this report Dr. James R. Houston was Technical Director of ERDC and COL James R. Rowan, EN, was Commander.

Executive Summary

The U.S. Army Engineer District, Detroit (LRE), proposes construction of a new lock at the Soo Locks on the St. Mary's River near Sault Ste. Marie, MI, which will replace the existing Davis and Sabin locks in the North Canal. The Poe Lock is currently the only facility at Soo Locks capable of handling the Great Lakes system's largest vessels. These large vessels account for more than half of the potential carrying capacity of the Great Lakes fleet and significant economic consequences result from disruption of services at the Poe Lock. The new lock will have the same capacity as the Poe Lock and will accommodate a vessel draft of 28 ft.

Engineering studies were necessary to investigate the hydraulic performance of the lock filling and emptying system, ice drawing and flushing for the lock, and the flow conditions in the approaches during lock filling and emptying. A laboratory model was used for evaluation of the filling and emptying system and the ice flushing and drawing experiments. A numerical model was used to help evaluate the flow conditions in the approaches during lock filling and emptying.

Lock chamber performance was based on filling and emptying times, hawser forces, surface roughness, and system energy losses. The intakes were evaluated based on energy losses, vortex tendencies, and the resulting flow patterns in the upper approach during lock filling. Performance of the outlet was based on water-surface bulking and the resulting flow patterns in the lower approach during lock emptying. Flow conditions in the upper and lower approaches were evaluated based on the surge heights generated from the locking operations. It is expected that the new lock will have upper approach ice congestion problems similar to those experienced at the existing Soo Locks. The only means of passing ice from the upper to lower approach with the proposed design will be to lock the ice through, either ahead of the vessel or as a separate ice lockage. For this reason, a major objective of the ice tests in the physical model is to maximize ice lockage performance.

The original design for the filling and emptying system did not perform as needed. Vortices formed in the upper approach during lock filling and were stronger than desired. Vortex formation is common with a through-the-sill intake as the flow required to fill the lock is confined between the lock approach walls. Vortex formation is a concern for safety reasons as well as hydraulic efficiencies. Small craft can experience difficulties from strong vortices and ice and debris may be pulled down and clog the trash racks, resulting in slower lock operations. Several modifications were evaluated in the upper approach and in the vicinity of

the intakes. Placing a 3-ft thick ported roof between the upstream bulkhead sill and the intakes, type 6 intake design, reduced vortex strength the most during lock filling.

The filling time required to keep the hawser forces to an acceptable level was much slower than desired. The permissible filling time is the time required to fill the lock without exceeding the criteria set for the maximum hawser forces. The maximum hawser force for the Soo Lock model investigation was 15 tons. A filling time less than 15 min. was the objective and the permissible filling time with the original design was 20.5 min. Several modifications were made to the chamber ports to improve the design. Placing upstream facing baffles on the upper ports, horizontally mounted baffles above the lower ports, and reducing the total number of ports, type 12 chamber design, provided the best performance of the designs evaluated. These changes resulted in a more balanced distribution of flow entering the chamber during filling. The permissible filling and emptying times with the type 12 chamber design, based on maximum allowable hawser forces, were 13.0 and 12.4 min., respectively.

The outlet was also modified to improve the flow conditions in the outlet during lock emptying. Flow discharging from the outlets strikes the lower bulkhead sill and is directed toward the water-surface, causing upwelling. A 3-ft-thick ported roof was placed between the downstream end of the outlet and the upstream side of the lower bulkhead sill. This was designated the type 4 outlet design and was a slight improvement over the original design.

Ice drawing and flushing experiments were performed using combinations of ice valves installed in the upper and lower lock culverts, valved manifolds mounted in the upper lock gates, and the lock filling and emptying valves. The upper ice valves were about equal to the combined use of filling valves and the manifolds in the upper miter gates during ice flushing. During ice drawing experiments, the lower ice valves brought the ice farther into the lock, although having the ice in direct contact with the lower miter gates would interfere with their operation. The surface water currents created by the through-the-sill culvert intakes drew ice directly in contact with the upper miter gates, which would make them difficult to open. A high flow air curtain, located 120 ft upstream of the miter gates, prevented this ice from reaching the gates. To create an upstream flow field sufficient to negate the downstream currents caused by lock filling would require a compressor capacity of 1500 cfm. Strong downstream-blowing winds would probably render the air curtain ineffective, however.

1 Introduction

Background

The U.S. Army Engineer District, Detroit (LRE), proposes construction of a new lock at the Soo Locks on the St. Mary's River near Sault Ste. Marie, MI. The lock will replace the existing Davis and Sabin locks in the North Canal. Currently, the Poe Lock is the only facility at Soo Locks capable of handling the Great Lakes system's largest vessels. These large vessels account for more than half of the potential carrying capacity of the Great Lakes fleet.

Disruption of services at the Poe Lock quickly results in significant economic consequences. The new lock will have the same capacity as the Poe Lock and will be 1,288 ft¹ from pintle to pintle and 110 ft wide. The lock will accommodate a vessel draft of 28 ft.

The Prototype

The existing Soo Locks project consist of four locks, MacArthur, Poe, Davis, and Sabin. The locks are located side by side near the eastern extremity of Lake Superior on the St. Mary's River, which is the only water connection between Lake Superior and the other Great lakes (Figure 1). The Soo Locks form a passage around the St. Mary's River rapids. The MacArthur Lock was constructed in 1943 and is 800 ft in length and 80 ft in width. The Poe Lock is 1,200 ft in length, 110 ft in width and was completed in 1968. The Davis and Sabin (closed) Locks are both 1,350 ft in length, 80 ft in width and were constructed in 1914 and 1919, respectively. A U.S. Hydroelectric Power Plant is also located north of the locks.

The filling and emptying system for the new lock consists of an in-chamber longitudinal culvert system (ILCS) with flow controlled by four vertically mounted, horizontally pivoting butterfly valves. A plan and profile view of the original design, Plan A, filling and emptying system for the new lock is shown in Plate 1. Plan A consisted of an intake with four 12-ft square ports, with the butterfly valves located just downstream from each entrance. A profile of the upper approach, intakes, and upper miter sill is shown in Plate 2 and a plan view is

¹ A table of factors for converting non-SI units of measurements to SI units is presented on page vii.

shown in Plate 3. The culverts downstream from the valves were also 12 by 12 ft. Each culvert then transitioned to 4-ft-high by 23-ft-wide culvert with a 3-ft-wide splitter wall located in the center. Each culvert inside the chamber contained 10 pairs of ports in the upper and lower ends of the chamber. The throat dimensions of the port were 2.5 by 2.0 ft and the ports were 3-ft thick (the culvert roof thickness). The ports were located at the top of the culvert as shown in Plate 4 and the port-to-culvert area ratio was 2.0. Ice valves were located at each end of the culvert inside the chamber to assist in moving ice through the project. Plates 5 and 6 provide details of the upper ice valves. The filling and emptying culverts transitioned back to a 12- by 12-ft culverts near the lower pintle. Four 12- by 12-ft butterfly valves located at the end of the culvert were used to empty the lock. Details of the outlet area are shown in Plate 7.



Figure 1. Vicinity map

Ice and debris lockages are common at many Corps locks. To lock ice, the emptying valves are opened, creating water currents that draw ice from the upper approach into the lock chamber. Once the chamber is lowered, the filling valves are opened to flush the ice into the lower approach. Conventional filling and emptying systems are inefficient for locking ice owing to low water velocity or “dead zones” that exist at the upper and lower ends of the chamber beyond the limits of the filling and emptying ports.

Purpose and Scope

The purpose of the physical model investigation was to evaluate the hydraulic performance of the lock filling and emptying system and to modify the design, if necessary, to achieve acceptable performance. A numerical model investigation was also conducted to assess the flow conditions in the lock approaches during filling and emptying and the impact of these conditions on vessels in the

approaches. Lock chamber performance was based on filling and emptying times, hawser forces, surface roughness, and system energy losses. The intakes were evaluated based on energy losses, vortex tendencies, and the resulting flow patterns in the upper approach during lock filling. Performance of the outlet was based on water-surface bulking and the resulting flow patterns in the lower approach during lock emptying. Flow conditions in the upper and lower approaches were evaluated based on the surge heights generated from the locking operations.

It is expected that the new lock will have upper approach ice congestion problems similar to those experienced at the existing Soo Locks. The only means of passing ice from the upper to lower approach with the proposed design will be to lock the ice through, either ahead of the vessel or as a separate ice lockage. For this reason, a major objective of the ice tests in the physical model is to maximize ice lockage performance.

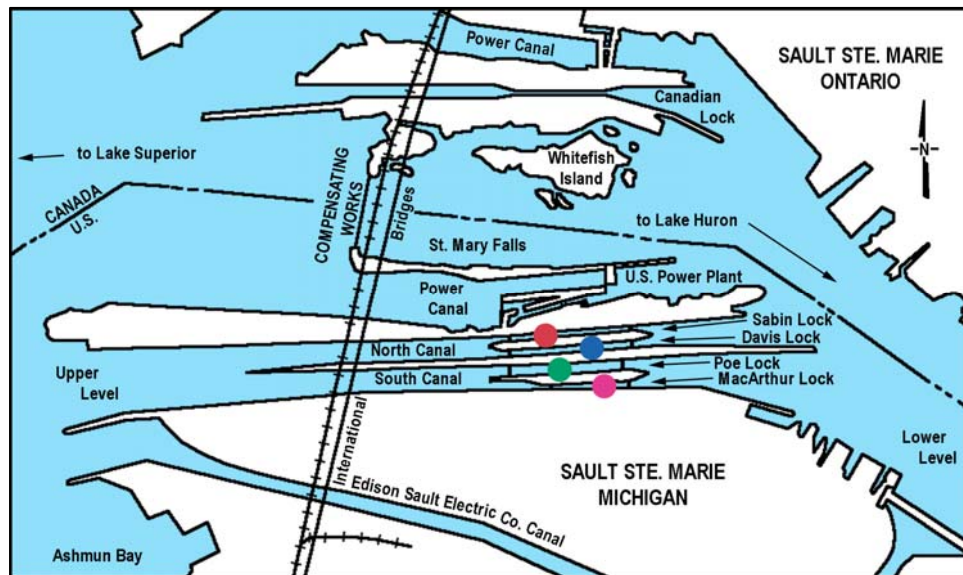


Figure 2. Layout of existing project

2 Physical Model

Description

The entire filling and emptying system was reproduced at a 1:25-scale, along with approximately 500-ft lengths of the upper and lower approaches. A layout of the model is shown in Plate 8. Photos of the 1:25-scale model are shown in Figures 3a-i. Overall views of the model looking downstream and upstream are provided in Figures 3a and 3b. The intakes with the four ports and butterfly valves located just downstream from each entrance are shown in Figure 3c. The vertical rods shown contain the rack mechanism used to operate the gear connected to the butterfly pivot. The culverts contained 10 pairs of ports in the upper and lower ends of the chamber, as shown in Figure 3d. Figure 3e shows a close-up view of one of the ports. Ice valves were located at each end of the culvert inside the chamber, as shown in Figures 3f and 3g. The filling and emptying culverts transitioned back to a 12- by 12-ft culvert near the lower miter gates, Figure 3h. Four 12- by 12-ft butterfly valves located at the end of the culvert were used to empty the lock. Figure 3i shows a view looking upstream at the outlet and valves.

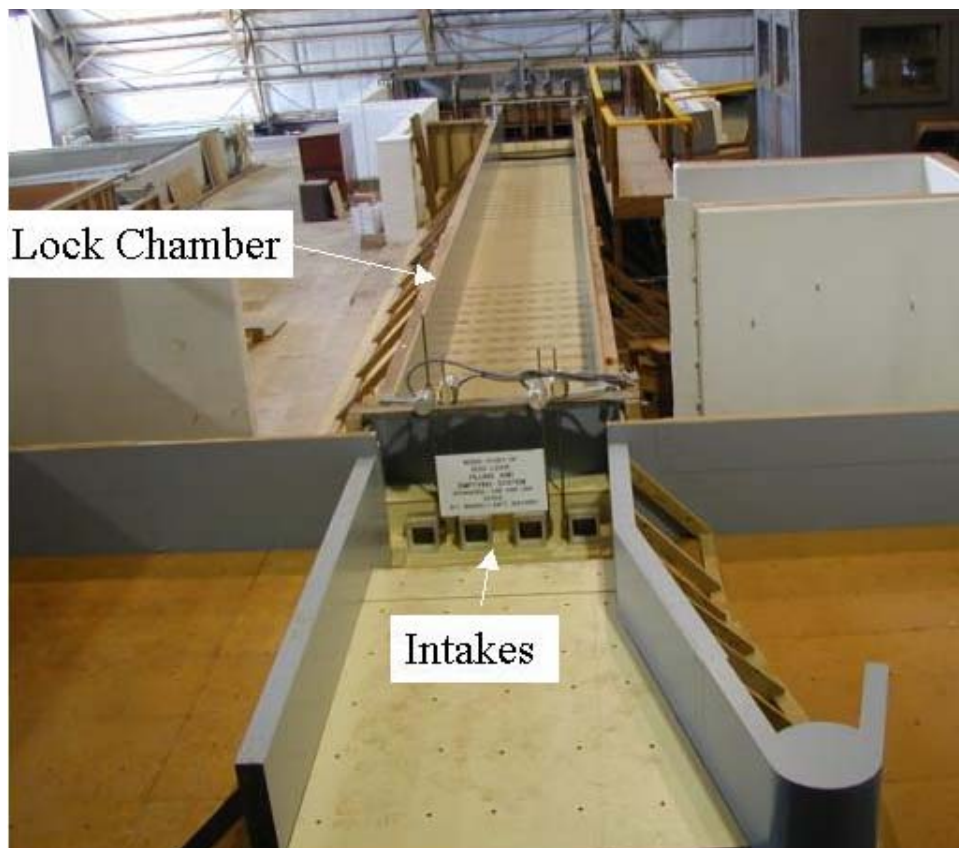
The filling and emptying system was fabricated from acrylic. The lock walls and floor and the upper and lower approaches were constructed from plastic-coated plywood. The filling and emptying valves were made of brass.

Appurtenances and Instrumentation

Water was supplied to the model through a circulating system. The upper and lower pools were maintained at near constant elevations during the filling and emptying operations using constant head skimming weirs in the model headbay and tailbay. During a typical filling operation, excess flow was allowed to drain over the weirs at the beginning of the fill operation and minimal flow over the weir was maintained at the peak discharge, thereby minimizing the drawdown in the upper reservoir. The opposite of this operation was performed during lock emptying. Upper and lower pool elevations were set to the desired level by adjusting the skimming weirs and reading piezometers placed in calm areas of the upper and lower pools. Water-surface elevations inside the chamber were determined from electronic pressure cells located in the middle and on each end of the lock chamber. Histories of the end-to-end water-surface differential were also recorded during filling and emptying. Dye and confetti were used to study

subsurface and surface current directions. Pressures throughout the systems were measured with piezometers (open-air manometers). Pressures obtained in this manner are considered average pressures because of the reduction in frequency response resulting from the use of nylon tubing.

An automated data acquisition and control program, Lock Control,¹ was used to control valve operations and collect pressure and strain gauge data. Fifteen data channels were used: eight for control of the filling and emptying valves, four for pressure data, and three for collecting strain gauge information. The data were usually collected at a sampling rate of 50 hz. Some of the hawser force and lock filling and emptying data were collected at 10 hz. These data were then processed using a computer program, LOCKDXF.² The processed data were used to determine lock filling and emptying times, longitudinal and transverse hawser forces, and differential pressures.



a. Overall view looking downstream

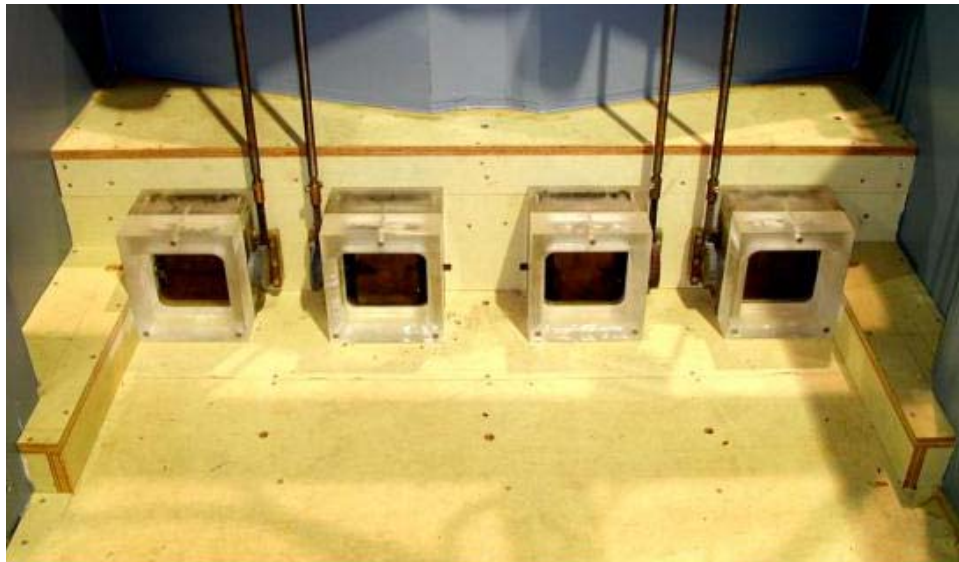
Figure 3. 1:25-scale model of the filling and emptying system (Sheet 1 of 9)

¹ Written by Dr. Barry W. McCleave, Information Systems Development Division, Information Technology Laboratory, ERDC.

² Written by Dr. Richard L. Stockstill, Navigation Branch, Coastal and Hydraulics Laboratory, ERDC.



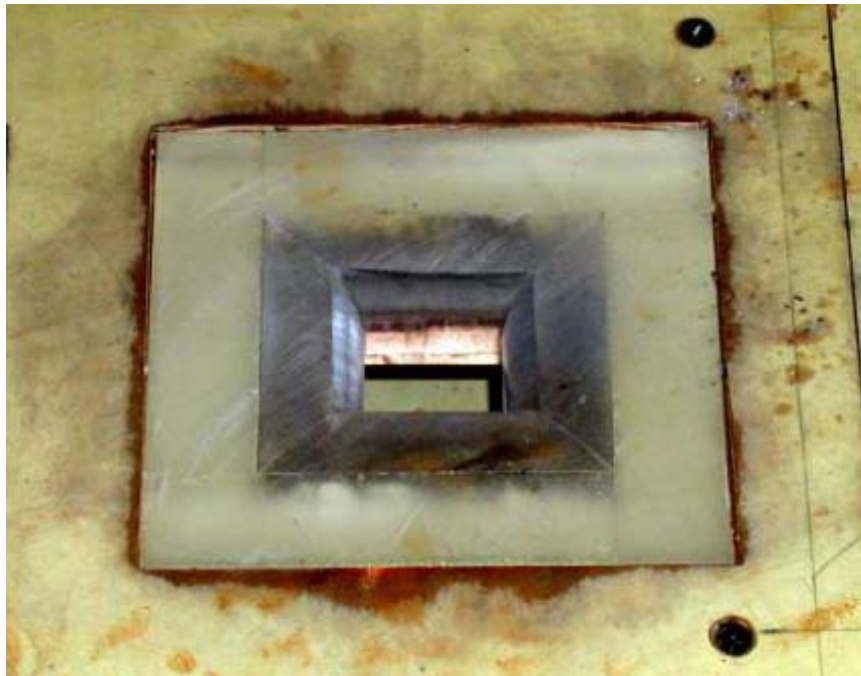
b. Overall view looking upstream
Figure 3. (Sheet 2 of 9)



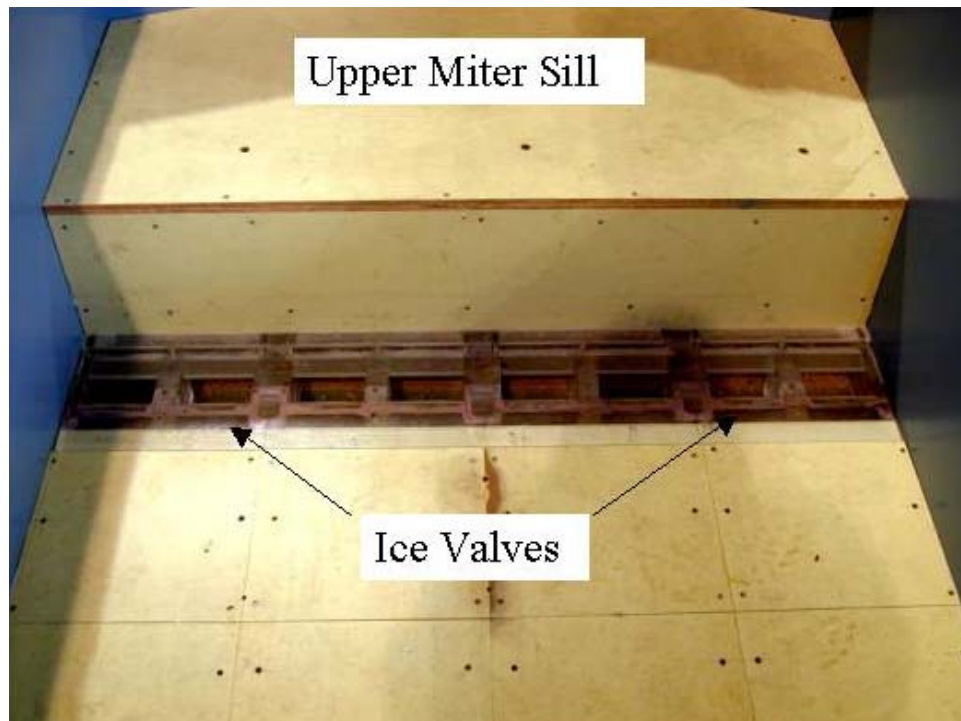
c. Close-up view of intakes
Figure 3. (Sheet 3 of 9)



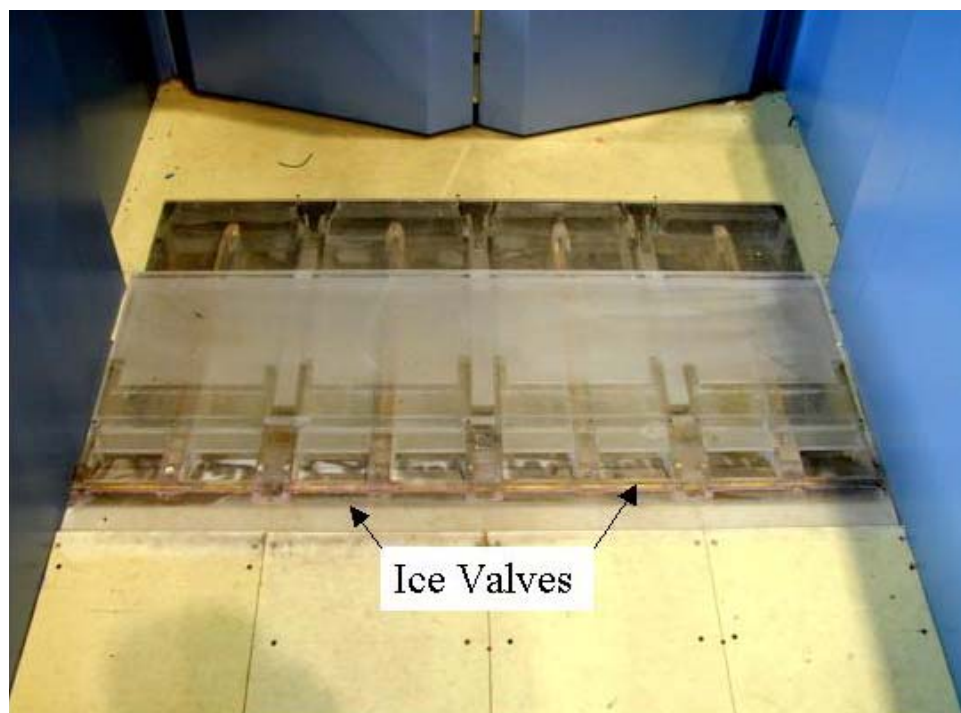
d. Ports inside lock chamber
Figure 3. (Sheet 4 of 9)



e. Close-up of port
Figure 3. (Sheet 5 of 9)



f. Upper ice valves
Figure 3. (Sheet 6 of 9)



g. Lower ice valves
Figure 3. (Sheet 7 of 9)



h. Lower miter gates and culvert transition
Figure 3. (Sheet 8 of 9)



i. Outlets and valves
Figure 3. (Sheet 9 of 9)

Figure 4 shows a hawser-pull (force links) device used for measuring the longitudinal and transverse forces acting on a tow in the lock chamber during filling and emptying. Three such devices were used: one measured longitudinal forces and the other two measured transverse forces on the downstream and upstream ends of the tow, respectively. These links were machined from aluminum and had SR-4 strain gauges cemented to the inner and outer edges. When the device was mounted on the tow, one end of the link was pin-connected to the tow while the other end was engaged to a fixed vertical rod. While connected to the tow, the link was free to move up and down with changes in the water-surface in the lock. Any horizontal motion of the tow caused the links to deform and vary the signal, which was recorded with a personal computer using an analog-to-digital converter. The links were calibrated by inducing deflection with known weights. Instantaneous pressure and strain gauge data were recorded digitally with a personal computer.

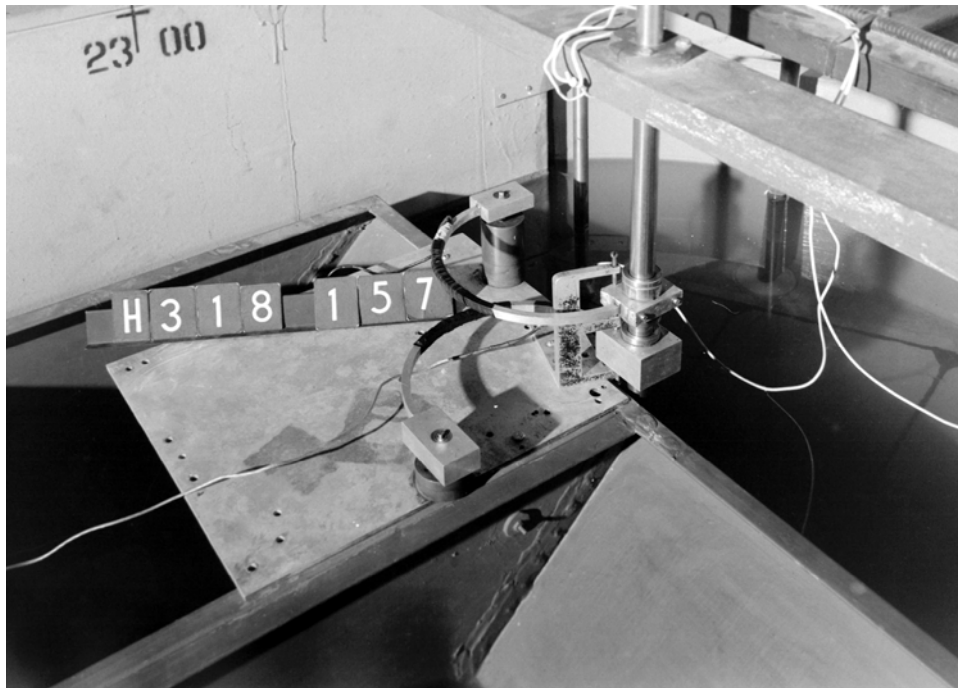


Figure 4. Hawser-pull (force links) measuring device

Similitude Considerations

Kinematic similitude

Kinematic similarity can be used for modeling free-surface flows in which the viscous stresses are negligible. Kinematic similitude requires that the ratio of inertial forces ($\rho V^2 L^2$) to gravitational forces ($\rho g L^3$) in the model be equal to that of the prototype. Here, ρ is the fluid density, V is the fluid velocity, L is a characteristic length, and g is the acceleration due to gravity. This ratio is generally expressed as the Froude number, N_F .

$$N_F = \frac{V}{\sqrt{gL}} \quad (1)$$

where L , the characteristic length, is usually taken as the flow depth in open-channel flow.

The Froude number can be viewed in terms of the flow characteristics. Because a surface disturbance travels at celerity of a gravity wave $(gh)^{1/2}$, where h is the flow depth, the Froude number describes the ratio of advection speed to the gravity wave celerity. Evaluation of the lock chamber performance primarily concerns modeling of hawser forces on moored barges during filling and emptying operations. These hawser forces are generated primarily by slopes in the lock chamber water-surface. The tow's bow-to-stern water-surface differentials are the result of long period seiches or oscillations in the lock chamber. Seiching is gravity waves traveling in the longitudinal direction from the upper miter gates to the lower miter gates.

Dynamic similitude

Modeling of forces is a significant purpose of the laboratory investigation. Appropriate scaling of viscous forces requires that the model be dynamically similar to the prototype. Dynamic similarity is accomplished when the ratios of the inertia forces to viscous forces (μVL) of the model and prototype are equal. Here, μ is the fluid viscosity. This ratio of inertia to viscous forces is usually expressed as the Reynolds number

$$N_R = \frac{VL}{\nu} \quad (2)$$

where ν is the kinematic viscosity of the fluid ($\nu = \mu/\rho$) and the pipe diameter is usually chosen as the characteristics length, L , in pressure flow analysis.

Similitude for lock models

Complete similitude in a laboratory model is attained when geometric, kinematic, and dynamic similitudes are satisfied. Physical models of hydraulic structures with both internal flow (pressure flow) and external flow (free surface) typically are scaled using kinematic (Froudian) similitude at a large enough scale so that the viscous effects in the scaled model can be neglected. More than 50 model and 10 prototype studies of lock filling and emptying systems have been investigated (Pickett and Neilson 1988). The majority of these physical model studies used a scale of 1 to 25 (model to prototype). Lock model velocities scaled using kinematic similitude (model Froude number equal to prototype Froude number) in a 1:25-scale model have maximum Reynolds numbers at peak discharges on the order of 10^5 , yet the corresponding prototype values are on the order of 10^7 .

Boundary friction losses in lock culverts are empirically described using the “smooth-pipe” curve of the Darcy-Weisbach friction factor, where the headloss is expressed as

$$H_f = f \frac{\ell V^2}{D 2g} \quad (3)$$

where H_f is the headloss due to boundary friction, f is the Darcy-Weisbach friction factor, ℓ is the culvert length, and D is the culvert diameter. The Darcy-Weisbach friction factor for turbulent flow in smooth pipes is given in an implicit form (Vennard and Street 1982)

$$\frac{1}{\sqrt{f}} = 2.0 \log(N_R \sqrt{f}) - 0.8 \quad (4)$$

Because f decreases with increasing N_R , the model is hydraulically “too rough.” The scaled friction losses in the model will be larger than those experienced by the prototype structure. Consequently, the scaled velocities (and discharges) in the model will be less and the scaled pressures within the culverts will be higher than those of the prototype. Low pressures were not a major concern with the Soo Lock design; however, the lower discharges would in turn result in longer filling and emptying times in the model than the prototype will experience. Prototype filling and emptying times for similar designs will be less than those measured in a 1:25-scale lock model.

Modeling of lock filling and emptying systems is not entirely quantitative. The system is composed of pressure flow conduits and open-channel components. Further complicating matters, the flow is unsteady. Discharges (therefore N_F and N_R) vary from no flow at the beginning of an operation to peak flows within a few minutes and then return to no flow at the end of the cycle. Fortunately, though, engineers now have about 50 years of experience in building large-scale models and subsequently studying the corresponding prototype performance. This study used a 1:25-scale Froudian model in which the viscous differences were small and could be estimated based on previously model-to-prototype comparisons. Setting the model and prototype Froude numbers equal results in the following relations between the dimensions and hydraulic quantities:

Characteristic	Dimension ¹	Scale Relation Model:Prototype
Length	$L_r = L$	1:25
Pressure	$P_r = L_r$	1:25
Area	$A_r = L_r^2$	1:625
Velocity	$V_r = L_r^{1/2}$	1:5
Discharge	$Q_r = L_r^{5/2}$	1:3,125
Time	$T_r = L_r^{1/2}$	1:5
Force	$F_r = L_r^3$	1:15,625
¹ Dimensions are in terms of length.		

These relations were used to transfer model data to prototype equivalents and vice versa.

Plastic Ice Material and Scaling

The scaled piece size distribution of the plastic model ice was based on observed ice runs on the St. Claire River and analysis of photos of brush ice in the Poe Lock in March 1999. These data are plotted in Figure 5 with a curve fitted empirically. A crushed polyurethane plastic ice material successfully simulated ice jam processes in a physical model study of the upper Niagara River, sponsored in part by the New York Power Authority. The size distribution of this “NYPA” ice matches reasonably well with the less than or equal to 50 percent and finer portion of the field-observed ice piece size. The larger size fractions were sawn into 0.252-in.-thick (6.4-mm-thick) polyethylene squares. The specific gravity of the two plastic types is 0.92, similar to 0.916 for freshwater.

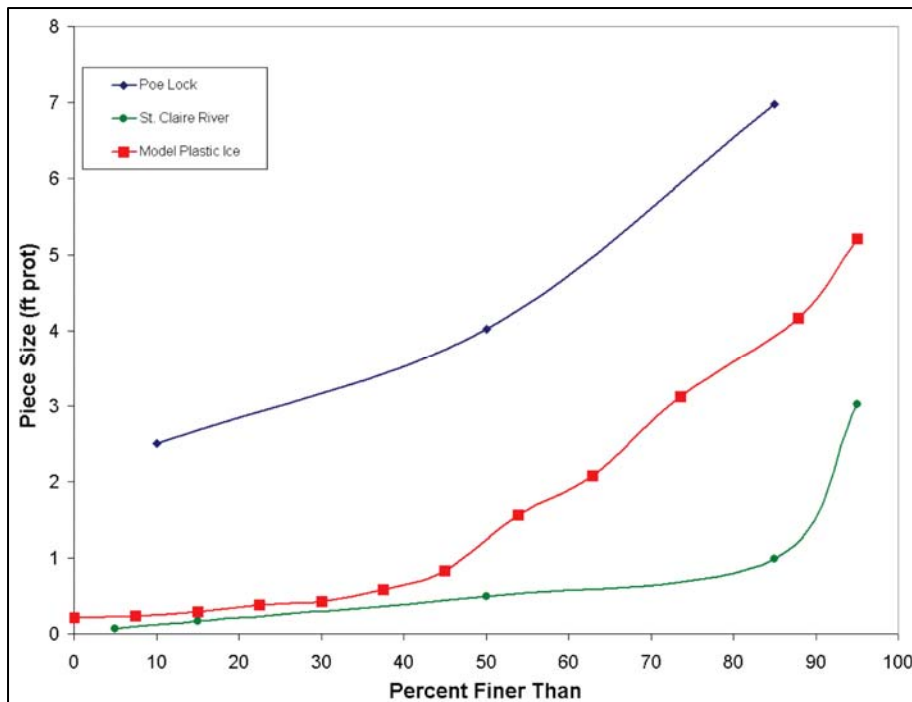


Figure 5. Piece size distribution of plastic ice material compared to field observations

Experimental Procedures

The various elements of the lock system were evaluated on the basis of data obtained during typical filling and emptying operations. Performance was based primarily on hawser forces on tows in lockage, roughness of the water surface, pressures, and time required for filling and emptying. Quantification of energy loss coefficients was made using fixed-head (steady-flow) conditions with the culvert valve or miter gates, or both, fully opened or closed.

3 Model Experiments and Results

Headloss Measurements

Loss coefficient

Piezometers were placed at selected locations in the filling and emptying system to determine loss coefficients for the system components. These measurements were used to quantify loss coefficients for various components of the system. Energy loss through each component is expressed as

$$H_{L_i} = K_i \frac{V^2}{2g} \quad (5)$$

where K_i is the loss coefficient for component i , and V is the culvert velocity computed for that component. The total headloss through the system is

$$H_L = \sum H_{L_i} = \sum K_i \frac{V^2}{2g} \quad (6)$$

The loss coefficients for the individual components determined for the filling operations are shown in Table 1. The loss coefficients for the filling system were obtained by holding a steady upper pool and discharge, closing the upper miter gates with the lower miter gates open, closing the emptying valves, and opening the filling valves. The total filling system loss coefficient was 3.60.

Table 1 Loss Coefficients Plan A Design Filling System	
System Component	Component Loss Coefficient
Intake	1.14
Transition	0.38
U/S Culvert	0.25
Manifold	1.83
Total	3.60

Lock coefficient

Another method to evaluate the efficiency or energy losses of a lock system is to compute an overall lock coefficient. The lock coefficient is defined as

$$C_L = \frac{V}{\sqrt{2gH_L}} \quad (7)$$

Equating the headloss, H_L , in each expression shows the relation between the lock coefficient and loss coefficient.

$$K = C_L^{-2} \quad \text{or} \quad C_L = K^{-0.5} \quad (8)$$

where K is the sum of each K_i . The lock coefficient computed from the loss coefficients (3.6) is 0.5.

This method of computing the lock coefficient from the steady state head loss measurements does not truly represent the system because, in normal operations, the flow is unsteady. The individual loss coefficients do indicate which components should be modified to improve the chamber performance.

An equation typically used by the U.S. Army Corps of Engineers to compute the overall lock coefficient is:

$$C_L = \frac{2A_L\sqrt{H+d} - \sqrt{d}}{A_c(T - kt_v)\sqrt{2g}} \quad (9)$$

where

A_L = area of lock chamber, ft²

H = initial head, ft

d = overtravel, ft

A_c = area of culverts, ft²

T = filling time, sec

k = a constant

t_v = valve opening time, sec

g = acceleration due to gravity, ft/sec²

Refer to Davis (1989) for additional information on the development of Equation (9). The term $T - k t_v$ is the lock filling or emptying time for the hypothetical case of instantaneous valve operation and is determined directly from the filling times associated with the various valve times. The operation times during filling will be discussed in a later paragraph. The lock coefficient computed for these conditions during filling was also 0.5 and during emptying was 0.46.

Typical lock coefficients, determined from previous model studies performed for varying types of filling and emptying systems, for filling range from 0.6 to 0.8 and for emptying from 0.5 to 0.7.

Intake Vortex Experiments

Plan A intake design

Experiments were performed to evaluate the tendency for vortices to form in the upper approach during filling operations for different valve schedules. The Alden Research Lab vortex strength classification scale, Plate 9, was used to determine the strength of the vortex based on visual observations. The scale classifies a coherent surface swirl as a type 1 vortex and a vortex with a full air core that enters the intake as a type 6 vortex. Vortices stronger than type 3 that form in a 1:25-scale model indicate a potential for strong vortex formation in the prototype. Time histories of vortex formation during lock filling with an upper pool el of 601.6 and a lower pool of 580.1 for 2-, 4-, and 8-min valve operations are shown in Plate 10. Multiple tests were performed because of the unsteady nature of vortex formation. Sufficient time is allowed between the tests to minimize residual flume currents. The tests indicate that type 4 vortices occurred on the left and right sides of the approach for all valve operations tested. A vortex was usually observed first on the left side of the approach just upstream from the left two intakes. This vortex would vary in strength and, when the strength decreased, a vortex formed on the right side of the approach. This vortex often appeared stronger. The vortices form as a result of the geometry of the miter gate recesses and the bulkhead sill and the flow conditions in the upper approach. Flow separation and circulation create the vortices.

Previous model studies, conducted with through-the-sill intakes, developed modifications in the approach to reduce the tendency for the strong vortices to form. Streamlining the flow into the intakes by modifying the miter gate recesses and bulkhead sill helped reduce vortex formation. Reducing the approach velocities by deepening the approach also helps improve flow conditions.

Type 2 intake design

Vanes were placed in the upper approach between the face of the upper miter sill and the bulkhead sill. In addition, the structural walls located in the upper approach at the corners of the lock walls and floor were removed and the invert el of the miter recesses were raised to the same el as the miter sill (562.4). These modifications were designated the type 2 intake design (Plate 11). Experiments were performed with 4- and 6-min valve operations to document the strength of the vortices during filling. Strong vortices were observed on both the left and right sides of the approach with the 4-min valve. The strength of these vortices was slightly reduced with the 6-min valve operation; however the vortices were still stronger than desired. Plate 12 presents time histories of the vortex strength observed during lock filling for the 4- and 6-min valve operations with the type 2 intake design.

Type 3 intake design

The type 3 intake design consisted of changing the slope on the upstream side of the bulkhead sill from 1V on 0.6H to 1V on 1.8H as shown in Plate 13. The intent was to prevent the flow separation shown in Figure 6 and help spread the approach flow throughout the entire depth. This should reduce the approach velocities and the vortex strength. Plate 14 provides the time histories of vortex strength observed with 4- and 6-min valve operations and the type 3 intake design. The vortices still formed during filling; however, the strength was reduced from that observed with the type 2 design. The strength was still higher than desired.

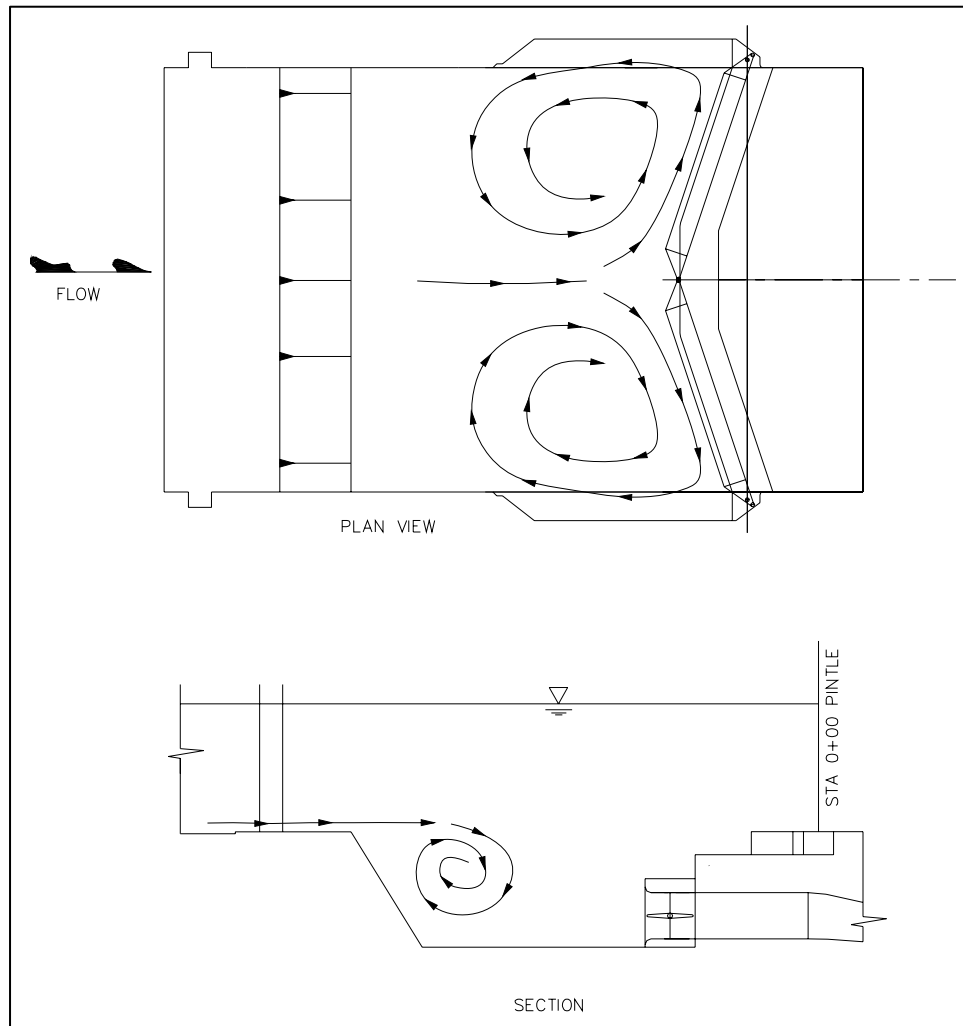


Figure 6. Schematic of flow with original bulkhead sill

Type 4 intake design

The intake was modified by extending the upstream face of the upper miter sill to match the entrance to the intakes. This design, type 4 intake design, is shown in Plate 15. This design provided a more streamlined entrance and

eliminated the reentrant flows. Plate 16 provides the time histories of the vortex experiments for the 4-, 6-, and 8-min valve operations. Nine tests were performed with the 6-min filling valves to determine the potential for a type 4 vortex. None was observed during these nine tests. There were noticeable vortices with the 6-min filling valves on the left side of the approach between 6 and 9 min into the filling operation. Type 3 vortices formed in three out of nine tests. Type 3 vortices were observed in all nine tests on the right side of the approach with the 6-min filling valves. Vortices still formed for all three valve operations, although they were not as strong as with previous designs. The flow entering the intakes was more streamlined with the type 4 design. The maximum strength vortex was a type 3 and it was observed for all three valve operations. The strongest vortex usually formed on the right side when the vortex activity on the left side reduced. The criteria indicate that, with a 1:25-scale model, vortices stronger than a type 3 are not desired. In this study, the vortex strength is right on the edge of the criteria. In the model, the trashracks are not included. The trashracks will create additional headloss and probably reduce the vortex strength. If good intake flow conditions in the model are achieved without a trashrack, this assures that these conditions will be acceptable in the prototype as the prototype will have a trashrack.

A qualitative test was done by placing a section of bar screen material in front of the intakes to observe the flow conditions for the 6-min filling valve operation. The vortex activity was noticeably reduced. This bar screen probably caused more headloss than a typical trashrack. The test did indicate that a trashrack would probably help reduce the vortex strength for the intakes.

Type 5 intake design

Vanes similar to the type 2 design were installed with the type 4 design as shown in Plate 17. The tests with a 6- and 8-min valve indicated that type 3 vortices still formed, but their strength appeared slightly less than that observed with the type 4 design.

Plan A Design Chamber Performance Without Ship

Lock filling

Experiments were performed to evaluate chamber performance. The initial tests were conducted without the ship in the chamber to observe the water-surface during locking operations and determine the filling and emptying times associated with the valve operations. The tests consisted of documenting filling and emptying times and water-surface differentials in the chamber to gain insight into what valve operations might cause high hawser forces. Typical time histories obtained during filling with an upper pool el of 601.6 and a lower pool el of 580.1 and a 2-min filling valve are shown in Plate 18. The lock water surface reached the upper pool el in 11.2 min and this was considered the filling time with these conditions. The water-surface differential (positive means the upstream water surface is greater than the downstream water surface) indicates

that, initially, the water level is higher in the upper end of the chamber. This differential was determined from pressure cells located in the upper and lower ends of the chamber. Between 1 and 2 min into the filling operation, the downstream water surface becomes greater than the upstream water surface and remains this way for the remainder of filling. The maximum water-surface differential measured and averaged from three experiments was -0.63 ft.

The filling time with the 4-min valve was 12.1 min and the maximum water-surface differential measured and averaged from three experiments was -0.30. The filling time with the 8-min valve was 14.1 min and the maximum water-surface differential measured and averaged from three experiments was -0.16. The filling curves and water-surface differentials determined with the 4- and 8-min valves are shown in Plate 18.

Lock emptying

The emptying system for the Plan A design was evaluated in the same manner as the filling system. Plate 19 provides typical time histories obtained during emptying with an upper pool el of 601.6 and a lower pool el of 580.1 and 2-, 4-, and 8-min emptying valves. The emptying time with the 2-min valve was 12.1 min. The emptying times with the 4-min valve were 13.3 min and 15.7 min with the 8-min valve. The maximum water-surface differentials measured and averaged from three experiments were 0.06 and 0.028 with the 4-, and 8-min emptying valve operations, respectively. The water-surface differentials were much less during emptying.

Operation times for filling and emptying with no vessel in the chamber are shown in Plate 20.

Outlet Experiments

The next experiments evaluated the water-surface bulking or upwelling in the lower approach for valve operations of 2, 4, and 8 min. The maximum rise above the lower pool el was 2.3 ft and occurred with the 2- and 4-min valve operations on the right side (looking downstream) of the lower approach at the bulkhead sill. Results from the outlet experiments are shown in Table 2. The outlet flow, directed toward the surface by the bulkhead sill, causes the bulking and there was no significant bulking observed on the downstream side of the lower miter gates.

Table 2 Outlet Experiments, Plan A Filling and Emptying System, Upper Pool El 601.6, Lower Pool El 580.1			
Valve Operation, min	Location	Time, min	Maximum Rise in WSEL, ft
2	Left Wall	4.6	2.0
	Right Wall	3.9	2.3
4	Left Wall	5.8	1.5
	Right Wall	6.3	2.3
8	Left Wall	10.0	1.6
	Right Wall	9.2	1.6

Plan A Design Chamber Performance with Ship

Experiments were conducted to determine hawser forces on the ship with an upper pool el of 601.6 and 580.1 for various valve operations. A schematic of the ship reproduced for this model study is shown in Plate 21. The dimensions of the ship were 1,000 ft long by 105 ft wide, with a draft of 28 ft. The displacement weight for this size vessel was 90,000 tons. Criteria for hawser forces as stated in EM 1110-2-1604 (HQUSACE 1995) indicate that, for a ship of 50,000 tons, the forces should not exceed 10 tons and, for a ship of 170,000 tons, the hawser forces should not exceed 25 tons. Interpolation of this guidance for a ship that weighs 90,000 tons gives a hawser force not to exceed 15 tons. The target operation times for the new lock are 13 min for filling and 10 min for emptying, which are the operation times for the existing Poe Lock. An upper limit for filling was considered to be 15 min. The experiments without the ship in the chamber indicated that a filling time of 13-min was achieved with a 6-min filling valve operation.

Hawser forces during filling

The initial experiments with the ship in the chamber were conducted using 8-min filling valves and upper and lower pool el's of 601.6 and 580.1, respectively. Typical water-surface and hawser force measurements obtained with these conditions are shown in Plate 22. The upper time history is the longitudinal hawser force and the next lower two are the upstream and downstream transverse hawser forces. The filling curve is also provided. An upstream longitudinal force of 52 tons occurred between 5 and 6 min into the filling operation. The transverse forces were much lower than the longitudinal and the filling time was 14.4 min. As mentioned, the acceptable hawser force for a ship with this displacement is 15 tons. The filling time was under the upper limit of the acceptable filling time; however, the maximum upstream longitudinal hawser force was much higher than the acceptable force of 15 tons.

Additional experiments were conducted next with filling valve operations of 10, 12, 14, 18, and 20 min. A 20-min filling valve operation was required to obtain a maximum longitudinal hawser force of 15 tons. Plate 23 shows the time histories with the 20-min filling valve operation. An upstream longitudinal

hawser force of 15 tons was measured around 12 min into the filling operation. The filling time with the 20-min valve was 20.3 min, much slower than the desired filling time. Each hawser force experiment was usually repeated at least three times and the maximum hawser force measurements from each of these experiments were averaged and noted as the average maximum force for that valve operation. A table of the maximum hawser forces and the filling times determined for each experiment with the Plan A chamber design is provided in Table 3 and a plot of the average maximum hawser forces versus filling time for the valve operations tested is shown in Plate 24. This plot shows that, to achieve an upstream longitudinal hawser force of 15 tons, a filling time of around 20.5 min was necessary. This filling time was much higher than the target time desired.

Table 3
Filling Characteristics, Plan A Filling and Emptying System, 21.5-ft Lift, Upper Pool EI 601.6, Lower Pool EI 580.1

Valve Time, min	Hawser Forces, tons						Fill Time, min
	Longitudinal		U/S Transverse		D/S Transverse		
	U/S	D/S	Right	Left	Right	Left	
8.0	51.3	-11.1	6.6	-1.4	1.7	-4.8	14.6
	51.3	-10.4	4.9	-1.5	2.0	-3.4	14.6
	52.0	-10.1	5.7	-1.0	1.7	-3.6	14.4
Average	51.5	-10.5	5.7	-1.3	1.8	-3.9	14.5
10.0	39.0	-8.1	4.6	-0.8	1.9	-3.7	15.6
	39.8	-8.2	4.7	-0.5	1.2	-2.8	15.5
	38.7	-8.3	4.6	-0.8	1.1	-3.2	15.5
Average	39.2	-8.2	4.6	-0.7	1.4	-3.2	15.5
12.0	29.2	-7.3	3.5	-2.4	2.1	-3.0	16.8
	29.2	-6.1	2.7	-2.6	1.6	-3.1	16.7
	28.8	-7.3	4.1	-3.5	2.6	-2.6	16.4
Average	29.1	-6.9	3.4	-2.8	2.1	-2.9	16.6
14.0	24.6	-5.7	1.9	-2.9	1.5	-2.4	17.4
	24.1	-5.9	2.5	-1.9	1.8	-3.4	17.1
	24.7	-5.5	1.9	-2.2	2.0	-2.3	17.1
Average	24.5	-5.7	2.1	-2.3	1.8	-2.7	17.2
18.0	17.9	-5.1	1.6	-2.3	1.3	-1.5	19.2
	18.6	-4.8	1.7	-2.6	1.9	-1.6	19.2
	18.0	-5.3	2.3	-2.5	2.0	-2.2	19.2
Average	18.2	-5.1	1.9	-2.5	1.7	-1.8	19.2
20.0	15.3	-4.8	1.8	-2.2	2.0	-1.7	20.3
	15.0	-4.4	2.5	-2.1	2.0	-2.0	20.3
	15.8	-4.6	1.9	-2.4	2.1	-1.8	20.3
Average	15.4	-4.6	2.1	-2.1	2.0	-1.8	20.3

Hawser forces during emptying

Experiments to measure water-surface and hawser forces during emptying were conducted in a manner similar to those during filling. These forces were much lower than those measured with the same valve operations during filling. Typical time histories measured with the 8-min emptying valve are shown in Plate 25. The upstream longitudinal hawser force (7.2 tons) was the maximum force measured; it occurred about the time the lock was empty when the water level in the chamber drops below the lower pool level owing to inertia. This force was well below the 15-ton limit. The transverse hawser forces measured with the 10-, 12-, 14-, 18-, and 20-min emptying valve operations were all similar in magnitude and much smaller than those during filling. A table of the maximum hawser forces and the emptying times determined for each experiment is provided in Table 4 and a plot of the average maximum hawser forces versus emptying time for the valve operations tested is shown in Plate 26. The upstream longitudinal and both the upstream and downstream transverse hawser forces were similar for all valve operations tested. The downstream longitudinal hawser force was slightly higher with the 8-min emptying valve, but was still under 15 tons. It was clear that the chamber had to be modified to try and reach acceptable filling times and hawser forces.

Type 2 Chamber Design

Small deflectors (baffles) were placed across the upstream ports in the chamber to redirect the flow upstream during the filling operation. The baffles were placed on the downstream side of the ports and angled 45 degrees in the upstream direction. The vertical height above the port was 3 ft as shown in Plate 27. The baffles for each row of transverse ports were made as a solid unit and ran across (transverse) the chamber from lock wall to lock wall. This design was designated the type 2 chamber design.

Hawser forces during filling, type 2 chamber design

Water-surface and hawser force measurements were repeated with the type 2 chamber design. Typical time histories obtained with the 8-min filling valve operation are shown in Plate 28. The large upstream longitudinal hawser force observed with the original design was eliminated. The maximum hawser force was 17.1 tons and occurred on the downstream longitudinal hawser between 3 and 4 min into the filling operation. The baffles were effective in reducing the magnitude of the upstream longitudinal hawser forces measured with the original design. Table 5 provides the maximum hawser forces and the filling times determined for each experiment and a plot of the average maximum hawser forces versus filling time for the valve operations tested is shown in Plate 29. A filling time of just over 15 min was required to limit the hawser forces to 15 tons. This was a significant improvement over the original design. The water surface in the upstream half of the chamber during filling was much smoother compared to the original design. The upstream longitudinal hawser forces were essentially the same for filling valve operations between 8 and 20 min.

Valve Time, min	Hawser Forces, tons						Empty Time, min
	Longitudinal		U/S Transverse		D/S Transverse		
	U/S	D/S	Right	Left	Right	Left	
8.0	7.9	-7.5	2.0	-1.0	1.6	-1.5	16.3
	7.2	-7.1	1.2	-0.7	1.2	-0.7	16.3
	6.4	-8.3	1.3	-1.1	1.4	-0.9	16.3
Average	7.2	-7.6	1.5	-0.9	1.4	-1.0	16.3
10.0	6.8	-6.8	1.2	-1.1	1.5	-1.0	17.5
	6.1	-7.0	1.7	-1.1	1.8	-0.9	17.5
	6.4	-7.1	1.8	-1.0	1.5	-1.2	17.5
Average	6.4	-7.0	1.6	-1.1	1.6	-1.0	17.5
12.0	6.6	-5.1	2.7	-2.4	1.9	-2.0	18.8
	6.8	-5.5	2.3	-2.1	1.7	-1.8	18.0
	6.6	-5.3	1.5	-1.5	1.5	-1.6	18.4
Average	6.7	-5.3	2.2	-2.0	1.7	-1.8	18.4
14.0	6.7	-5.1	3.1	-2.1	2.0	-2.8	20.0
	6.9	-4.1	1.2	-1.0	1.0	-1.0	19.9
	6.2	-4.3	1.5	-0.8	0.9	-1.1	20.0
Average	6.6	-4.5	1.9	-1.3	1.3	-1.6	20.0
18.0	7.1	-3.7	1.4	-0.7	0.9	-1.0	21.3
	7.0	-4.3	2.8	-1.4	1.7	-2.0	21.3
	6.6	-3.6	0.9	-1.0	1.1	-0.8	21.3
Average	6.9	-3.9	1.7	-1.0	1.2	-1.3	21.3
20.0	6.5	-3.2	2.2	-1.4	1.3	-1.4	22.3
	6.4	-3.4	1.1	-0.9	1.0	-0.7	22.5
	6.2	-3.5	1.6	-1.1	1.4	-1.2	22.6
Average	6.4	-3.4	1.6	-1.1	1.2	-1.1	22.5

Hawser forces during emptying, type 2 chamber design

Hawser forces were also measured during emptying with the type 2 chamber design. Typical time histories of water-surface and hawser forces are provided in Plate 30 for an emptying valve operation of 8-min. A table of the maximum hawser forces and the emptying times determined for each experiment is provided in Table 6 and a plot of the average maximum hawser forces versus emptying time for the valve operations tested is shown in Plate 31. Valve speeds equal to or greater than 8 min did not result in hawser forces larger than 15 tons during emptying with the type 2 design chamber.

Table 5
Filling Characteristics, Type 2 Filling and Emptying System, 21.5-ft
Lift, Upper Pool EI 601.6, Lower Pool EI 580.1

Valve Time, min	Hawser Forces, tons						Fill Time, min
	Longitudinal		U/S Transverse		D/S Transverse		
	U/S	D/S	Right	Left	Right	Left	
8.0	6.5	-17.1	2.1	-2.2	1.4	-2.9	14.2
	6.2	-17.3	1.7	-2.0	1.4	-4.0	14.1
	6.0	-16.6	3.5	-3.0	1.5	-3.7	14.1
Average	6.2	-17.0	2.4	-2.4	1.4	-3.5	14.1
10.0	5.9	-14.3	2.5	-2.1	1.1	-2.9	15.2
	6.1	-14.3	3.6	-2.4	1.3	-4.1	15.2
	6.2	-13.9	2.2	-2.0	1.3	-3.0	15.2
Average	6.1	-14.2	2.8	-2.2	1.2	-3.3	15.2
14.0	6.5	-10.2	2.1	-1.1	1.3	-2.4	17.3
	6.4	-9.9	1.6	-1.4	1.0	-2.5	17.2
	6.7	-9.8	1.6	-0.9	1.4	-2.2	17.3
Average	6.5	-10.0	1.8	-1.1	1.2	-2.4	17.3
18.0	6.1	-8.4	1.8	-1.5	0.9	-2.3	19.5
	5.6	-8.5	1.5	-1.6	0.9	-1.7	19.4
	6.8	-8.4	1.9	-1.3	1.2	-2.0	19.5
Average	6.2	-8.4	1.7	-1.5	1.0	-2.0	19.5
20.0	6.4	-9.0	1.5	-1.2	0.9	-1.8	20.5
	6.6	-7.7	1.2	-1.2	0.8	-1.9	20.5
Average	6.5	-8.4	1.4	-1.2	0.9	-1.9	20.5

Plan A and Type 2 Chamber Design Hawser Forces

Comparison of the average maximum hawser forces determined during filling and emptying with the original (Plan A) and type 2 chamber designs are shown in Plates 32 and 33. The upstream longitudinal hawser forces with the type 2 chamber design were reduced significantly from those measured with the original design. The downstream longitudinal hawser forces were higher with the type 2 chamber design. The transverse hawser forces were slightly less with the type 2 chamber design. For all normal valve operations between 8 and 20 min, the transverse hawser forces were small with either design. Both the longitudinal and transverse hawser forces determined during emptying for valve operations between 8 and 20 min with both designs were less than 8.5 tons.

Table 6
Emptying Characteristics, Type 2 Filling and Emptying System,
21.5-ft Lift, Upper Pool EI 601.6, Lower Pool EI 580.1

Valve Time, min	Hawser Forces, tons						Empty Time, min
	Longitudinal		U/S Transverse		D/S Transverse		
	U/S	D/S	Right	Left	Right	Left	
8.0	5.6	-6.2	1.3	-1.0	1.0	-1.2	15.2
	5.8	-6.2	1.4	-1.4	1.3	-1.2	15.4
	6.5	-5.8	1.1	-1.4	1.5	-1.0	15.2
Average	6.0	-6.1	1.3	-1.3	1.3	-1.1	15.3
10.0	6.0	-5.0	1.7	-1.5	1.6	-1.0	16.5
	6.0	-5.8	2.4	-1.6	1.8	-1.5	16.5
	6.4	-5.5	1.0	-0.8	1.0	-0.5	16.4
Average	6.1	-5.4	1.7	-1.3	1.5	-1.0	16.5
14.0	6.2	-4.4	1.7	-1.3	1.4	-1.6	18.9
	7.0	-4.4	1.3	-1.0	1.2	-1.2	18.9
	6.2	-4.8	1.4	-1.1	1.5	-1.1	19.3
Average	6.5	-4.5	1.5	-1.1	1.4	-1.3	19.0
18.0	6.4	-3.7	1.8	-1.2	1.1	-1.7	21.6
	6.3	-3.9	1.3	-1.0	1.0	-1.4	21.3
	6.2	-4.3	1.1	-1.0	1.3	-1.2	21.3
Average	6.3	-4.0	1.4	-1.1	1.1	-1.4	21.4
20.0	7.3	-3.8	2.7	-1.6	1.6	-2.0	22.4
	6.7	-4.5	2.0	-2.3	1.6	-1.9	22.6
	5.8	-3.7	1.8	-1.2	1.0	-1.6	22.5
Average	6.6	-4.0	2.2	-1.7	1.4	-1.8	22.5

Water-Surface Differential Experiments

Experiments were performed next to measure water-surface differentials for different chamber designs. The water-surface differential represents the difference between the water level in the upper chamber and the lower chamber. Water-surface differential experiments were done because they were much faster than the hawser force experiments. Deploying the ship and measuring hawser forces each time sometimes required up to three weeks. Comparison of the water-surface differentials measured during the locking operations for different designs was used to determine the effectiveness of the design.

Comparisons were made with faster valve speeds because the water-surface differentials were larger. Plate 34 compares the water-surface differentials between the original (Plan A) and the type 2 chamber designs. A positive differential indicates the water level is higher in the upper end of the chamber and would result in a downstream longitudinal hawser force. The differential shown in Plate 34 with the Plan A design demonstrates why the large upstream longitudinal hawser forces were observed with this design. Between 2 and 8 min into the operation, a substantial negative differential or upstream hawser force occurred. Between 0.5 and 3 min, a positive differential occurred, which caused the

downstream longitudinal hawser force. A design with minimum differential and one where the resulting hawser forces do not have a dominant direction is preferred.

Type 3 Chamber Design

A modification was made to the type 2 chamber design in an effort to reduce the maximum downstream longitudinal hawser forces. A 6-in. radius was placed on the upstream edge of the baffle as shown in Plate 27. The concept was to slightly reduce the length of the baffle and to remove the sharp edge on the upstream end of the baffle. This baffle shape was designated the type 3 chamber design and a comparison of the water-surface differentials obtained with the types 2 and 3 chamber designs is shown in Plate 35. The water-surface differential measured with the type 3 chamber design was very similar to the type 2 chamber design, so no noticeable improvement was gained with this design.

Type 4 Chamber Design

The baffle design was modified by removing the solid unit that crossed the entire chamber and placing the rounded design from the type 3 chamber on each individual port. This modification was designated the type 4 chamber design and water-surface differential experiments were performed. The water-surface differential was not improved over the types 2 or 3 chamber designs. A comparison to the type 2 chamber design is shown in Plate 36. A noticeable positive differential occurred for about 1.5 min longer with the type 4 design, which would result in a longer period for downstream longitudinal hawser forces.

Type 5 Chamber Design

The baffles were removed from the downstream four rows of ports and water-surface differential experiments were performed. This modification was designated the type 5 chamber design and the water-surface differential measured with this design is compared to the type 2 design in Plate 37. The positive differential that occurred between 0.5 and 3 min was similar to the type 2 chamber design and a negative differential occurred after 3 min. This meant an upstream hawser force would occur after 3 min. Hawser force experiments were conducted next to further evaluate this design.

Hawser forces were measured with the type 5 chamber design during filling and emptying for selected valve operations. Typical time histories measured during filling with an 8-min valve are shown in Plate 38. A downstream longitudinal hawser force was observed for just over 5 min and then an upstream longitudinal hawser force was observed. Table 7 provides the results from the filling operation with the type 5 chamber design for 6-, 8-, and 10-min filling valves. Plate 39 shows a plot of the average maximum hawser forces measured with these valve operations. A filling time of 13.2 min was required to maintain

hawser forces of 15 tons. The permissible filling time was faster with the type 5 chamber design.

Table 7 Filling Characteristics, Type 5 Filling and Emptying System, 21.5-ft Lift, Upper Pool EI 601.6, Lower Pool EI 580.1							
Valve Time, min	Hawser Forces, tons						Fill Time, min
	Longitudinal		U/S Transverse		D/S Transverse		
	U/S	D/S	Right	Left	Right	Left	
6.0	13.0	-19.9	3.2	-1.2	1.4	-5.5	12.5
	12.4	-19.9	4.6	-2.3	1.2	-7.7	12.5
	12.9	-19.6	3.3	-1.1	1.7	-5.9	12.5
Average	12.8	-19.8	3.7	-1.5	1.4	-6.4	12.5
8.0	12.0	-13.1	2.2	-0.9	1.2	-5.0	13.6
	10.2	-12.8	4.5	-1.0	1.3	-7.5	13.6
	10.9	-13.6	2.4	-1.2	1.6	-4.6	13.7
Average	11.0	-13.2	3.0	-1.0	1.4	-5.7	13.6
10.0	9.0	-11.7	2.8	-0.7	0.9	-5.5	14.8
	8.0	-10.9	3.0	-0.7	1.3	-4.2	14.8
	8.1	-11.3	3.2	-1.2	1.2	-4.5	14.8
Average	8.4	-11.3	3.0	-0.9	1.1	-4.7	14.8

Typical time histories measured with the type 5 chamber design during emptying with a 3-min valve are shown in Plate 40. The maximum downstream longitudinal hawser force was 15.9 tons and occurred around 2 min into the emptying operation. Table 8 lists the hawser forces and emptying times determined with the type 5 chamber design and Plate 41 shows the plot of the average maximum hawser forces. The permissible emptying time determined with the type 5 chamber design was 12.2 min.

The type 5 chamber design performed better than the type 2 chamber design in terms of filling time and hawser forces; however, the water surface was rougher.

Types 6-9 Chamber Designs

Additional experiments were performed with a different baffling arrangement to try and improve the surface roughness observed with the previous chamber designs. A solid baffle was placed across the chamber 3 ft above all ten rows of the downstream ports. A section view of this design is shown in Plate 27 for the type 6 chamber design. The lock was filled using a 4-min filling valve with the 21.5-ft lift. The surface roughness observed above the lower ports was considerably improved with this design. The surface over the last four rows of ports in the upper end of the chamber, which did not have any baffling, was still very rough.

Table 8
Emptying Characteristics, Type 5 Filling and Emptying System,
21.5-ft Lift, Upper Pool EI 601.6, Lower Pool EI 580.1

Valve Time, min	Hawser Forces, tons						Empty Time, min
	Longitudinal		U/S Transverse		D/S Transverse		
	U/S	D/S	Right	Left	Right	Left	
3.0	6.4	-15.7	1.1	-1.7	1.0	-2.1	12.1
	6.4	-15.9	1.3	-1.0	0.9	-1.4	12.1
	6.6	-15.4	1.3	-0.9	0.8	-1.2	12.1
Average	6.5	-15.7	1.2	-1.2	0.9	-1.6	12.1
4.0	6.6	-11.9	1.5	-1.5	1.1	-1.5	12.7
	6.6	-12.1	0.8	-0.7	0.6	-1.0	12.6
	6.5	-11.9	1.2	-1.0	0.7	-1.2	12.6
Average	6.6	-12.0	1.2	-1.1	0.8	-1.2	12.6
6.0	5.9	-7.6	2.0	-1.8	2.4	-1.9	14.0
	6.1	-7.7	1.3	-1.1	1.6	-1.0	13.9
	5.9	-8.3	1.4	-1.1	1.3	-0.7	13.9
Average	6.0	-7.9	1.6	-1.3	1.8	-1.2	13.9
8.0	6.1	-6.3	3.2	-2.2	2.3	-2.3	14.8
	6.1	-7.0	1.3	-1.3	1.6	-0.9	15.0
	6.4	-6.3	0.8	-1.0	1.2	-0.8	14.9
Average	6.2	-6.5	1.8	-1.5	1.7	-1.3	14.9
10.0	6.3	-6.0	1.1	-0.7	1.4	-0.6	16.4
	6.0	-5.7	1.6	-1.0	1.7	-0.8	16.2
	6.3	-5.8	1.4	-0.8	1.5	-0.9	16.2
Average	6.2	-5.8	1.4	-0.8	1.5	-0.8	16.3

The lower baffles used with the type 6 chamber design were then placed over the last four rows of the upper ports (type 7 chamber design). The surface roughness was observed during lock filling with 4-min filling valves. The water surface above the last four rows of ports was still rough, indicating that the baffles were not effective. The jets were discharging from these ports in a downstream direction and did not have much impact with the baffles.

The baffles for the seventh row were changed to the upstream facing type (type 3 chamber design in Plate 27) and the lock was again observed during filling with a 4-min filling valve. This design was designated the type 8 chamber design. The surface roughness above the last four rows of upper ports was improved from the type 7 chamber design; however, the surface was still considered rough. The baffles placed above the ports were not effective for any of the upper ports.

The baffles used on the upper ports with the type 3 design were placed on rows 1, 2, 4, 6, 8, and 10. The jets discharging from these rows of ports would be redirected upstream and the jets discharging from the remaining rows (3, 5, 7, and 9) would be in the downstream direction. The concept was that the interaction between the jets would help dissipate energy and result in a smoother surface. This design was the type 9 chamber design. Conditions in the chamber were

observed during lock filling with a 4-min filling valve. The surface was still rougher than desired with this design. A comparison of the water-surface differentials during filling with the types 9 and 5 designs, shown in Plate 42, indicate very little difference in the water-surface conditions in the chamber between the two designs.

Type 10 Chamber Design

The baffles on the last three rows of upper ports were located as shown in Plate 43. The baffles deflected the flow downstream in an effort to reduce the magnitude of the downstream longitudinal hawser force, and to provide a smoother surface than the previous designs. The surface was observed during lock filling with 4-min filling valves and the 21.5-ft lift. The surface roughness above rows 8-10 (upper ports) was still excessive and had moved slightly downstream from the type 9 chamber design.

Type 11 Chamber Design

The last two rows of the upper ports were covered to prevent flow from discharging from these ports. The upstream facing baffles were in place for the remaining upper rows (1-8). The baffles on the lower ports remained the same as the type 10 chamber design. The water-surface differential during filling was measured with the 21.5-ft lift and the 4-min filling valves. Plate 44 compares the water-surface differential measured with the types 5 and 11 chamber designs. The upstream water-surface remained slightly higher than the downstream water-surface for the first 3 min into the filling operation and then there was very little difference in the upper and lower water levels for the remainder of filling. The filling time was 11.5 min with the 4-min valve. Hawser forces were measured next with the type 11 chamber design.

Typical time histories during filling with the type 11 chamber design and a 8-min filling valves are shown in Plate 45. The maximum downstream longitudinal hawser forces with the type 11 chamber design were increased with the 8- and 10-min filling valves compared to the type 5 chamber. The upstream longitudinal hawser forces were reduced, although with these valve operations the hawser forces were less than 15 tons for both designs. Table 9 provides the results of the hawser force measurements from the filling operation with the type 11 chamber design for 6-, 8-, and 10-min filling valves. Plate 46 compares the average maximum hawser forces measured with these valve operations and the type 5 chamber design. The permissible filling time was 14.0 min. The right transverse hawser forces were similar and the left transverse hawser forces were less with the type 11 chamber design.

Table 9
Filling Characteristics, Type 11 Filling and Emptying System, 21.5-ft Lift, Upper Pool EI 601.6, Lower Pool EI 580.1

Valve Time, min	Hawser Forces, tons						Fill Time, min
	Longitudinal		U/S Transverse		D/S Transverse		
	U/S	D/S	Right	Left	Right	Left	
6.0	8.9	-19.7	1.4	-3.7	2.4	-2.1	12.6
	6.7	-20.0	1.4	-3.6	3.4	-2.5	12.5
	6.9	-19.1	1.6	-3.1	3.8	-2.1	12.5
Average	7.5	-19.6	1.5	-3.5	3.2	-2.2	12.5
8.0	6.1	-15.9	1.1	-3.9	3.3	-2.1	13.6
	6.6	-15.3	1.3	-3.1	3.1	-2.5	13.7
	6.6	-15.9	1.4	-2.5	2.8	-2.7	13.7
Average	6.4	-15.7	1.3	-3.2	3.1	-2.4	13.7
10.0	6.1	-13.6	1.2	-2.4	1.4	-2.9	14.7
	6.4	-13.6	1.3	-2.3	2.5	-1.7	14.8
	6.6	-13.3	1.1	-2.5	2.2	-2.9	14.7
Average	6.4	-13.5	1.2	-2.4	2.0	-2.5	14.7

Hawser forces during emptying with the type 11 chamber design were also measured for 6-, 8-, and 10-min valve operations. Typical time histories measured during emptying with the 6-min valve are shown in Plate 47. The emptying time for the 6-min emptying valve was the same as for the type 5 chamber design. The hawser forces were all under 15 tons for the 6-, 8-, and 10-min valve operations.

The experiments conducted with the type 11 chamber design demonstrated that more ports were available than needed. Blocking off the last two rows of upper ports did not significantly change the filling and emptying times. The total port area, ΣA_{pi} , with the Plan A and types 2-10 designs was 800 ft² and the total area of the culverts, ΣA_{ci} , was 400 ft². The total area at the filling valves with the valves completely open was slightly over 500 ft². The port-to-culvert ratio with the Plan A and the types 2-10 chamber designs was 2. Generally, a ratio slightly less than 1 is best to maintain flow control at the ports during most of the lock operations. For the designs tested, flow control remains at the valves until the valves are opened sufficiently that control shifts to the culverts. Flow control was never established at the ports for these designs. Additional tests were made with rows of ports blocked off to determine chamber performance.

Type 12 Chamber Design

Upper rows 3, 5, 7, and 9 and lower rows 12, 14, 16, and 18 were blocked off. The upstream facing baffle was left in place on the open upper ports and the horizontal offset baffle design was used on the open lower ports as shown in Plate 48. This provided a port-to-culvert area ratio of 1.2. The water-surface differential and filling curve were determined with the type 12 chamber design during filling with 4-min filling valves. Because the water-surface differential or

filling curve were not much different from the type 11 design, hawser force experiments were conducted. The water surface was slightly rougher than observed with the type 11 chamber design, although the roughness was not considered excessive.

Typical time histories measured with the type 12 chamber design and a 6-min filling valves are Plate 49. Table 10 provides the results from the filling operation with the type 12 chamber design for 6-, 8-, and 10-min filling valves. Plate 50 shows a plot of a comparison of the average maximum hawser forces measured with these valve operations and the types 5 and 11 chamber designs. The upstream longitudinal hawser forces were similar to the type 11 chamber design and the downstream longitudinal hawser forces were slightly less than the type 5 chamber design. The transverse hawser forces were slightly lower than the other designs. The permissible filling time determined with the type 12 chamber design was 13.0 min. This was faster than both the types 5 and 11 designs.

Table 10 Filling Characteristics, Type 12 Filling and Emptying System, 21.5-ft Lift, Upper Pool EI 601.6, Lower Pool EI 580.1							
Valve Time, min	Hawser Forces, tons						Fill Time, min
	Longitudinal		U/S Transverse		D/S Transverse		
	U/S	D/S	Right	Left	Right	Left	
6.0	5.5	-16.9	2.4	-2.5	2.5	-1.9	12.6
	6.1	-16.9	1.9	-2.2	2.2	-1.5	12.6
	6.1	-16.9	1.3	-2.7	2.4	-1.8	12.7
Average	5.9	-16.9	1.9	-2.5	2.4	-1.7	12.6
8.0	6.3	-12.6	1.3	-1.7	2.0	-1.7	13.7
	6.0	-13.2	1.2	-1.6	1.8	-1.8	13.5
	4.5	-12.7	0.9	-1.7	1.5	-0.9	13.6
Average	5.6	-12.8	1.1	-1.7	1.8	-1.5	13.6
10.0	6.2	-10.1	1.4	-2.2	2.1	-2.0	14.6
	6.2	-10.1	0.8	-2.3	1.9	-0.7	14.6
	6.4	-10.1	0.7	-2.2	2.1	-1.0	14.6
Average	6.3	-10.1	1.0	-2.2	2.0	-1.2	14.6

The type 12 chamber design was the fastest filling system of those evaluated. Table 11 provides the permissible filling times for the designs evaluated using hawser forces measurements.

The type 12 chamber design was preferred over the other designs tested because the filling time met the target and fewer ports were required.

Table 11
Comparison of Permissible Filling Times with Different Filling and Emptying Designs

Design	Filling Time, min
Plan A	20.5
Type 2	15.3
Type 5	13.2
Type 11	14.0
Type 12	13.0

Hawser forces were also measured during emptying with the type 12 chamber design. Typical time histories measured with a 3-min valve operation are shown in Plate 51. The maximum downstream longitudinal hawser force exceeded 15 tons with the 2-min emptying valves. The maximum hawser forces were less than 15 tons for the remaining emptying valve operations tested. The average maximum hawser forces and emptying times determined are shown in Table 12 and a plot of this information is shown in Plate 52. The permissible emptying time determined with the type 12 chamber design was 12.4 min. This compares to 12.2 min determined with the type 5 chamber design. The permissible emptying time for the Plan A chamber design was 12.8 min. A comparison of the permissible emptying times is shown in Table 13.

Table 12
Emptying Characteristics, Type 12 Filling and Emptying System, 21.5-ft Lift, Upper Pool EI 601.6, Lower Pool EI 580.1

Valve Time, min	Hawser Forces, tons						Fill Time, min
	Longitudinal		U/S Transverse		D/S Transverse		
	U/S	D/S	Right	Left	Right	Left	
2.0	5.9	-27.3	1.1	-0.7	0.7	-1.5	12.1
	6.4	-26.6	1.3	-0.7	1.0	-1.4	11.9
	6.4	-27.0	1.3	-1.9	1.4	-1.6	11.9
Average	6.2	-27.0	1.2	-1.1	1.0	-1.5	12.0
3.0	6.3	-13.3	1.1	-0.9	0.9	-1.4	12.6
	5.9	-14.9	0.8	-0.9	0.9	-1.3	12.7
	6.1	-13.1	1.0	-0.6	0.9	-0.9	12.7
Average	6.1	-13.8	1.0	-0.8	0.9	-1.2	12.7
4.0	6.3	-10.6	1.0	-0.9	1.0	-1.0	13.1
	6.2	-11.3	1.2	-0.7	0.7	-1.4	13.1
	6.4	-11.1	1.0	-0.9	1.1	-1.2	13.1
Average	6.3	-11.0	1.1	-0.8	0.9	-1.2	13.1
6.0	5.7	-7.8	1.3	-1.4	1.2	-1.4	14.4
	5.7	-7.8	1.3	-1.4	1.2	-1.4	14.6
	6.6	-7.2	2.0	-2.1	1.2	-2.5	14.6
Average	6.0	-7.6	1.5	-1.6	1.2	-1.8	14.5

Table 13 Permissible Emptying Times	
Design	Emptying Time, min
Plan A	12.8
Type 5	12.2
Type 12	12.4

Numerical Model

The scope of work included evaluating the effect of the lock filling operation on vessels moored in the upper approach. As this work was to be performed numerically, it was started during the construction of the filling and emptying model. The numerical model LOCKSIM (Schohl 1999) was used to compute the filling characteristics for the Plan A filling and emptying design. LOCKSIM is a numerical model developed at the Tennessee Valley Authority's (TVA's) Engineering Laboratory for simulation of one-dimensional transient filling and emptying flow in navigation locks. LOCKSIM has the capability to model one-dimensional, subcritical, unsteady flow in open channels of uniform cross sections and river channels with non-uniform cross sections. The Preissmann's scheme (Cunge et al. 1980) often called the four-point weighted implicit numerical method, is used to solve the continuity and momentum equations.

A schematic representation of the Soo Lock project modeled with LOCKSIM is shown in Plate 53. The upper pool was modeled as a series of 10 river cross sections. The sections represented the changes in width encountered in upper approach channel, as shown in Plate 54. The upstream section (Xsect10) was made large (20,000 ft wide) to represent a reservoir. An invert el of 572 was used for the nine upstream sections and an invert el of 568 was used for the downstream section. The filling and emptying system was modeled by using diverging manifolds to represent the ports. The system was divided into eight culverts within the chamber and five diverging manifolds were placed in both the upstream and downstream halves of the chamber to represent the ports. Each manifold represented two ports. A schematic representation of the lock is shown in Plate 55.

Upper approach flow conditions

Initially, the conditions in the upper approach were evaluated based on the water-surface changes in the upper approach during lock filling operations. During lock filling, the water-surface near the chamber lowers as flow begins to enter the intakes and fill the chamber. This drop in water-surface causes an oscillation in the approach channel between the miter gates and the reservoir. The miter gates, the reservoir, and changes in the upper approach geometry reflect the oscillation. The water-surface elevations in the upper approach channel were computed for lock filling operations with an upper pool el of 600.7, a lower pool el of 579.2, and 2-, 3-, and 4-min valve operations. The valve operation refers to

the time required for the butterfly valves to go from closed to open at a near constant rotation. The valve curve is shown in Plate 56.

The areas between cross sections 5 and 4 and 4 and 1 were selected as likely locations for a vessel to moor during lock filling. The changes in water-surface (water-surface differential) that occurred between these cross sections during filling with 2-, 3-, and 4-min filling valves are shown in Plate 57. The positive water-surface (WS) differential indicates that the water surface at the upstream cross section is higher than at the downstream section. The largest positive differential was observed between cross sections 4 and 1 around 85 sec into the operation and the most negative differential occurred between cross sections 5 and 4 around 390 sec into the operation. Similar tendencies were seen with the 3- and 4-min valve operations.

To estimate hawser forces on a vessel moored in the upper approach between cross sections 5 and 4 and 4 and 1, the water-surface slopes were determined for the 2-, 3-, and 4-min valve operations. Neglecting the forces due to drag and inertia, assuming the ship acts as a single rigid vessel, and neglecting the effect of the vessel blockage area of the approach channel, we model the force required to hold the vessel in place as a function of water-surface slope only. The water-surface slopes were determined between cross sections 4 and 1 and 5 and 4 for filling operations with 2-, 3-, and 4-min valve operations. Plate 58 shows the slopes between cross sections 4 and 1 and indicates the steepest water surface slopes occurred with the 2-min valve. Similar results were observed for cross sections 5 and 4 also shown in Plate 58. The steepest slopes occurred between cross sections 4 and 1, indicating that hawser forces for a vessel moored in this area would be higher than for a vessel moored between cross sections 5 and 4.

Computation of the water-surface elevation during filling is helpful for the physical model operations. The model can be operated to simulate the drawdown in the upper approach during filling by adjusting the discharge spilled over the constant head weirs prior to model filling operations. The water-surface elevations for cross sections 1-4 during filling with 2-, 3-, and 4-min valve operations are shown in Plate 59. The maximum drop below the upper pool occurred with a 2-min filling valve at 95 sec into the operation at cross section 1 and was 1.3 ft below the upper pool. The maximum rise above the upper pool also occurred with the 2-min valve. The water surface reached 0.85 ft above the upper pool between 6 and 7 min into the filling operation. Water-surface elevations computed during filling for the 3- and 4-min valve operations are shown in Plate 59. The lowest drop in water-surface occurred at cross section 1 for both the 3- and 4-min valves and was 1.1 ft below the upper pool el.

The initial computations using the LOCKSIM model were done before the physical model results were obtained. The coefficients for the components of the Plan A filling and emptying system were refined slightly, based on the filling and emptying times determined from the physical model results. The water surface elevations, slopes, and differentials determined for the cross sections in the upper approach showed no noticeable changes using the newer coefficients. With a 2-min filling valve, the maximum difference in the water surface elevation at cross section 1 was 0.07 ft. The initial results determined from the LOCKSIM model

were considered valid and representative of the Plan A filling and emptying system.

The numerical simulations of the water-surface elevations in the upper approach show that the water surface fluctuates during the filling operation. The water level near the lock drops below the upper pool el during the initial filling operation and then tends to fluctuate below and above the upper pool el for several min after the filling valves have completely opened. The amount the water level fluctuates around the upper pool el depends on the valve opening speed. The faster the valve opening time is, the greater is the deviations from the upper pool. Closer to the lock (say between cross section 4 and 1), the duration of the drop in the water surface approximates the valve opening time. During this time, a vessel between cross sections 4 and 1 would tend to move toward the lock. Farther upstream from the lock (between cross section 5 and 4) the duration of the water surface drop is slightly longer than the valve opening time, although the magnitude of the drop is less.

Lower approach flow conditions

LOCKSIM simulations were also performed to determine flow conditions in the lower approach during lock emptying. Immediately below the miter gates, the flow is highly 3-dimensional because of the discharge from four separate outlets and the impact of the jet flow on the lower bulkhead sill. The jet impacts the lower bulkhead sill and is redirected toward the surface, which causes water-surface bulking as described in the outlet experiments. The area farther downstream was the focus of this investigation. Four cross sections were established in the lower approach at the locations shown in Plate 60. If a ship moors in the lower approach, it would likely be between cross sections 12 and 13 or 13 and 14. The water-surface elevations during lock emptying were determined in these areas for 2-, 3-, and 4-min valve operations.

The changes in water-surface (water-surface differential) that occurred between these cross sections during filling with 2-, 3-, and 4-min filling valves are shown in Plate 61. The positive water-surface (WS) differential indicates that the water surface at the upstream cross section is higher than at the downstream section. The largest positive differential was observed with the 2-min emptying valve between cross sections 12 and 13 around 2 min into the operation. The most negative differential observed between cross sections 12 and 13 occurred just after 3 min into the operation. The water-surface differentials were less for the 2- and 3-min emptying valve operations.

The water-surface slopes were determined between cross sections 12 and 13 and 13 and 14 for emptying with 2-, 3-, and 4-min valve operations. Plate 62 shows the slopes between cross sections 12 and 13 and indicates that the steepest water surface slopes occurred with the 2-min valve. Similar results were observed for cross sections 13 and 14, also shown in Plate 51. The steepest slopes occurred between cross sections 12 and 13, indicating that hawser forces for a vessel moored in this area would be higher than for a vessel moored between cross sections 13 and 14. These forces would change direction during the emptying operation. For example, if a vessel were moored in the area between cross

section 12 and cross section 13, and a 2-min valve was used to empty the lock, a downstream longitudinal hawser force would occur for the first 2.5 min and then an upstream longitudinal hawser force would occur between 2.5 and 4 min. The direction of the force changes back and forth during the emptying operation because of the reflections of the gravity waves. The energy in the waves eventually dissipates.

The results of the LOCKSIM simulations for the lower approach show that a vessel moored downstream from cross section 13 (just over 1,800 ft from the lower gates) should not experience high hawser forces during lock emptying. If a vessel is moored between the lock and cross section 12 during emptying, the hawser forces will be higher, especially for faster emptying valve operations. The calculations used to determine water-surface slope do not take into account the effects of the vessel, wind, and ice. If the vessel moors downstream from cross section 12, the vessel effects should be small. If wind or ice, or both, are extreme, additional analyses may be needed to help quantify the increased hawser forces.

Ice Passage Investigations

To eliminate the upper dead zone and provide full culvert flow for flushing ice from the lock chamber, large valved ports were constructed in the roofs of the model culverts, just downstream of the upper miter sill (Figure 3f). Similarly, to minimize the size of the lower dead zone while drawing ice into the lock, valved ports were located in the culvert roofs 100 ft upstream of the lower miter gates (Figure 3g). Details of the ice valves are shown in Plates 5 and 6. Initial tests were performed with the large valved ports.

Additional tests examined the ice flushing performance of ports in the upper miter gates, based on similar systems at St. Lawrence Seaway locks and also the existing Poe Lock at the Soo. A final series of tests examined upper approach ice accumulation near the intakes. During lock filling, water currents can draw ice against the upper miter gates, making them difficult to open. Owing to their proximity to the gates, through-the-sill intake designs are particularly susceptible to this problem. A high-flow air curtain was also tested as a means of retaining ice upstream of the intakes, preventing its interference with the miter gates.

All ice tests used the Type 12 chamber design with a port-to-culvert-area ratio of 1.2 and upstream-facing baffles on the upper ports (Plate 48). With a 7-min valve, filling time was 13 minutes and emptying time was 12.7 min with a 3-min valve.

Three groups of ice passage tests were conducted. The first two test groups drew ice into the lock (Figure 7) and flushed it from the lock chamber (Figure 8). These relate to ice lockage performance. The third group of tests examined ice accumulation in the upper approach near the culvert intakes during lock filling (Figure 9). For each test group and condition, open water surface velocity distributions were measured as well as total culvert discharge. Initial and final ice surface extent and thickness were documented, as well as the timing and progression

of ice movement during the tests. Unless otherwise specified, all lengths, velocities, discharges, and times are reported in prototype units.



Figure 7. Test drawing ice from upstream approach into lock chamber viewed from upstream



Figure 8. Test flushing ice from lock chamber viewed from downstream



Figure 9. Upper approach ice accumulation test

Drawing ice into the lock chamber

Two ice drawing cases were tested, first with the lock at high pool, the upper miter gates open, and the culvert emptying valves fully opened. Conditions for the second case were the same, except the lower ice valves were opened, increasing surface water velocities in the upper portion of the lock chamber as shown in Figure 10. Each case was repeated for consistency. Figure 11 shows the position of the downstream edge of the ice accumulation vs. time as the ice moved into the lock chamber. A significant difference is that, for the lower ice valve case, the ice front progressed at a nearly constant rate until contacting the lower miter gates, while in the emptying valve case, the ice front slowed to a stop about 150 ft upstream of the lower miter gates. The two cases produced maximum discharges in the lock chamber at 15,480 and 17,120 cfs, respectively. For both cases, final ice accumulation thickness in the lock chamber ranged from 1.25 to 2.0 ft from downstream to upstream.

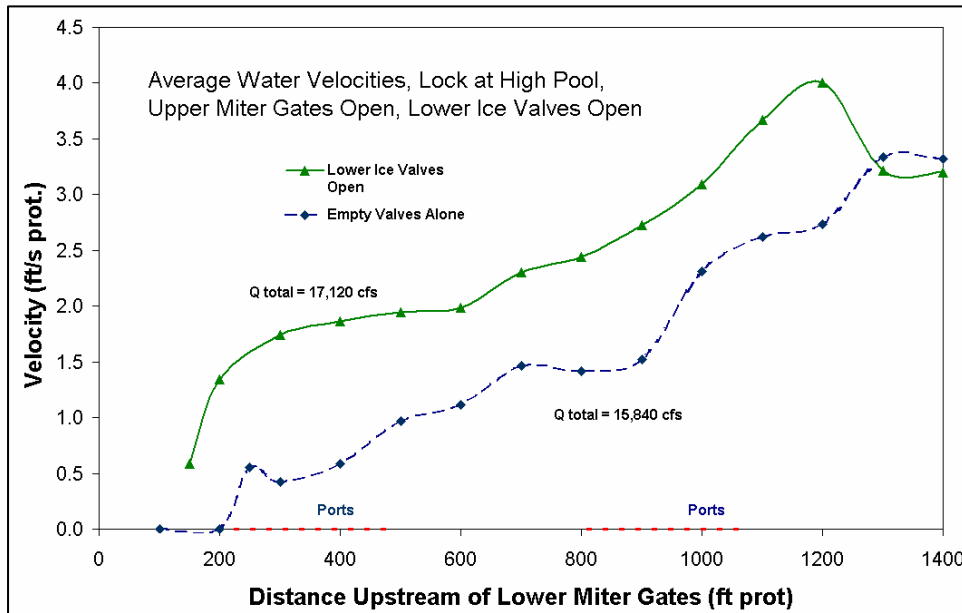


Figure 10. Surface water velocities for ice drawing tests

Flushing ice from the lock chamber

Four ice flushing cases were tested, with the lock at low pool and the lower miter gates open. The first case used fully open filling valves and, in the second case, the upper ice valves were opened to create water currents for ice flushing (Figure 12). A third test examined the ice moving effect of six 4-ft-diameter manifolds installed at the upper miter gates at the low pool level (Figure 13). Figure 14 shows longitudinal surface water velocity profiles for the three ice flushing cases.

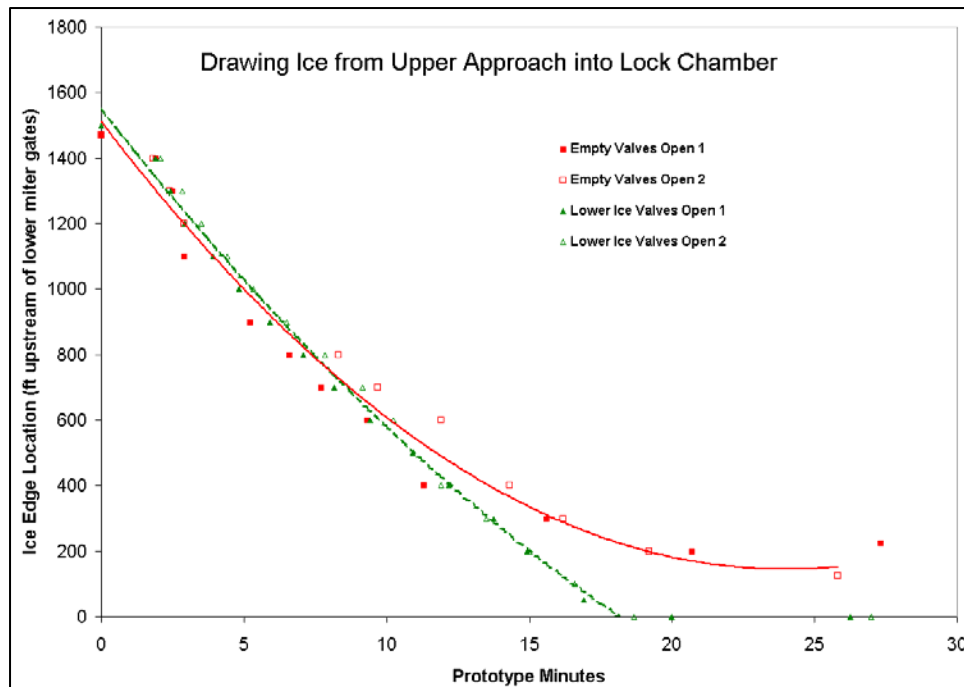


Figure 11. Ice edge position while drawing ice into lock

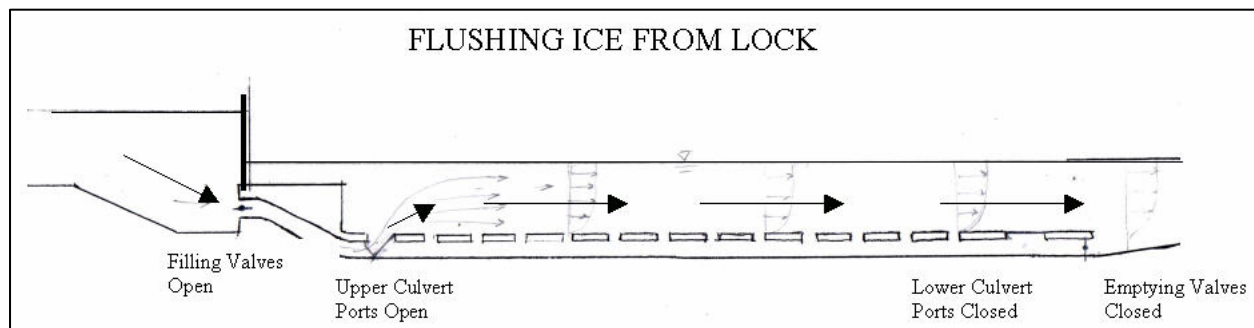


Figure 12. Longitudinal section showing use of upper ice valve to increase water currents out of the lock chamber

At the start of the ice flushing tests, ice covered the lock chamber surface from the upper miter gates to within about 200 ft from the lower miter gates, with an average accumulation thickness of 2.0 ft. Figure 15 plots percent ice coverage vs. time as the tests progressed.

Using only the filling valves (10,360 cfs), the ice mass tended to pull apart near the downstream end and move out in about 20 minutes. An interesting result is that all the ice moved out and no ice remained in the upstream dead zone, as is commonly the case with ice flushing using only filling valves. This better-than-average ice flushing performance could be the result of the upstream facing baffles on the upstream filling and emptying ports.



Figure 13. Manifolds in upper miter gates to create surface currents for ice flushing

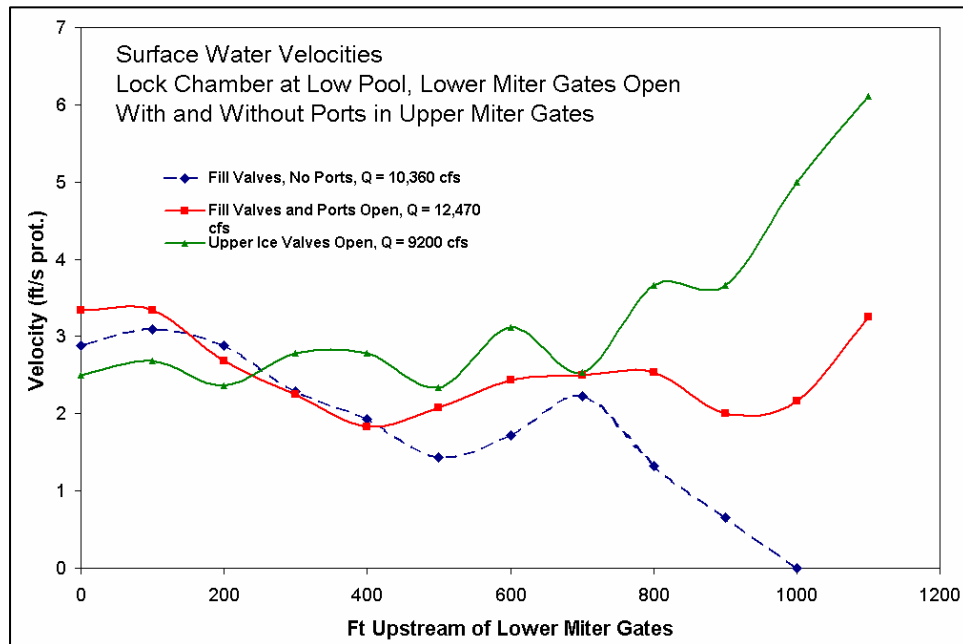


Figure 14. Surface water velocities for ice flushing cases

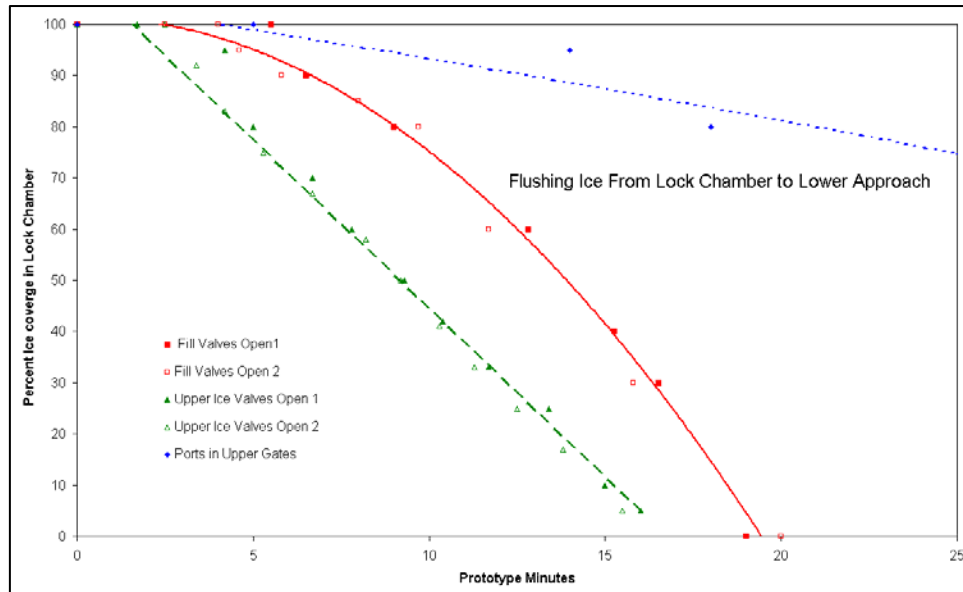


Figure 15. Percent ice coverage vs. time for ice flushing cases

In the upper ice valve case (9,200 cfs), the ice mass, rather than pulling apart and progressively moving out from the downstream end, compressed at the upstream end and moved out as one slug, in about 16 min. As a final case, the ice was flushed from the chamber using only flow from the manifolds in the gates, requiring an average time of 77 min.

Ice accumulation near culvert intakes

A series of tests documented ice movement in the upper approach during lock filling. The model lock has 4 butterfly-valve-controlled through-the-sill intakes located about 20 ft upstream of the gate miter. As an initial condition, a boom retained a 1.5- to 2.0-ft-thick ice accumulation upstream of the bullnose about 300 ft from the miter gates. The boom was removed just before starting the fill, allowing the ice to drift towards the intakes.

Figure 16 plots centerline surface water velocity vs. distance upstream of the miter gates during lock filling. Note the decrease in surface velocity from a maximum of about 2 to 0 ft/sec at the gates. In spite of this deadzone, which results from the intake location near the channel bottom, the ice is drawn in contact with the miter gates by about 2.5 minutes after the valve opening (Figure 17).

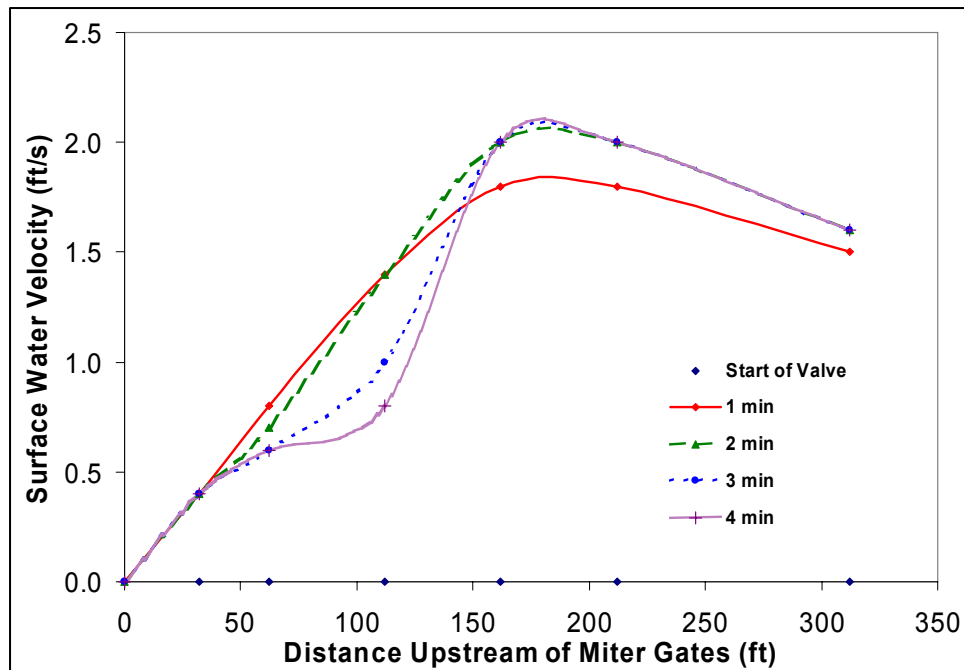


Figure 16. Upper approach centerline surface water velocity profiles during lock filling

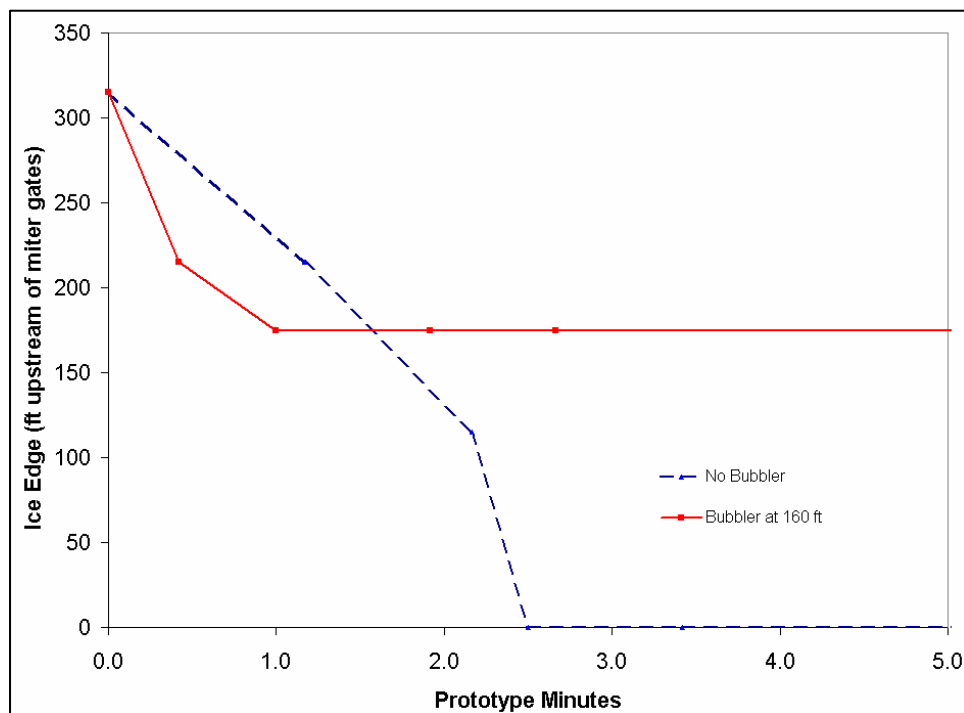


Figure 17. Position of upper approach ice edge vs. time during lock filling

A 110-ft-long high flow air curtain was placed across the upper approach 120 ft upstream of the miter gates (Figure 18). At a model airflow of 4.4 standard cubic ft/min per ft (SCFM/ft), the air curtain produced diverging flow fields with surface velocities on the order of 0.4 to 0.5 ft/sec (model). Figure 19 plots the

CHL average surface water velocity vs. airflow per unit width, along with data from lab experiments at CRREL and field measurements. Extrapolation of the data in Figure 19 indicates that a 110-ft-long high flow curtain at the New Soo Lock, supplied by a 1500 cfm compressor, would create prototype surface flows of about 2 ft/sec and likely prevent ice from being drawn into contact with the upper miter gates during lock filling.



Figure 18. High-flow air curtain retaining upper approach ice during lock filling

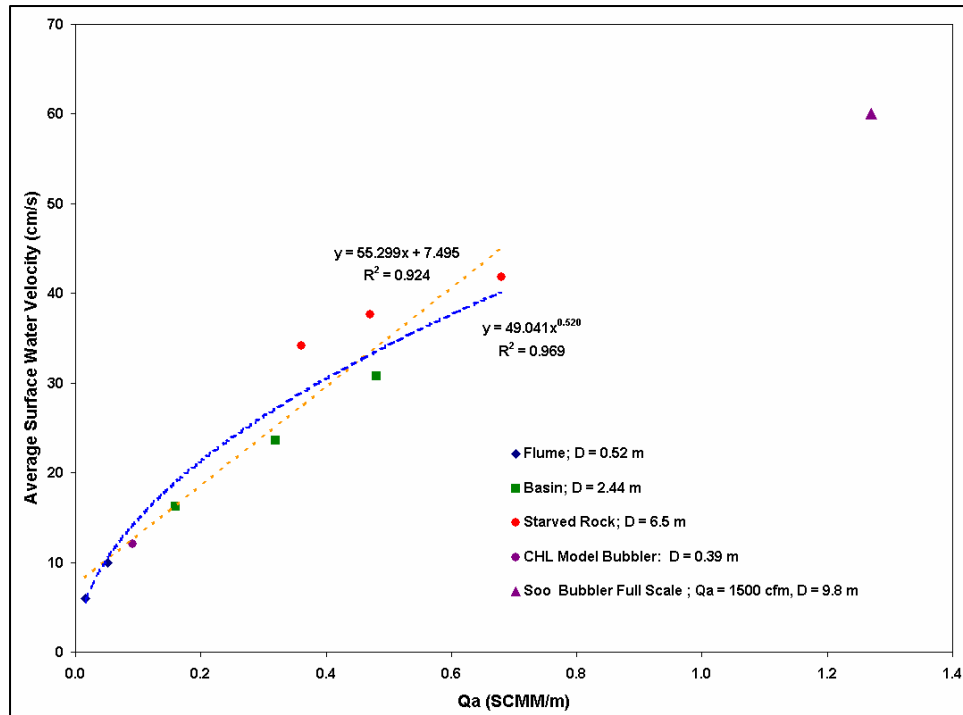


Figure 19. Average surface water velocity vs. unit airflow to the bubbler diffuser

Ice lockage times for the new Soo Lock model compared with average times observed at the existing Poe Lock are shown in Table 14.

Table 14 Comparison of Ice Lockage Times			
Operation	New Soo Lock using Ice Valves	New Soo Lock using F/E Valves	Existing Poe Lock using F/E Valves
Draw ice into chamber	17	23	25
Close upper miter gates	1	1	1
Lower chamber	13	13	12
Open lower miter gates	1	1	1
Flush ice from chamber	13	19	25
Close lower miter gates	1	1	1
Raise chamber	13	13	13
Open upper miter gates	1	1	1
Open water lockage time	30	30	34
Ice drawing/flushing time	30	42	50
Total ice lockage time	60	71	84

Additional Intake and Outlet Experiments

Additional intake and outlet experiments were conducted in an effort to improve the performance of these components.

Type 6 intake design

The type 6 intake design consisted of a ported roof 3 ft thick beginning at the downstream edge of the upper bulkhead sill and ending at the face of the intakes as shown in Plate 63. A total of 50 ports, each 5 ft square, was located in the roof above the intake. The ports would help spread the flow more evenly in the upper approach and reduce the strength of the vortices during lock filling. Experiments were conducted with 3-, 5-, and 8-min valve operations to document vortex formation in the upper approach and three tests were conducted for each valve operation (Plate 64). The vortex strength was reduced from that observed with the type 5 intake design. Typically, type 2 vortices formed on the right side of the approach with the 3- and 5-min valve operations. The maximum strength vortex observed on the left side of the approach was a type 2. A type 4 vortex was observed on the right side in one of the three experiments conducted with the 8-min valve operation and in the other two experiments the maximum strength on the right side was a type 1. Minimal vortex activity was observed on the left of the approach with the 8-min valve operation.

The permissible filling time determined with the type 6 intake design was 14 min. This is slightly slower than the 13.0 min determined with the type 5 intake and type 12 chamber. The ported area caused slightly more intake losses.

Type 7 intake design

The port shape with the type 6 intake design was changed from square to circular (Plate 65). The number of ports remained the same (50) and the radius of each port was 2.87 ft, which provided the same area per port as the 5-ft square ports. Similar vortex formation was observed with the round ports using 3-, 5-, and 8-min valve operations (Plate 66). Typically, type 2 vortices formed on the right side of the approach and weaker vortices formed on the left side. The maximum vortex observed in all experiments was a type 3 and occurred twice in one of the three experiments with the 3-min valve operation. The permissible filling time determined with the type 7 intake design was 14 min (Table 15).

Table 15 Comparison of Permissible Filling Times with Different Intake Designs, Upper Pool EI 601.6, Lower Pool EI 580.1	
Design	Filling Time, min
Plan A	20.5
Type 5 Intake and Type 12 Chamber	13.0
Type 6 Intake and Type 12 Chamber	14.0
Type 7 Intake and Type 12 Chamber	14.0
Type 6 – Square Ports, Type 7 Round Ports	

Types 2 and 3 outlet designs

The type 2 outlet design consisted of a ported roof section 3 ft thick that began at the downstream end of the outlet and ended at the upstream edge of the lower bulkhead. A total of 60 ports, each 2 by 2.5 ft, was located as shown in Plate 67. The total port area in the roof was 300 ft² compared to an area of 576 ft² at the outlet. Significant bulking was observed with the original design outlet and the ported roof section was developed with the thought of suppressing the bulking and distributing the outlet flow over a larger area. The maximum rise in water surface over the lower pool el measured with the type 2 design is shown in Table 16. No significant improvement was observed with the type 2 outlet design.

Table 16 Outlet Experiments, Types 2 and 3 Outlet Designs, Upper Pool EI 601.6, Lower Pool EI 580.1			
Valve Operation, min	Location	Maximum Rise in WSEL, ft	
		Type 2 Outlet	Type 3 Outlet
3	Right Wall	2.1	1.7
5	Right Wall	1.6	1.8
8	Right Wall	1.8	1.5

The port shape in the roof was changed from square to circular as shown in Plate 68 for the type 3 design outlet. A total of 60 ports, each with a 1.25 ft radius, was placed in the roof. The maximum rise in water surface over the lower pool el measured with the type 2 design is shown in Table 16. No improvement was observed from the original or type 2 design outlets. Table 17 lists the permissible emptying times determined for the type 2 and 3 outlet designs, along with the original design outlet (Plan A). The emptying times were approximately 30 percent slower with the types 2 and 3 outlet designs. These slower emptying times were considered unsatisfactory.

Table 17 Permissible Emptying Times, Upper Pool EI 601.6, Lower Pool EI 580.1	
Design	Emptying Time, min
Plan A Chamber	12.8
Type 5 Chamber	12.2
Type 12 Chamber	12.4
Type 2 Outlet and Type 12 Chamber	16.2
Type 3 Outlet and Type 12 Chamber	16.1
Type 4 Outlet and Type 12 Chamber	13.3

Type 4 outlet design

The rectangular ports with the type 2 outlet design were increased in size to 4 by 5 ft to form the type 4 outlet design shown in Plate 69. The number of ports

remained at 60. This provided a total ported area in the roof of 1,200 ft². This provided more than twice the area than the existing area at the outlet. Table 18 provides the maximum rise in water surface above the lower pool for emptying valve operations of 2, 3, 4, and 8 min. The maximum rises in water surface ranged from 1.5 to 2.4 ft, which was similar to those determined with the previous designs. The permissible emptying time was 13.3 min as listed in Table 17. This was slightly slower than the original outlet with the type 12 chamber (12.4 min), but faster than the types 2 and 3 outlets. The outlet conditions were improved slightly from the original design in that the bulking was spread more evenly over the lower approach, even though the maximum values of water surface rise were similar.

Table 18 Outlet Experiments, Type 4 Outlet Design, Upper Pool EI 601.6, Lower Pool EI 580.1		
Valve Operation, min	Location	Maximum Rise in WSEL, ft
2	Left Side	2.0
	Center	2.0
	Right Side	2.3
3	Left Side	2.1
	Center	2.2
	Right Side	2.1
4	Left Side	2.3
	Center	2.4
	Right Side	2.3
8	Left Side	1.8
	Center	2.0
	Right Side	1.5

4 Conclusions and Recommendations

Lock Filling and Emptying System

The lock chamber performance was evaluated for the 12 different chamber designs to try and achieve acceptable filling and emptying times and avoid excessive surface roughness during filling. Large upstream longitudinal hawser forces were measured with the Plan A design during filling. These large forces were caused by the dominant downstream direction of the jets issuing from the upper ports in combination with the longitudinal seiching of the water surface. A 20-min filling valve operation was required to keep hawser forces from exceeding 15 tons. This type of operation maintained flow control at the filling valves and reduced the flow into the chamber sufficiently to prevent large forces. Maintaining flow control at the valves defeats the purpose of a properly designed filling and emptying system. If a filling time of 20 min was acceptable, the entire filling system could be downsized to give the same performance as a large system controlled by the filling valves. Excessive surface roughness was also observed during filling with the Plan A design.

A variety of baffling arrangements was investigated next to try and reduce the permissible filling time and surface roughness. Any baffling placed on the lock floor would reduce the clearance to the bottom of the vessel, so the height of the baffles was kept to a minimum. The upstream facing baffles placed on the downstream side of the upper ports worked very well to redirect the jets discharging from the upper ports and keep a more balanced water level in the chamber during filling. The largest hawser forces measured using the upstream facing baffles were now in the downstream direction and were significantly lower than those measured with the Plan A chamber design. The permissible filling time was reduced by more than 5 min. The upstream baffles were modified slightly by rounding the upstream end and placing the baffles on each individual port rather than having them span the entire chamber downstream from each row of ports. The downstream longitudinal hawser forces were still the largest measured with this design (the type 4 chamber design) and further attempts were made to better distribute the flow entering the chamber during filling. The type 5 chamber design accomplished a better flow distribution; however, the surface roughness at both ends of the chamber was excessive.

The flow distribution and surface roughness were then evaluated with baffling on the lower end of the chamber and by removing some of the ports. The type 12 chamber design, which consisted of upstream facing baffles on the upper ports, offset horizontal baffling on the lower ports, and 40 percent of the ports removed was the best design evaluated and, without additional testing would be the recommended design. The permissible filling time met the target filling time of 13 min and the surface roughness was not excessive. The permissible emptying time, 12.4 min, was longer than the desired time of 10 min. The port and culvert configuration would need to be changed to reduce the permissible emptying time to 10 min. A larger culvert would be necessary. The 10 min target time for emptying was based on the current operation at the Poe Lock. The Poe Lock has a split lateral filling and emptying system, which is more hydraulically efficient than the longitudinal culvert system. This system has culverts in each lock wall that are 17 ft high by 13 ft wide and provide more culvert area than the new Soo Lock design.

Additional testing of the filling and emptying ports is recommended to try and develop an angled port design for the upper ports and a baffled design for the lower ports. The new port design, if successful, would eliminate the baffling placed on the lock floor that was necessary with the type 12 chamber design. The new port would be designed to redirect the jet discharging from the upper ports in an upstream direction. This may be difficult to accomplish as the port thickness is only 3 ft. The lower ports would be designed to include a horizontal baffle to break up the vertically discharging jet and reduce the surface roughness. If these additional tests are performed, results will be published as an appendix to this report.

The experiments performed on the intake showed that vortices form on both sides of the upper approach during lock filling. These vortices were stronger than desired with the original design intake. Several modifications were evaluated to try and reduce the vortex strength. Entrance conditions were improved by facing off the intakes to eliminate the borda effects and adding vanes to separate flow into each intake (type 5 intake design). The vortex strength was further reduced by placing a ported roof between the downstream side of the upper bulkhead sill and the intake face (type 6 intake design). This design spread the inflow over a larger area in the upper approach. The intake losses were slightly higher resulting in a permissible filling time 1 min longer than the type 5 intake design with the type 12 chamber design. Without any additional testing, the type 6 intake would be the recommended design. As horizontally mounted trashracks will be needed with this design, a method to clean these trashracks must be developed.

The outlet flow conditions with the original design were quite rough looking. The flow discharging from each of the culvert outlets struck the lower bulkhead sill and was directed toward the water-surface. Surface upwelling or bulking was observed in four distinct locations in the lower approach and was most noticeable along the lock walls. No excessive bulking was observed on the downstream side of the lower miter gate. A ported roof was placed over the outlet area between the outlets and the upstream side of the lower bulkhead sill to spread the outlet discharge over a larger area. The type 4 outlet design spread the flow better than the types 2 or 3 outlets. The maximum rise in water surface above the lower pool level during emptying operations was similar for all designs. Without additional

testing, the type 4 outlet design would be the recommended design. The area in the vicinity of the outlets needs to be lowered and baffle blocks could then be used to help dissipate the energy of the outlet flow. Also, moving the lower bulkhead sill farther downstream would provide more area for energy dissipation.

In summary, without any additional testing to further improve the performance of the filling and emptying design, this study recommends the type 6 intake, the type 12 chamber, and the type 4 outlet designs. It is recommended that additional tests be conducted to evaluate the hydraulic performance of angled ports for the upper chamber ports and baffled ports for the lower chamber ports.

Upper and Lower Approach Flow Conditions

The results from the numerical model simulations in the upper approach during lock filling showed that the largest hawser forces for a ship moored in the upper approach would occur in the area from the upper pintle to approximately 1,200 ft upstream and would be higher with fast valve speeds. Vessels moored within 1,200 ft of the upper lock pintle will be drawn toward the lock for a period during lock filling roughly equivalent to the valve opening time. Vessels moored in the lower approach greater than 1,800 ft from the lower gates should not experience significant hawser forces during lock emptying. These numerical results do not take into account the effects of the vessel, wind, or ice.

Ice Investigations

Table 10 compares ice lockage times for the new Soo Lock model with average times observed at the existing Soo Poe Lock. In all cases, no extra time was included to clear ice for miter gate operation. Based on the model test results, total ice lockage times were 71 and 60 min, respectively, for the filling and emptying valve and ice valve cases. This compares to an observed ice lockage at the Poe Lock that required 84 minutes on 30 March 2002. As a point of reference, based on observations at Mel Price Lock on 8 January 2002, an ice quantity equivalent to a conventional ice lockage can be passed over a vertical lift gate and sluiced through a 1,200-ft-long lock chamber in about 10 minutes.

Ice drawing

Model test results indicate that the lower ice valves will decrease the time required to draw ice into the chamber by 5 min (from 23 to 17 min). Use of the lower ice valve brought the ice directly into contact with the lower miter gates, while use of the emptying valves drew the ice to within 150 ft of the lower miter gates. Although the ice valve brought the ice farther into the lock, having the ice in direct contact with the lower miter gates would interfere with their operation.

Ice flushing

Use of the upper ice valves decreased ice-flushing time by 4 min (from 19 to 15 min). Both times are less than the observed time for the Poe Lock of 25 min. Based on the model ice flushing tests using the filling valves, the type 12 chamber design with its upstream facing baffles appears to be more effective for ice flushing than the split bottom lateral system of the existing Poe Lock which, used by itself, is incapable of clearing ice from the upper third of the chamber. In terms of ice flushing performance, the upper ice valves were about equal to the combined use of filling valves and the manifolds in the upper miter gates.

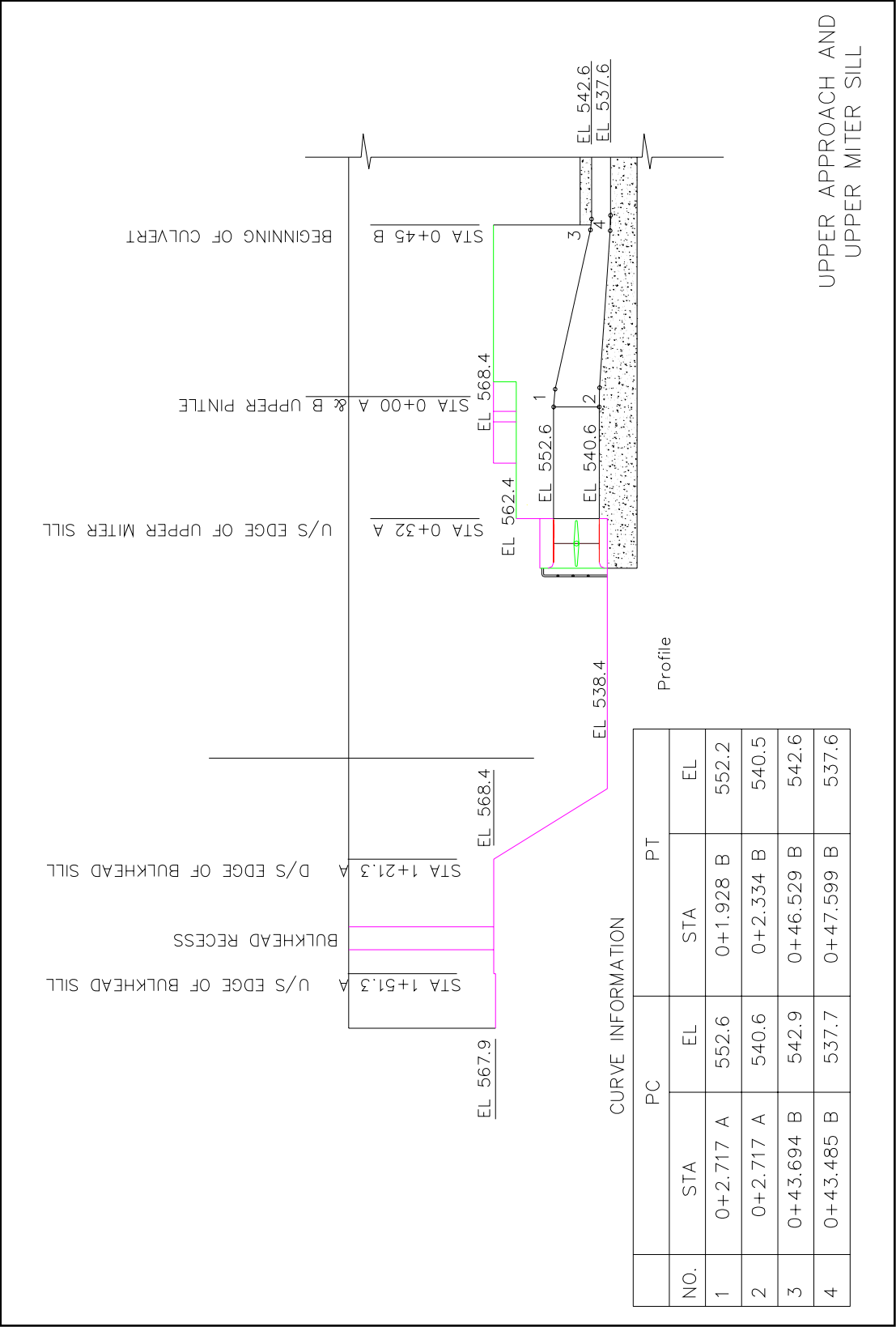
Upper approach ice accumulation near intakes during lock filling

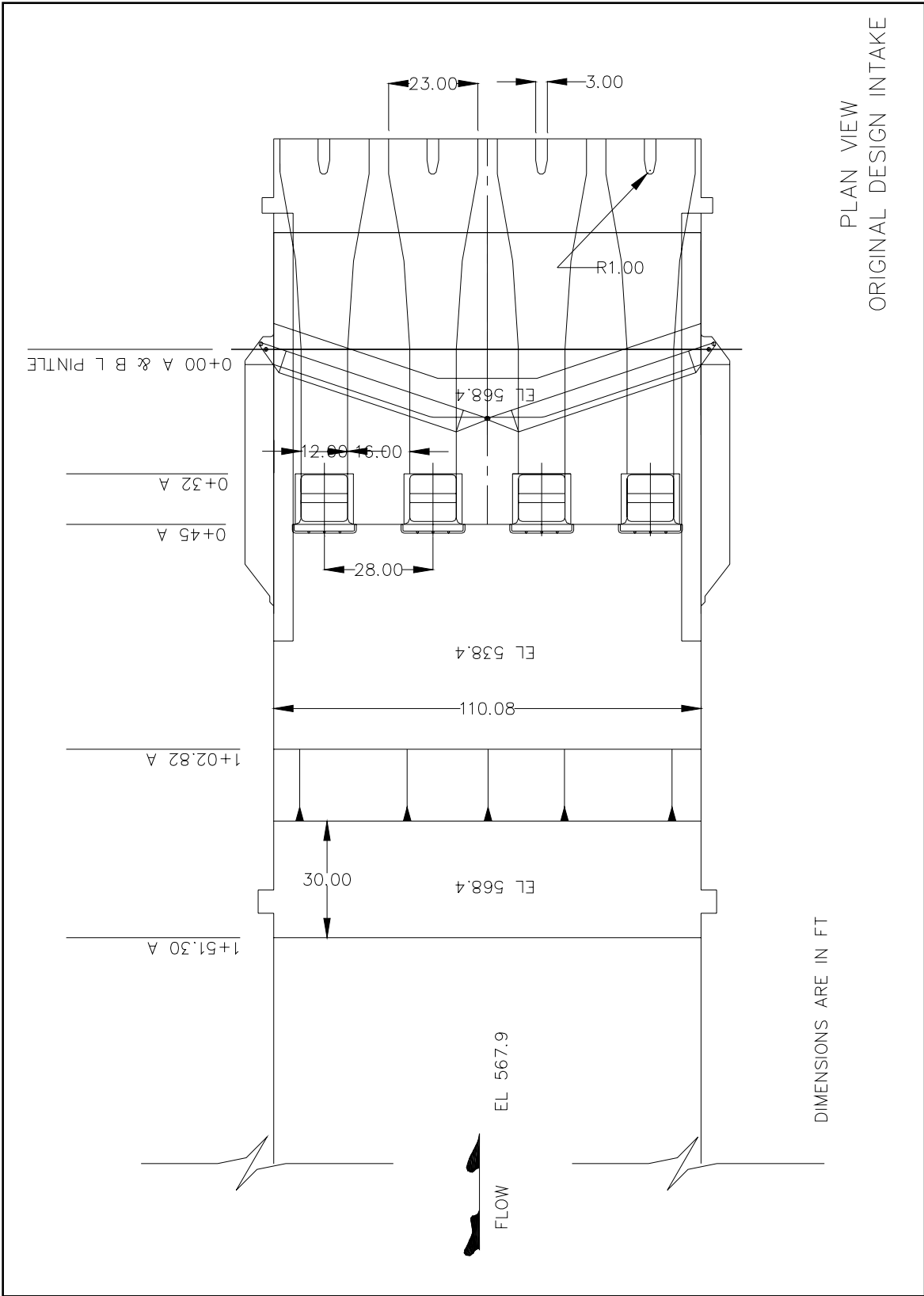
The surface water currents created by the through-the-sill culvert intakes drew ice directly in contact with the upper miter gates, which would make them difficult to open. A high flow air curtain located 120 ft upstream of the miter gates prevented this ice from reaching the gates. To create an upstream flow field sufficient to negate the downstream currents created by lock filling would require a compressor capacity of 1,500 cfm. Strong downstream-blowing winds would probably render the air curtain ineffective, however.

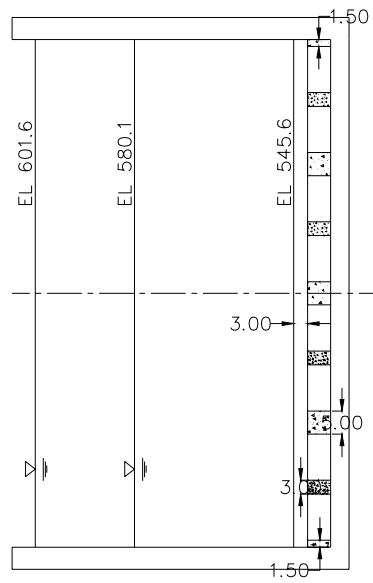
References

- Cunge, J. A., Holly, F. M., Jr., and Verway, A. (1980). "Practical aspects of computational river hydraulics," Pittman Publishing, Boston, MA.
- Davis, J. P. (1989). "Hydraulic design of navigation locks" Miscellaneous Paper HL-89-5, U.S. Army Engineer Waterways Experiment Station, Vicksburg, MS.
- Headquarters, U.S. Army Corps of Engineers. (1995). "Hydraulic design of navigation locks," EM 1110-2-1604, Washington, DC.
- Pickett, E. B. and Neilson, F. M. (1988). "Lock hydraulic system model and prototype study data," Miscellaneous Paper HL-88-1, U.S. Army Engineer Waterways Experiment Station, Vicksburg, MS.
- Vennard, J. K., and Street, R. L. (1982). *Elementary fluid mechanics*, 6th edition, John Wiley and Sons, New York.
- Schohl, G. A. (1999). "User's manual for LOCKSIM: Hydraulic simulation of navigation lock filling and emptying systems," Contract Report CHL-99-1, U.S. Army Engineer Waterways Experiment Station, Vicksburg, MS.

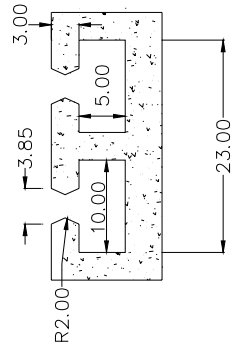
Plate 2



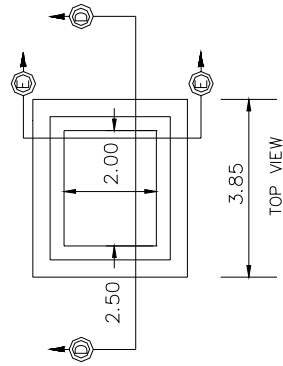




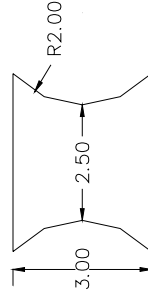
SECTION



SECTION THROUGH CENTER OF PORT

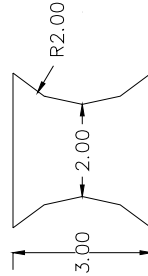


TOP VIEW



SECTION D-D

PORT DETAILS



SECTION E-E

CULVERT AND PORT DETAILS

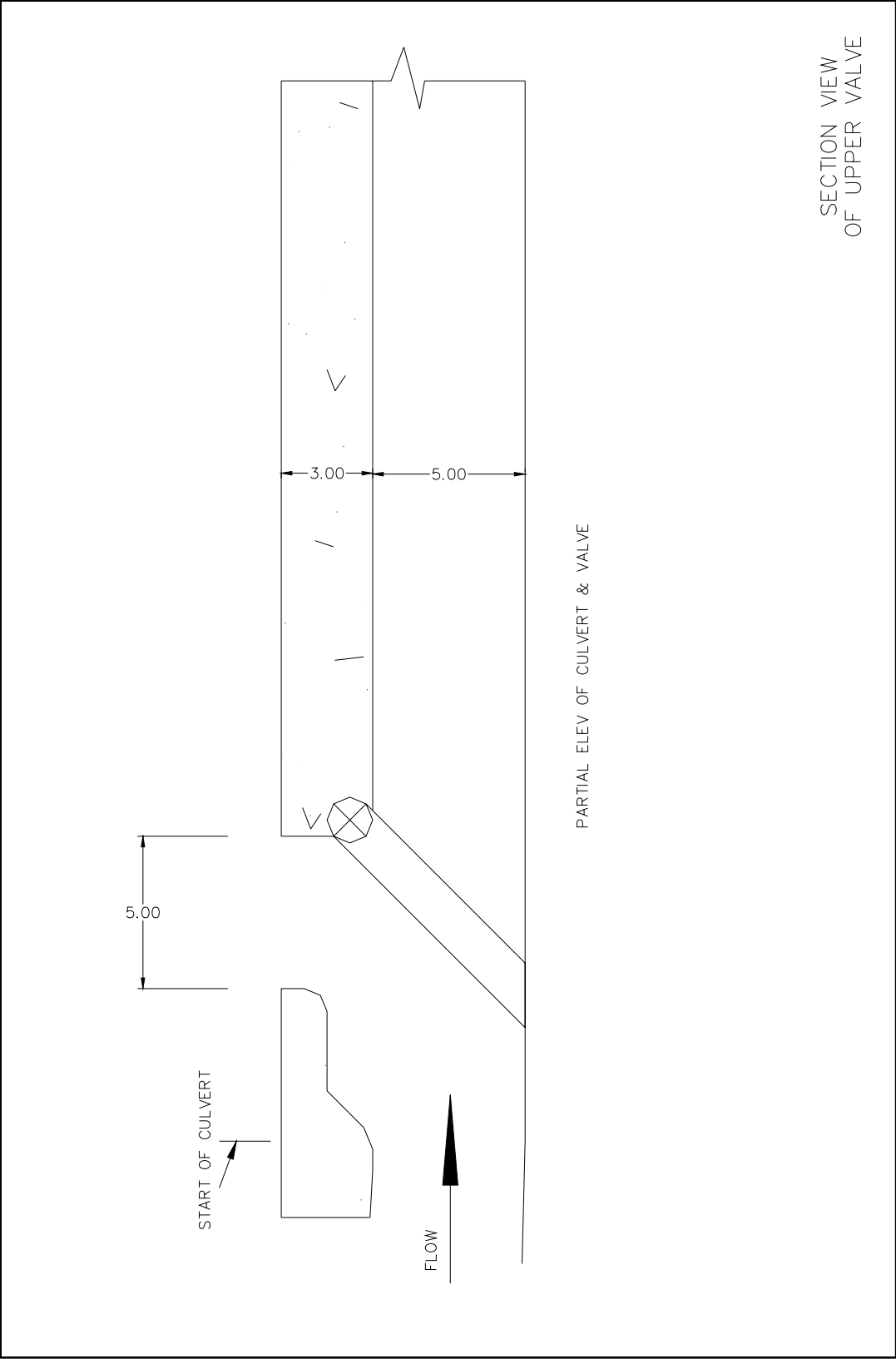


Plate 5

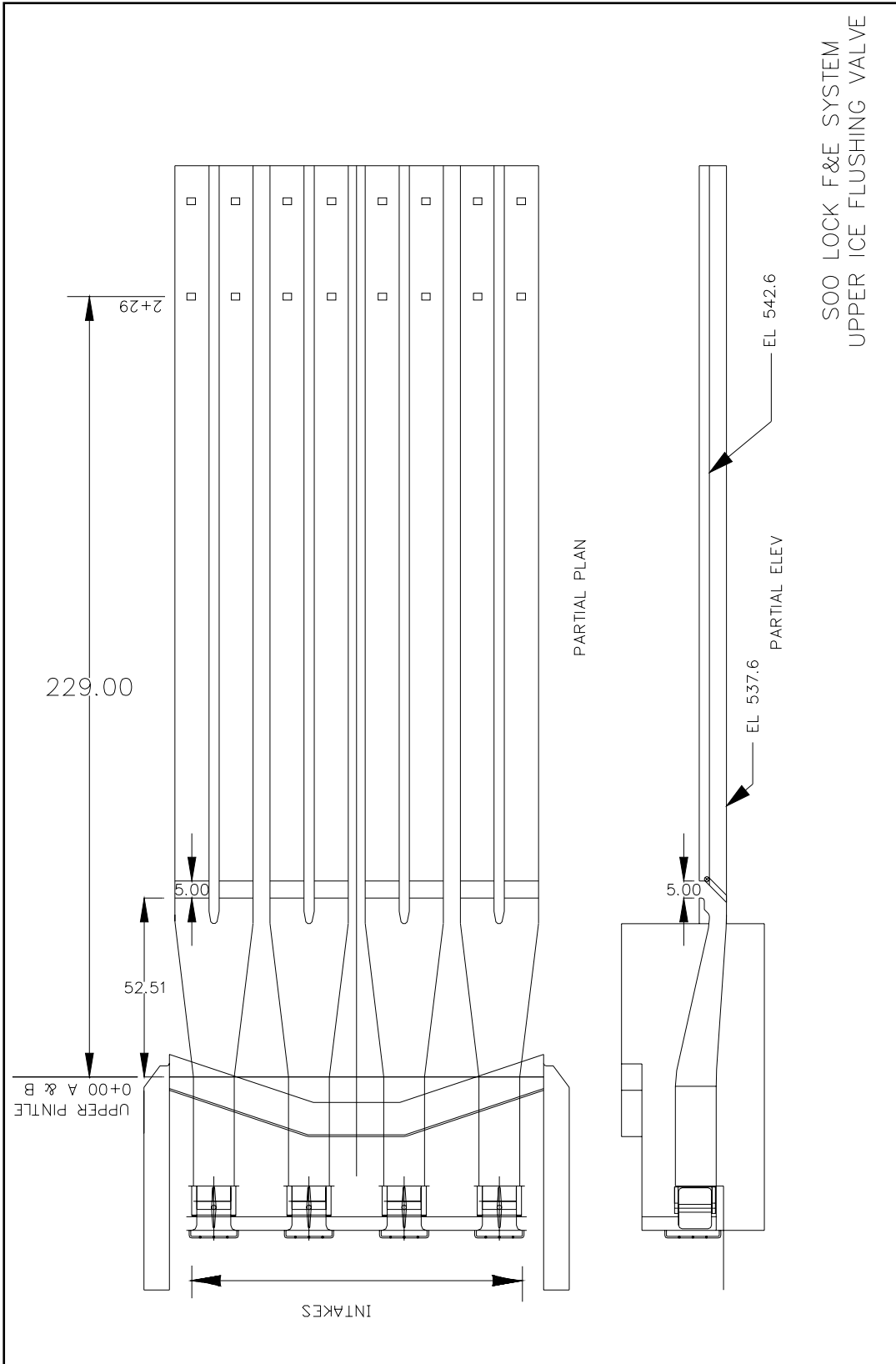
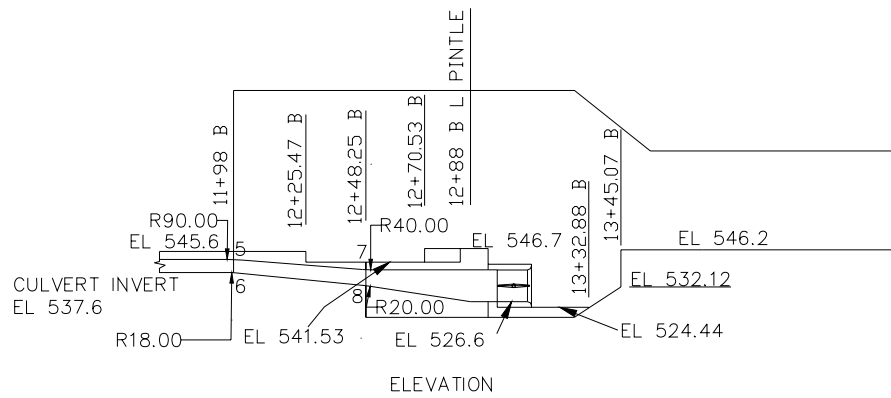
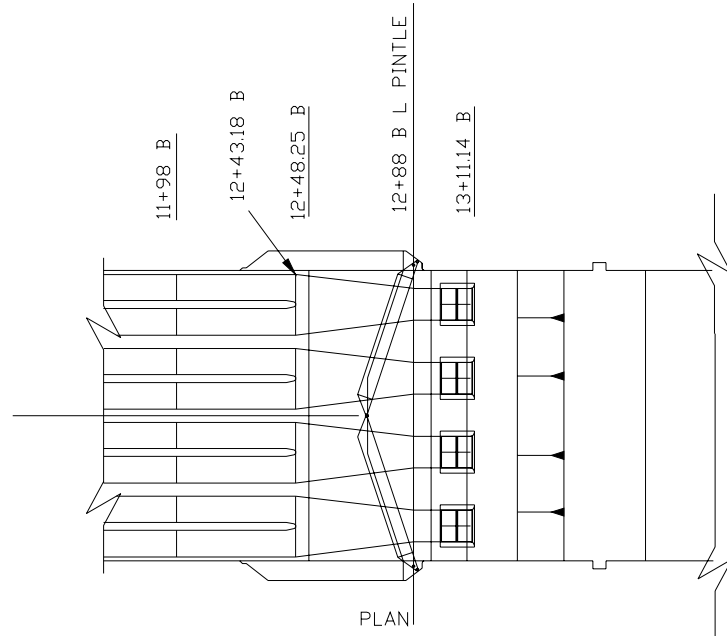


Plate 6



CURVE INFORMATION

NO.	PC		PT	
	STA	EL	STA	EL
5	11+95.53 B	542.6	12+01.33 B	542.34
6	11+97.31 B	537.6	11+98.80 B	537.52
7	12+46.90 B	538.78	12+50.03 B	538.65
8	12+48.25 B	532.62	12+49.90 B	532.38

DIMENSIONS ARE IN FT

SOO ILCS PLAN A
OUTLET AREA

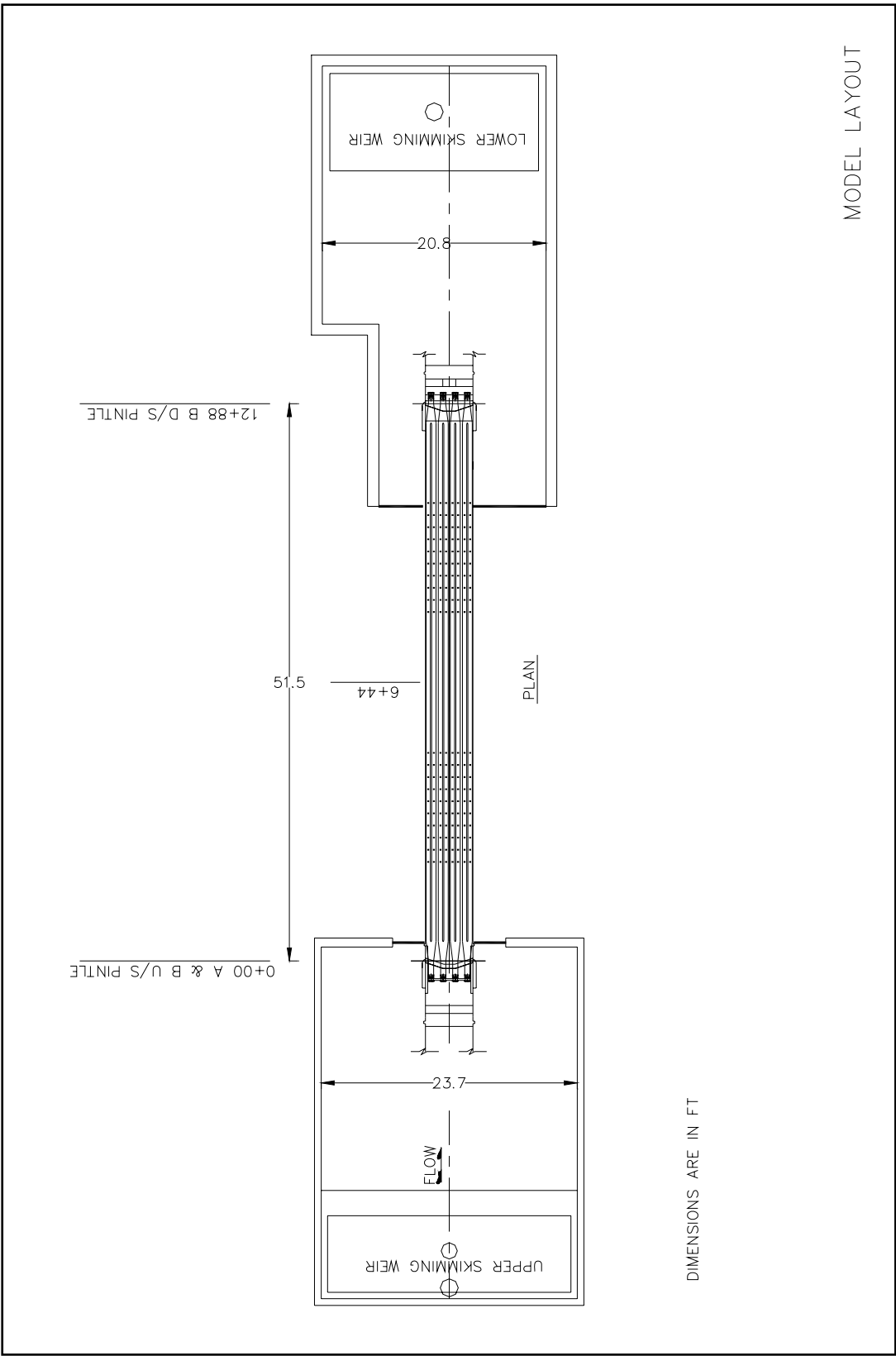

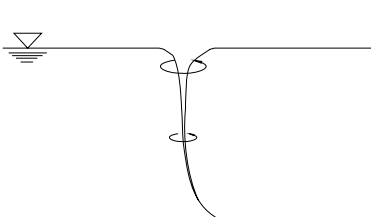


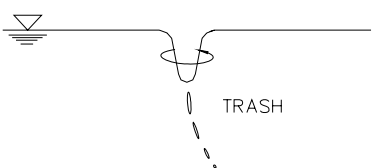
Plate 8

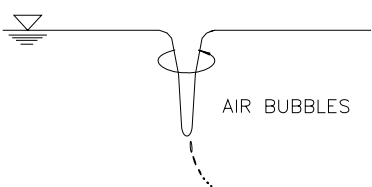
VORTEX
TYPE (VT)

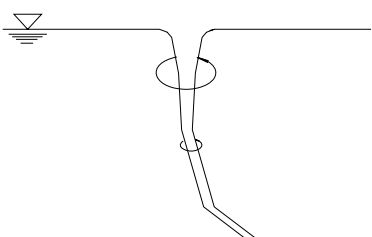
1  COHERENT SURFACE SWIRL

2  SURFACE DIMPLE
COHERENT SWIRL AT SURFACE

3  DYE CORE TO INTAKE
COHERENT SWIRL THROUGHOUT
WATER COLUMN

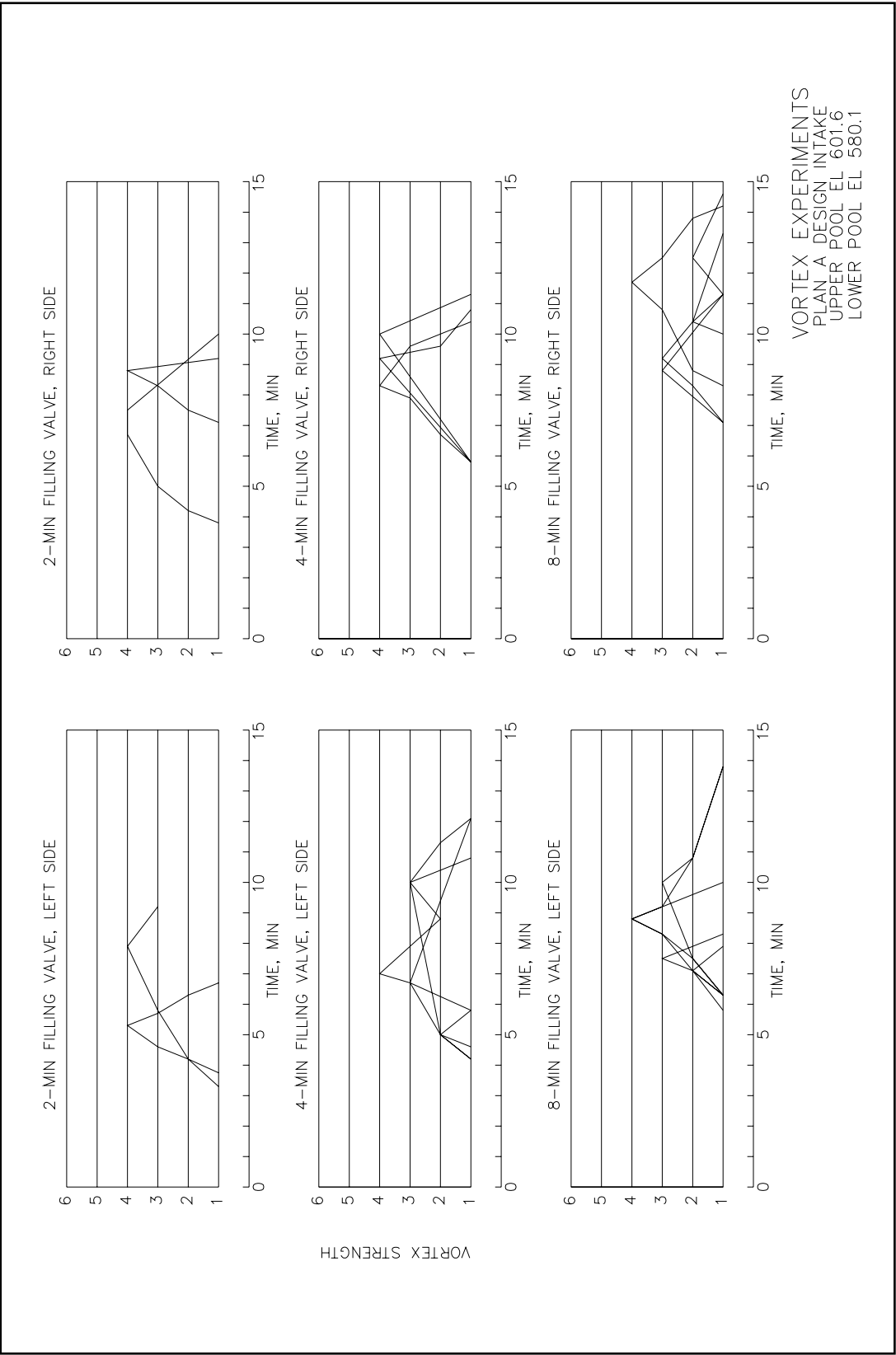
4  VORTEX PULLING FLOATING
TRASH, BUT NOT AIR
TRASH

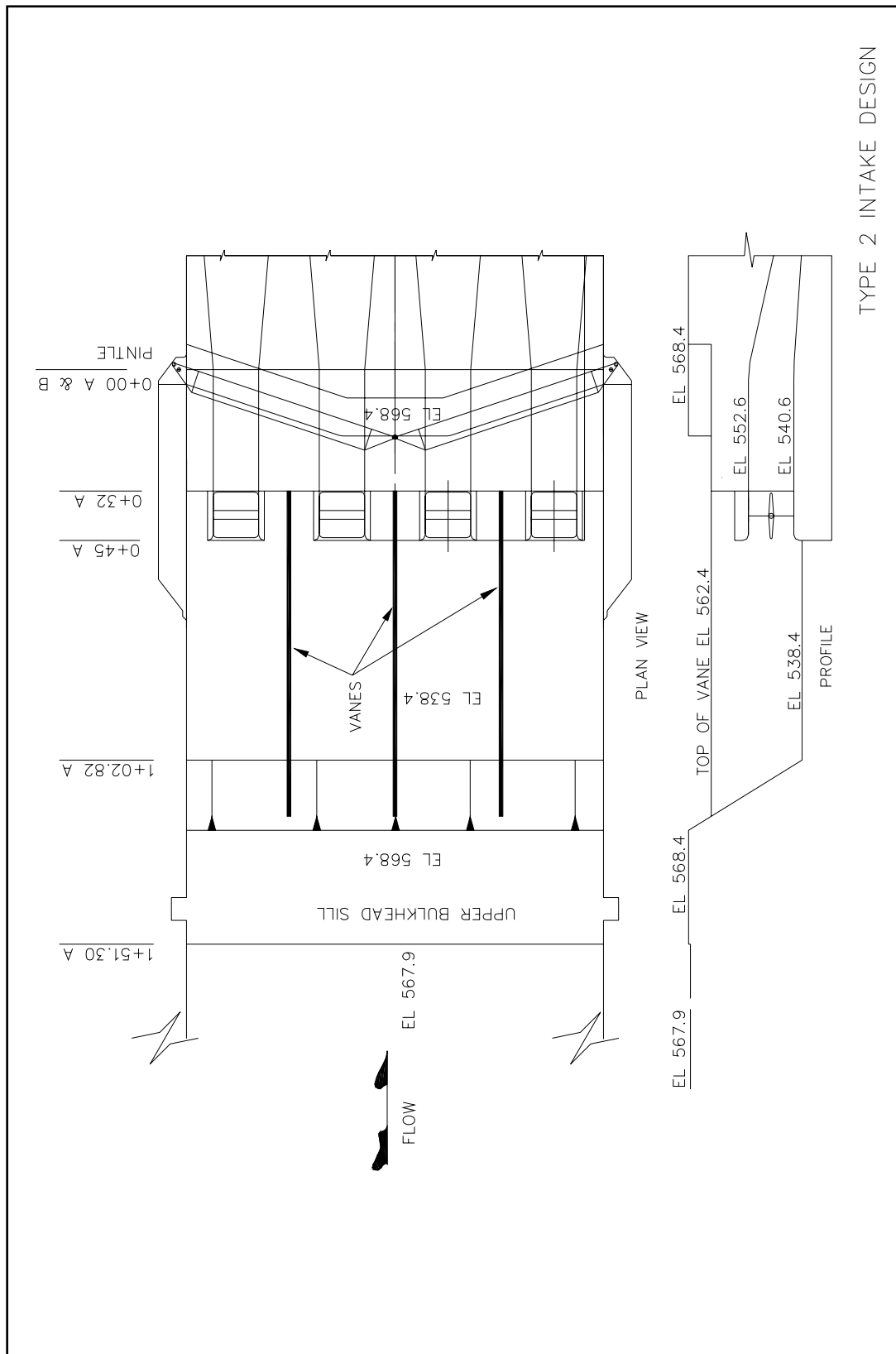
5  VORTEX PULLING AIR
BUBBLES TO INTAKE
AIR BUBBLES

6  FULL AIR CORE
TO INTAKE

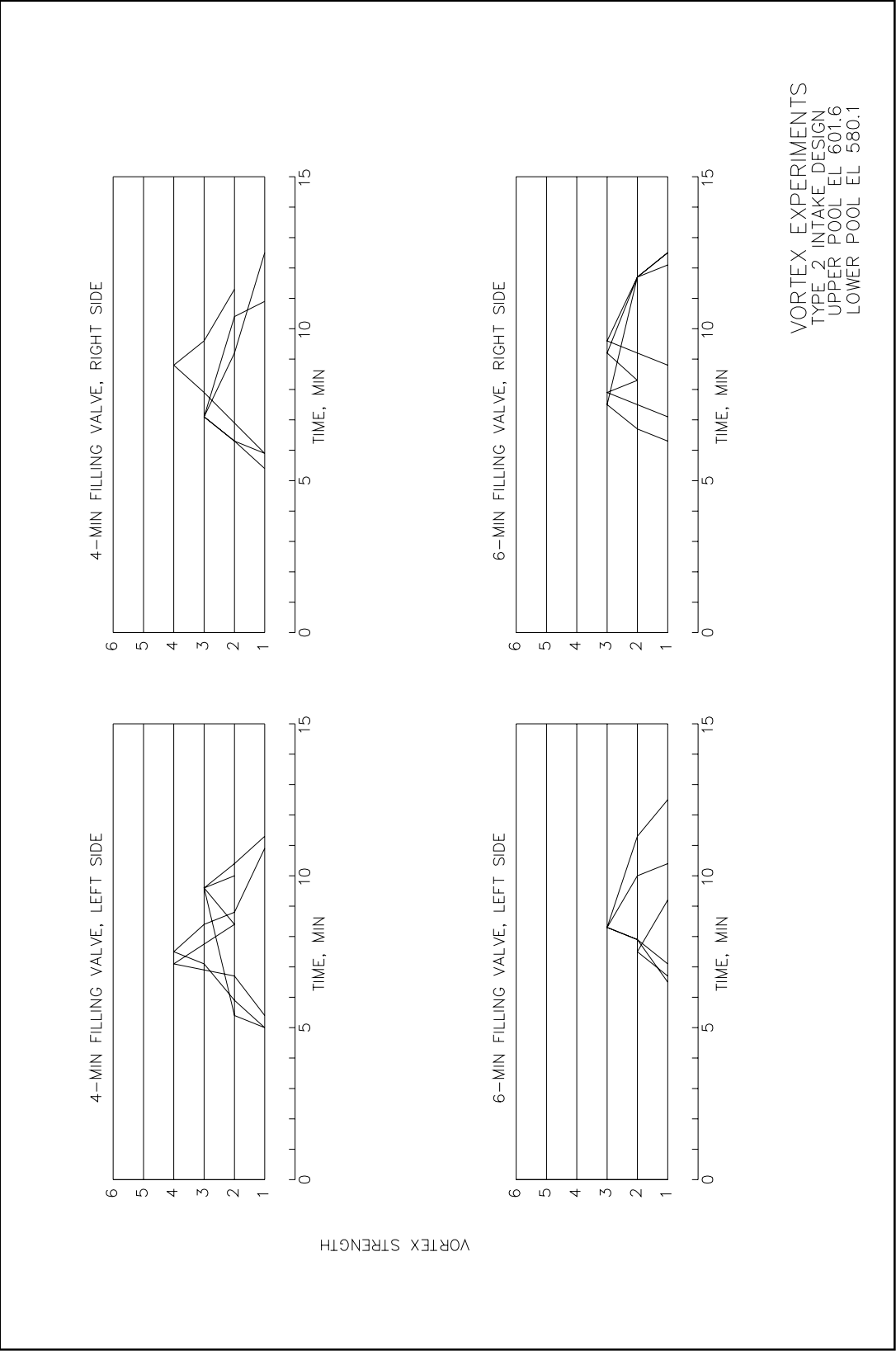
SOURCE: PADMANABHAN AND HECKER, 1984

ALDEN RESEARCH LAB
VORTEX TYPE CLASSIFICATION





TYPE 2 INTAKE DESIGN



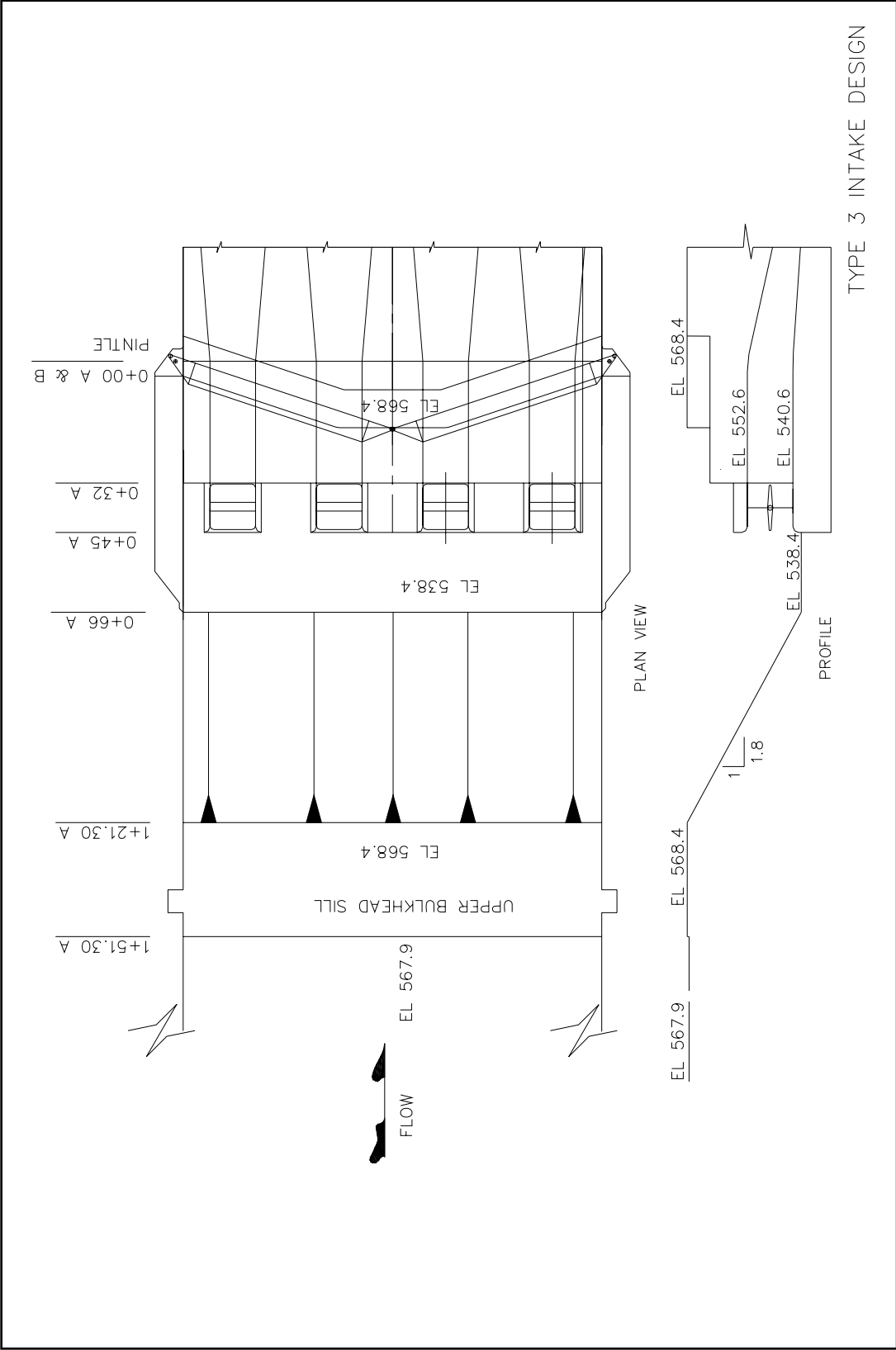
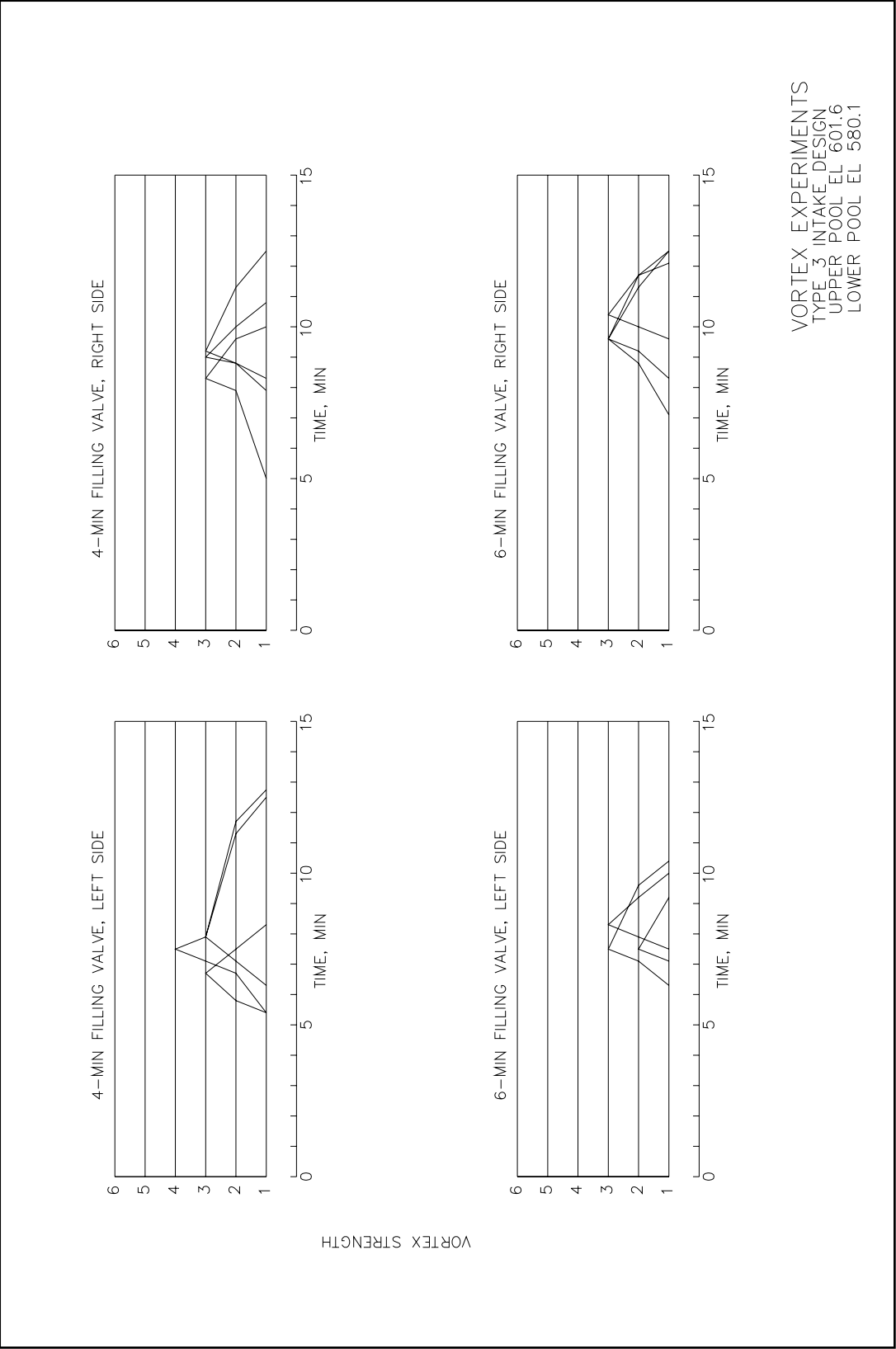


Plate 13



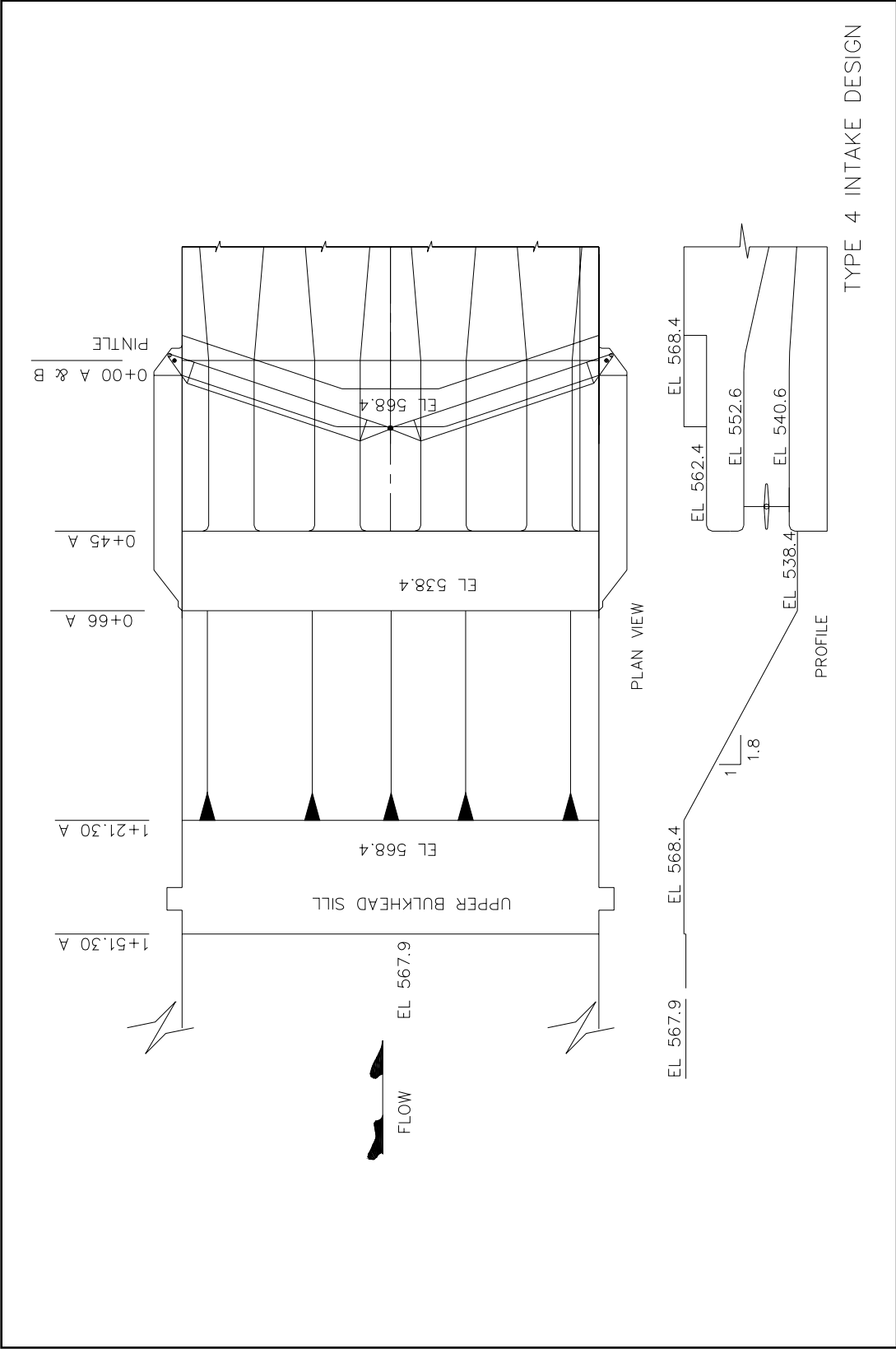
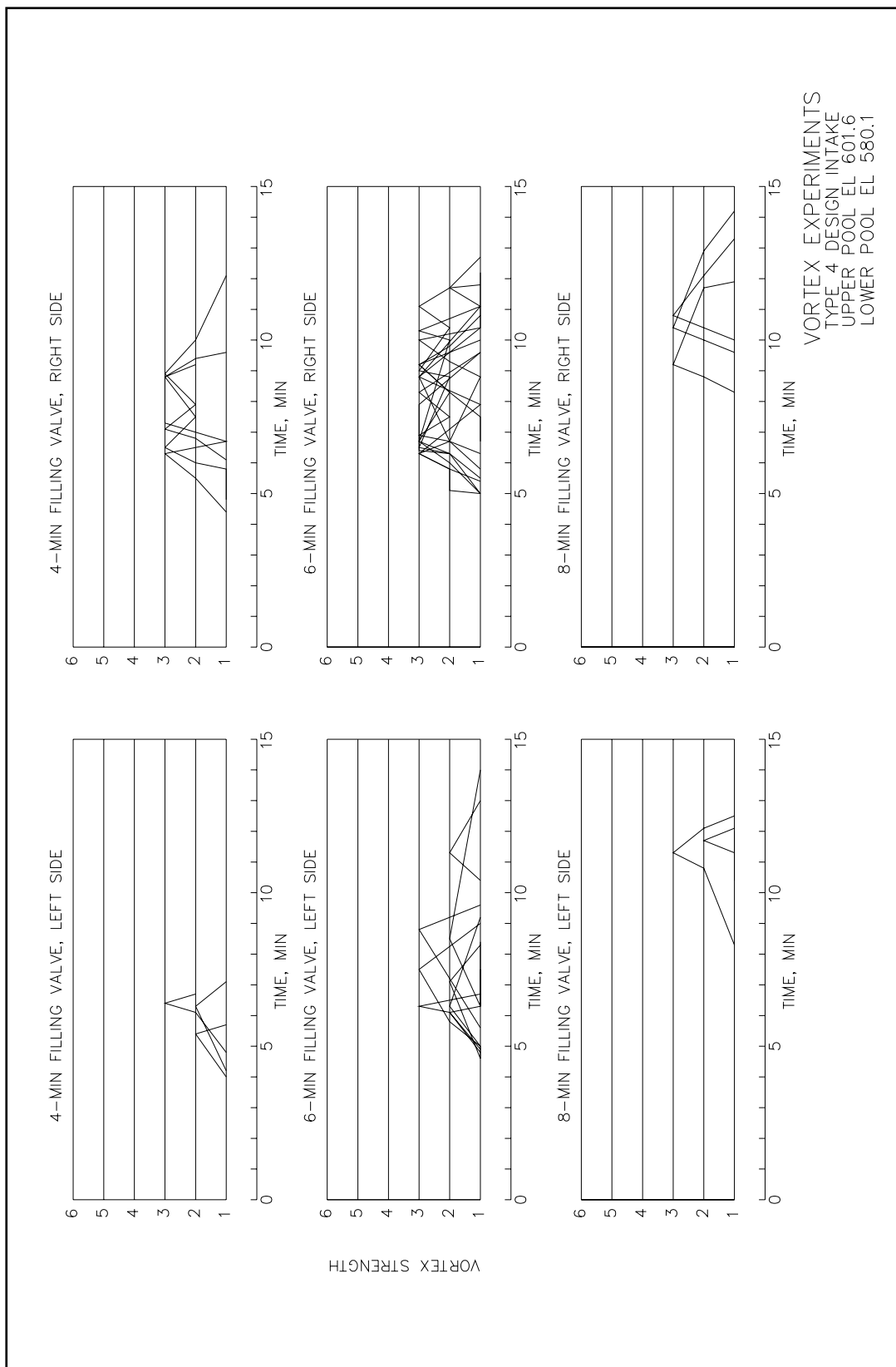
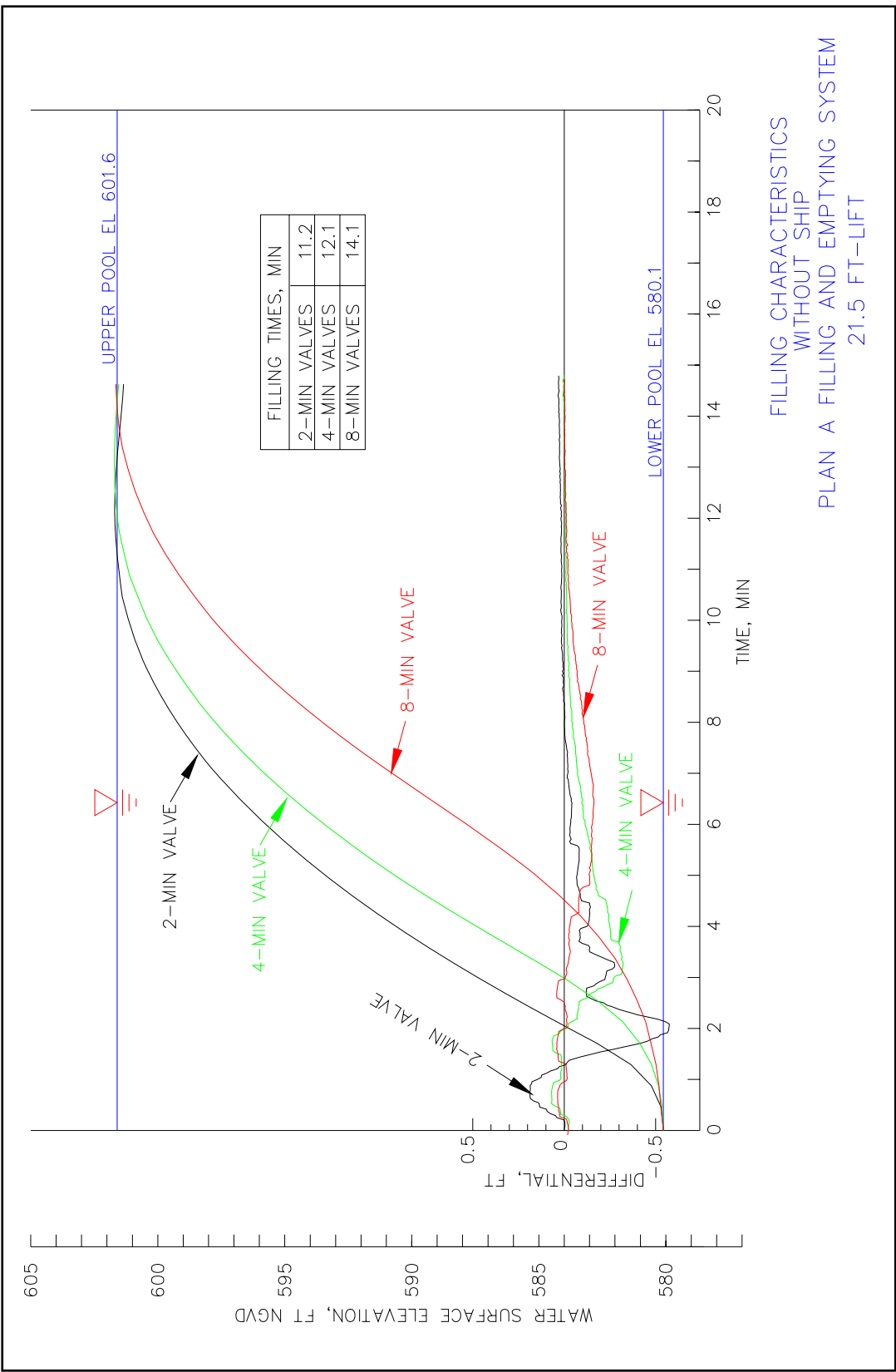


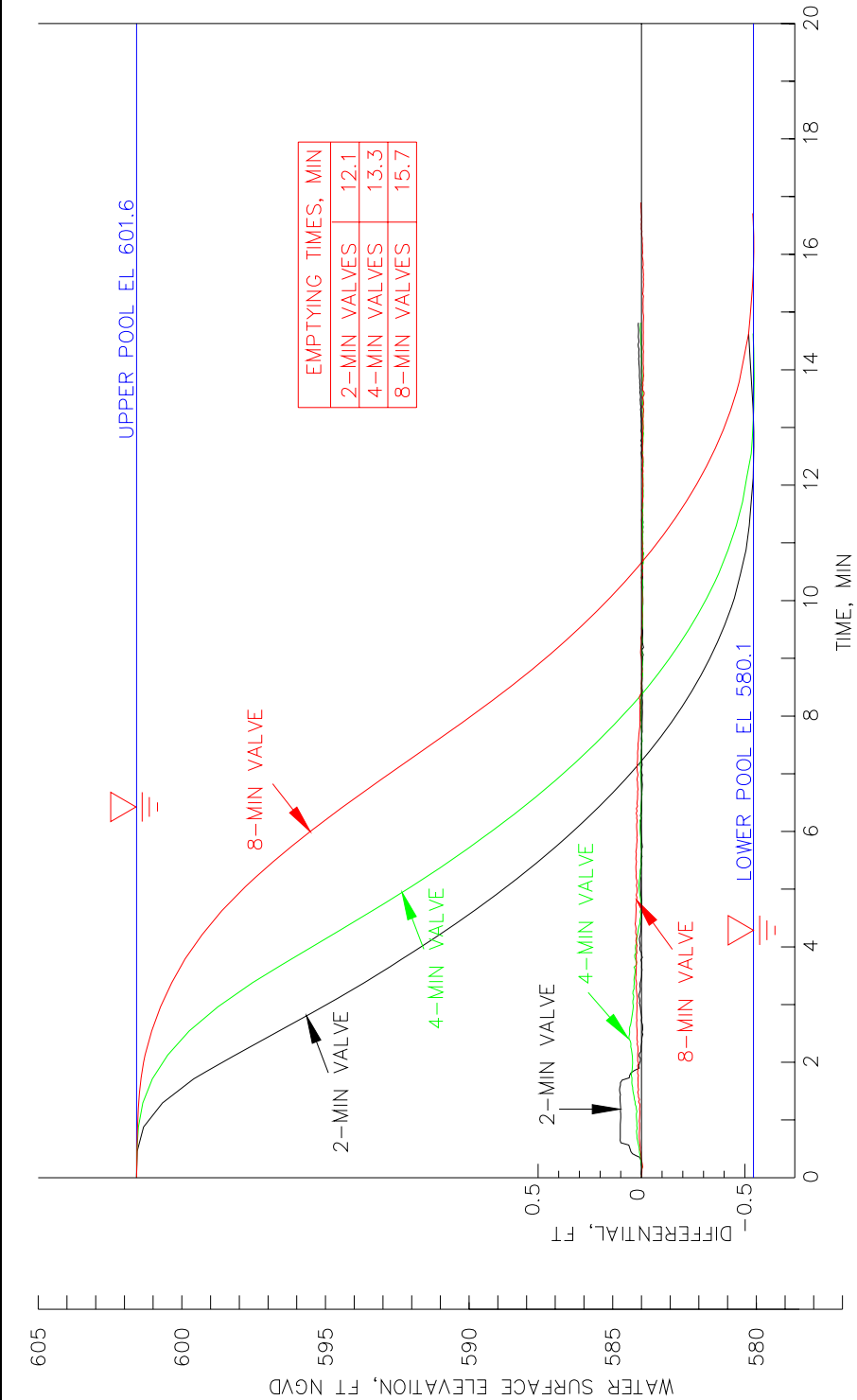
Plate 15



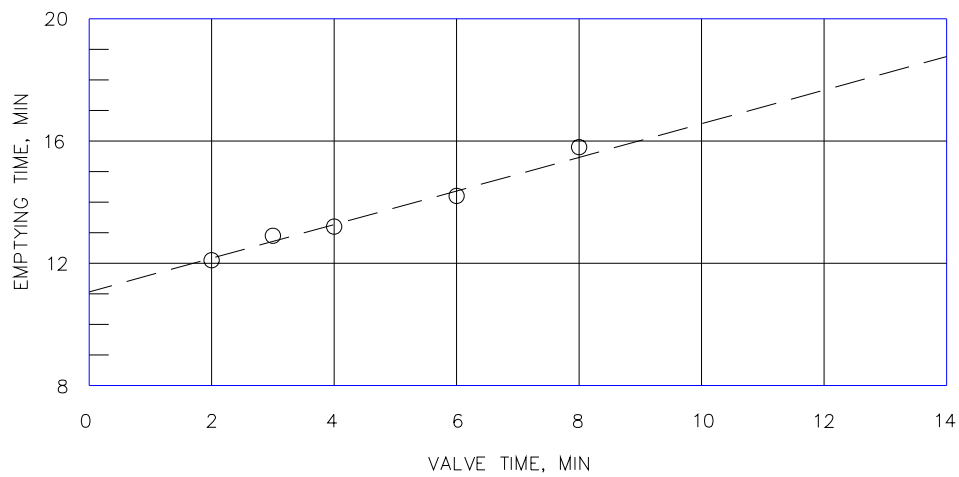
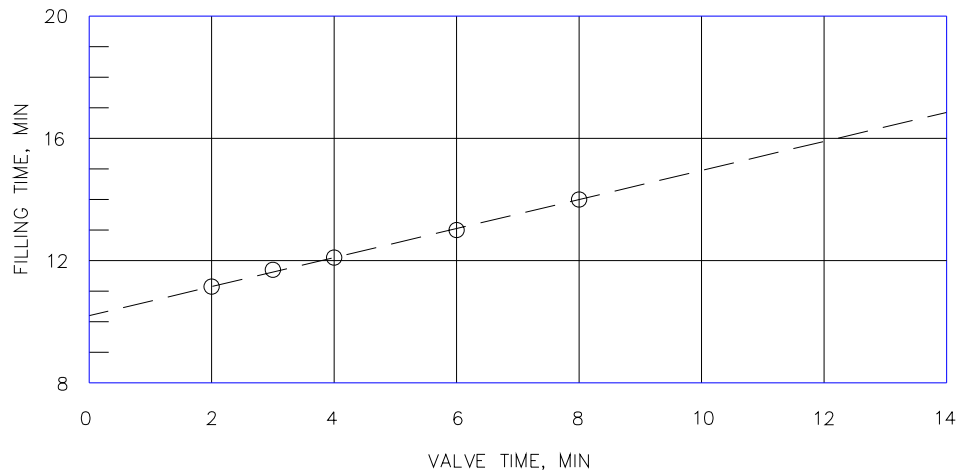




FILLING CHARACTERISTICS
WITHOUT SHIP
PLAN A FILLING AND EMPTYING SYSTEM
21.5 FT-LIFT



EMPTY CHARACTERISTICS
 WITHOUT SHIP
 PLAN A FILLING AND EMPTYING SYSTEM
 21.5 FT-LIFT



OPERATION TIMES FOR
PLAN A DESIGN
FILLING AND EMPTYING SYSTEM
21.5-FT LIFT
UPPER POOL EL 601.6
LOWER POOL EL 580.1

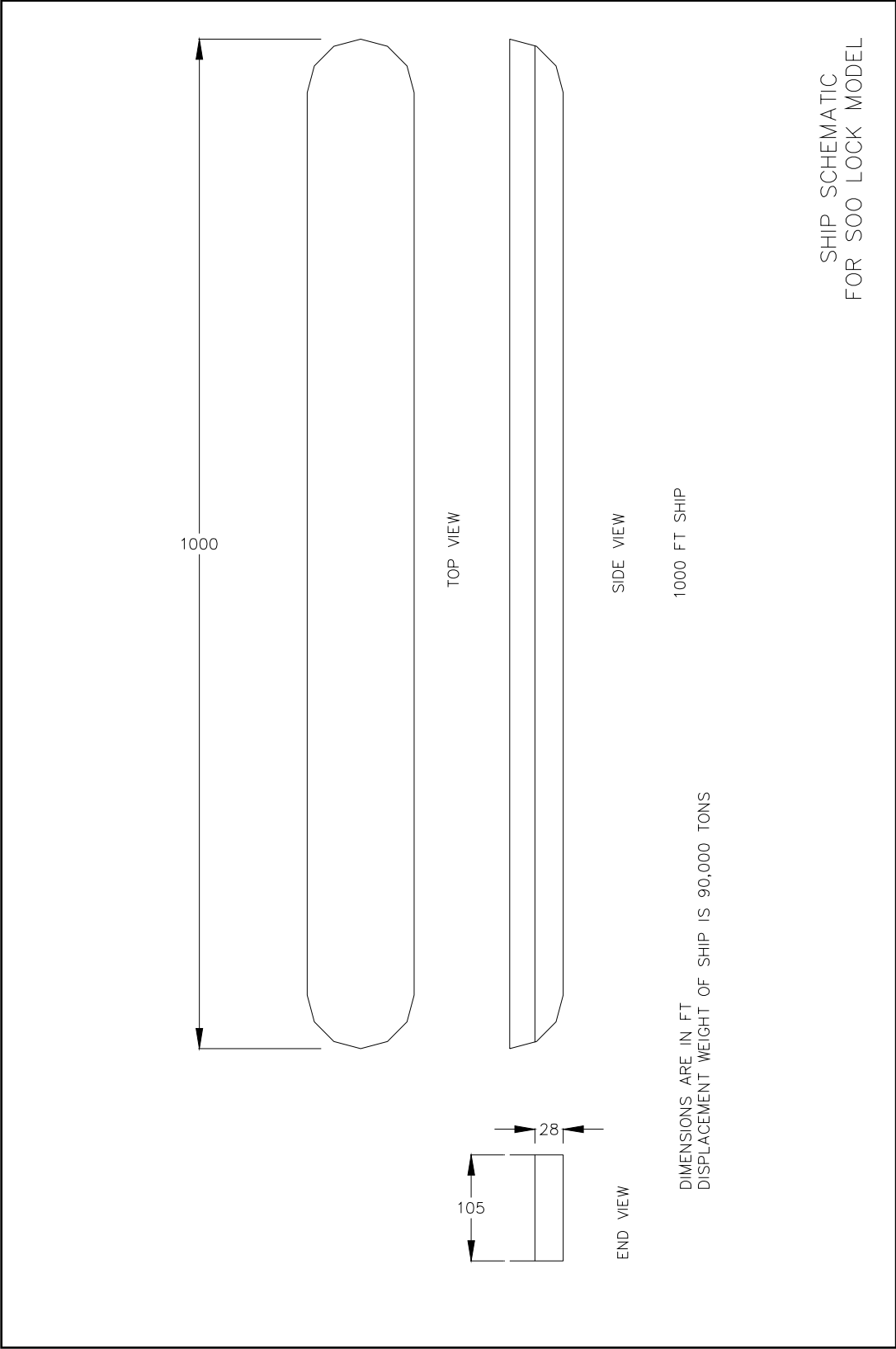


Plate 21

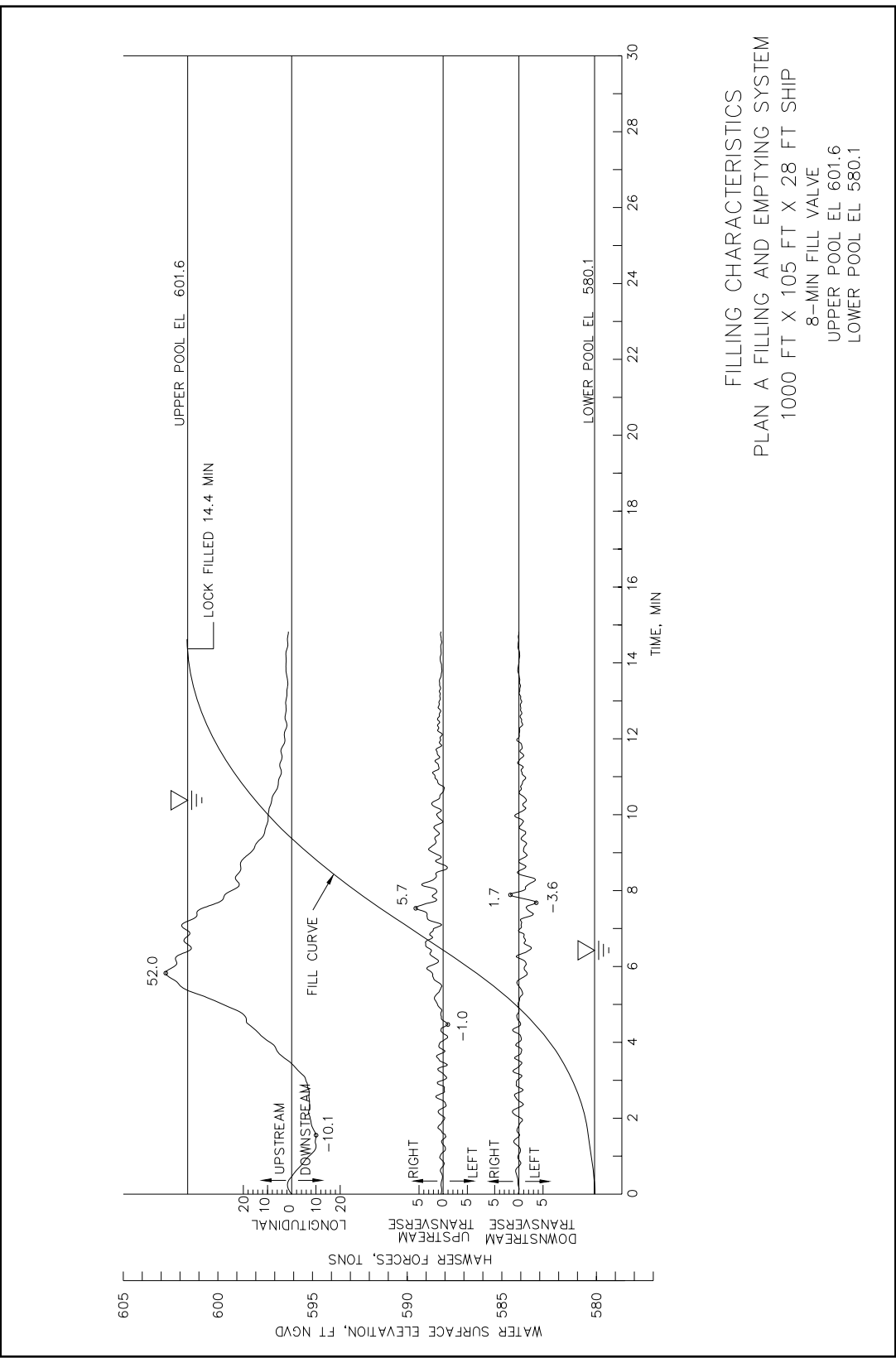
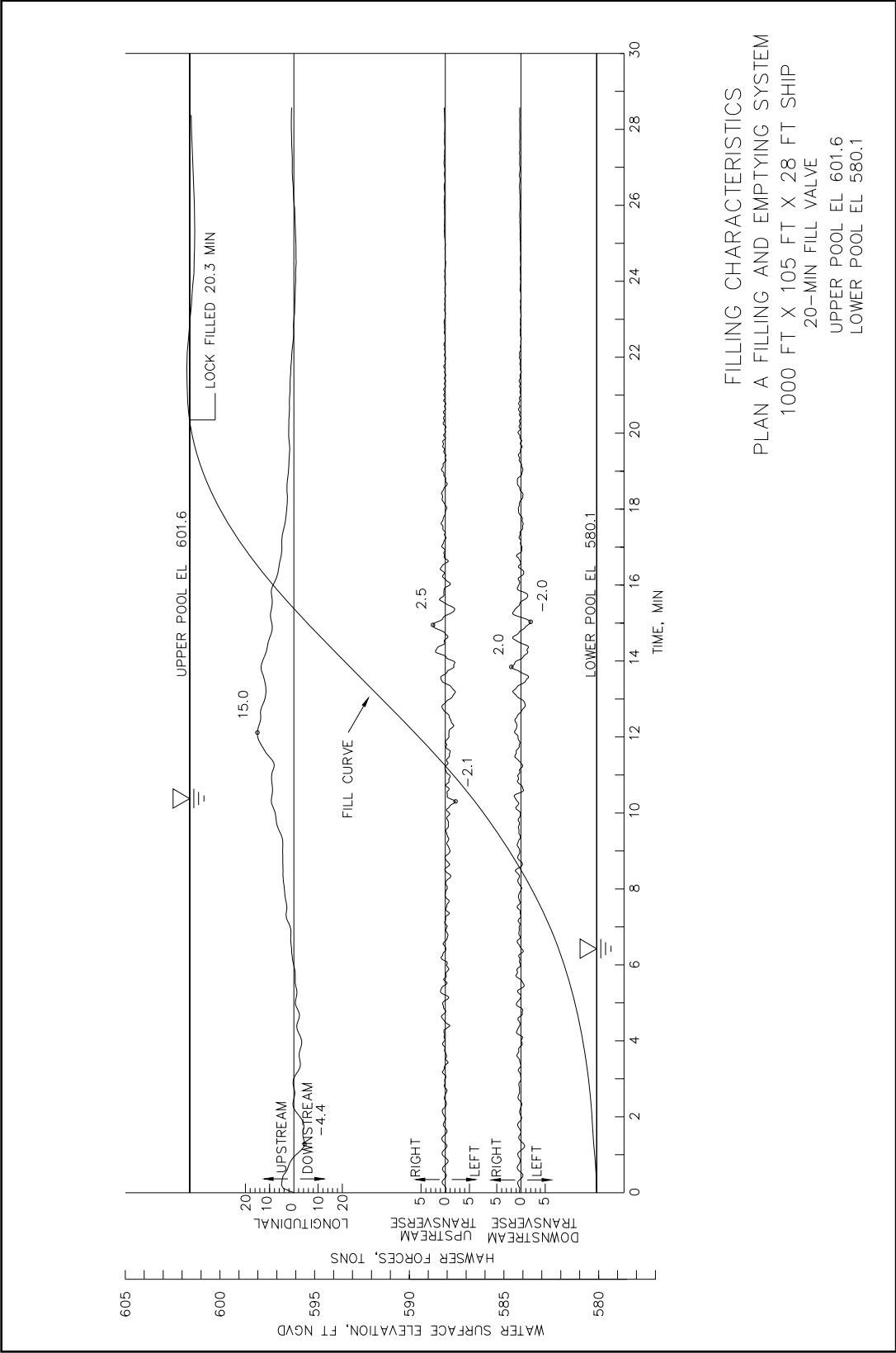
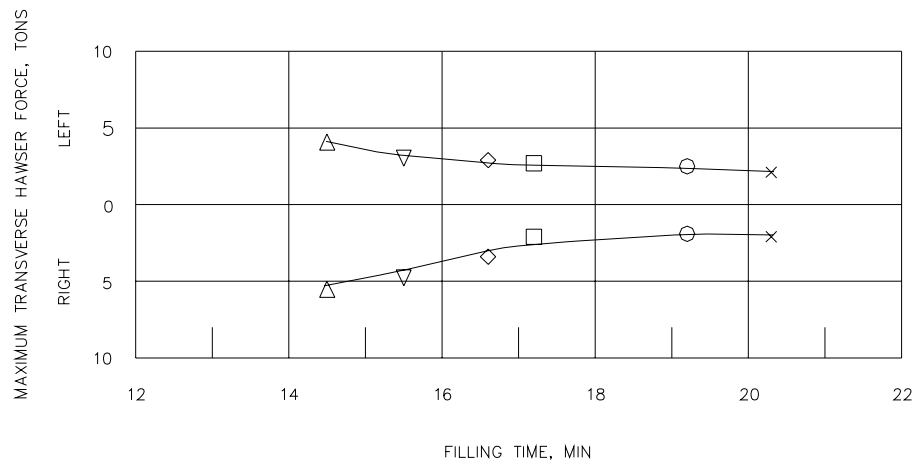
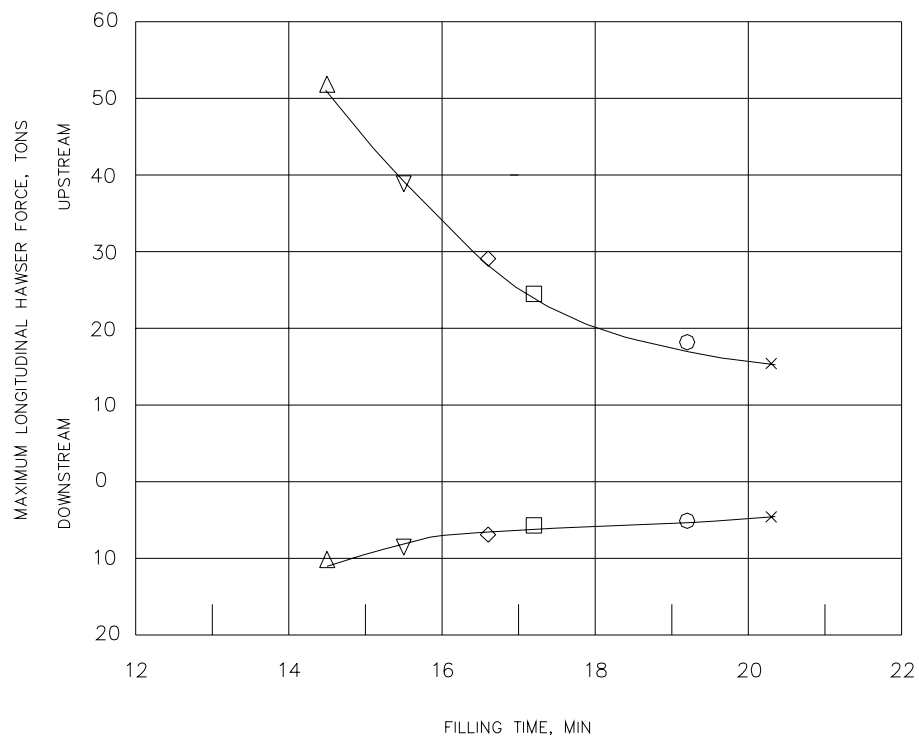


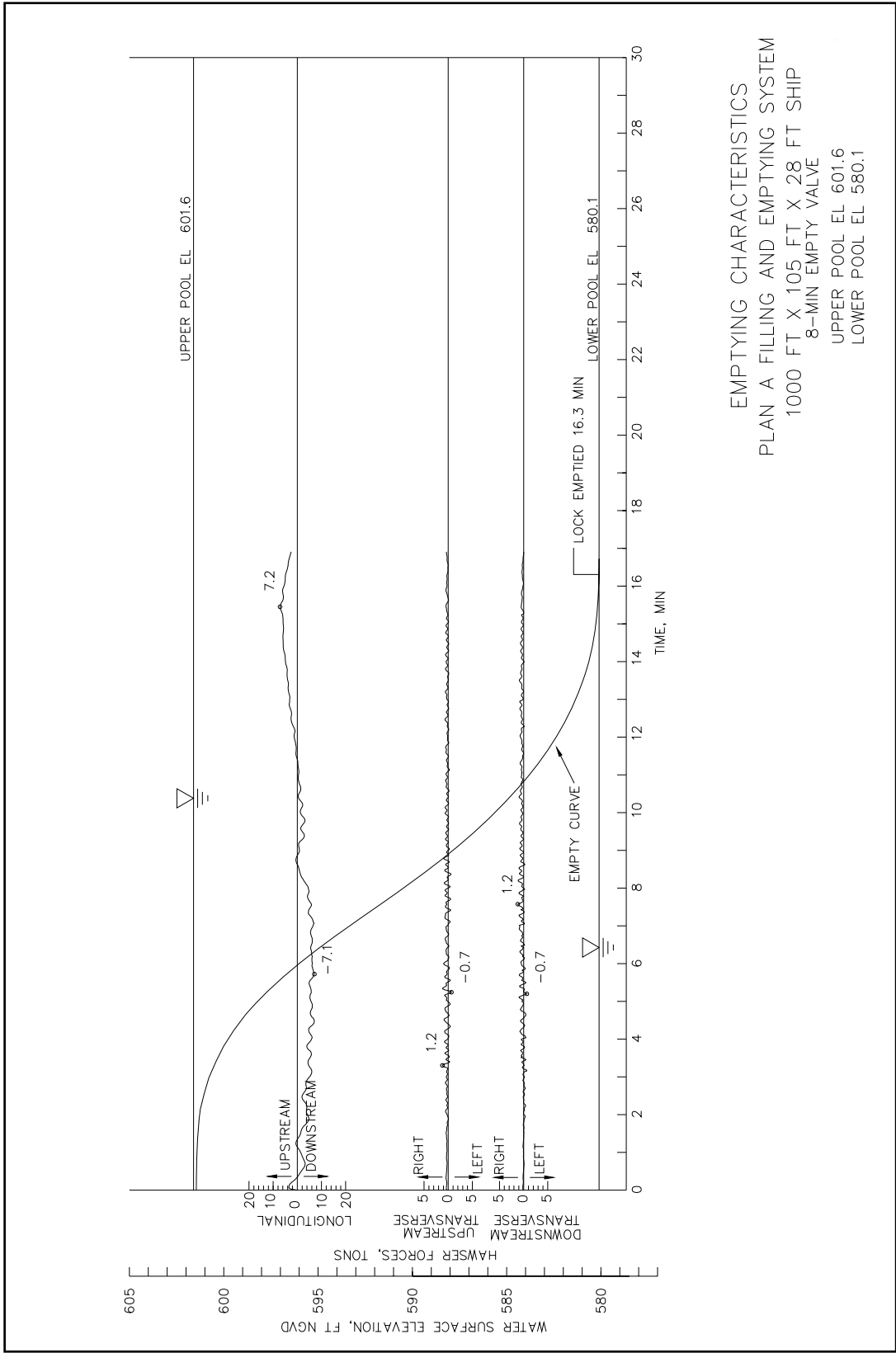
Plate 22

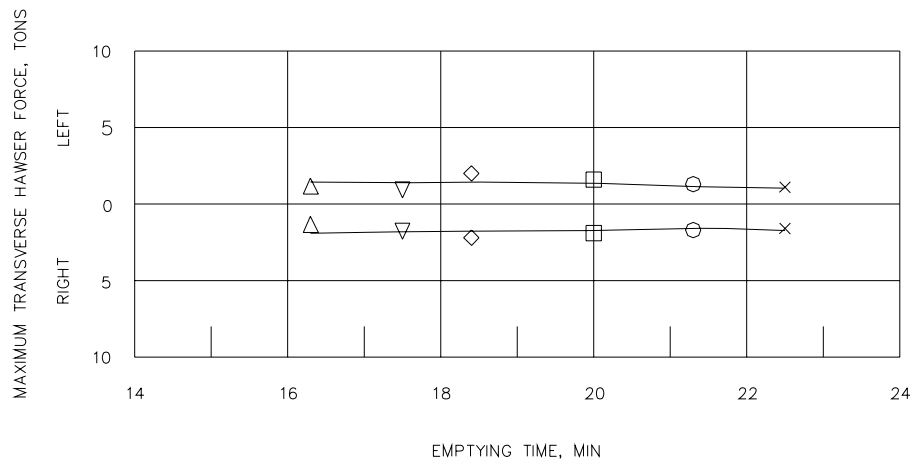
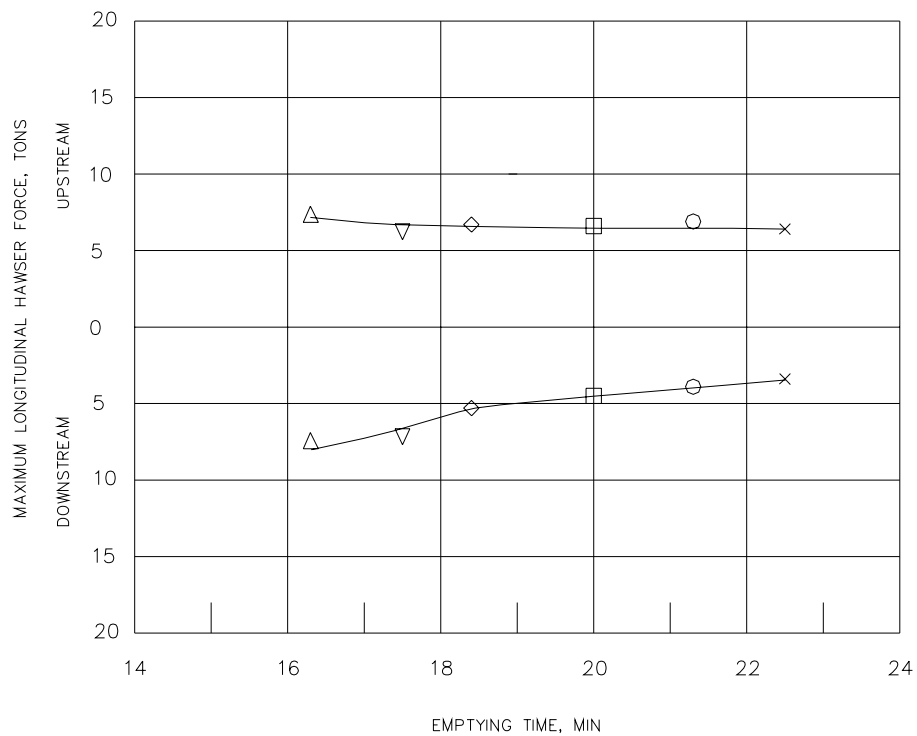




LEGEND	
SYMBOL	VALVE SCHEDULE, MIN
△	8
▽	10
◇	12
□	14
○	18
×	20

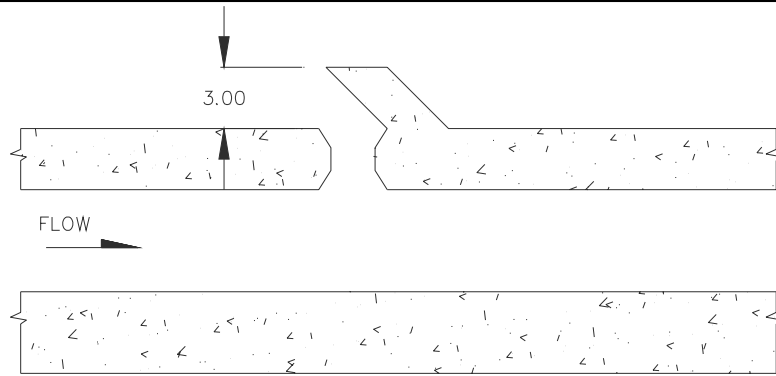
HAWSER FORCES
 DURING FILLING
 PLAN A DESIGN
 FILLING AND EMPTYING SYSTEM
 UPPER POOL EL 601.6
 LOWER POOL EL 580.1
 21.5-ft. LIFT



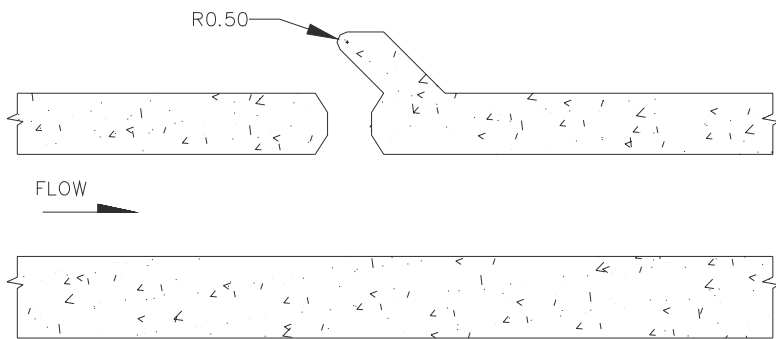


LEGEND	
SYMBOL	VALVE SCHEDULE, MIN
△	8
▽	10
◇	12
□	14
○	18
x	20

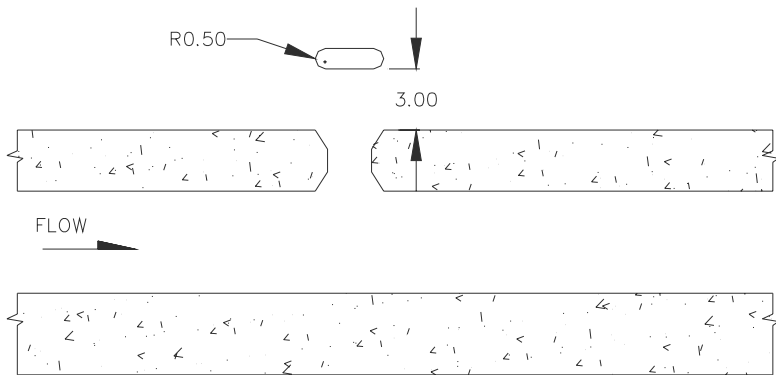
HAWSER FORCES
 DURING EMPTYING
 PLAN A DESIGN
 FILLING AND EMPTYING SYSTEM
 UPPER POOL EL 601.6
 LOWER POOL EL 580.1
 21.5-ft. LIFT



BAFFLES ON UPPER PORTS WITH TYPE 2 CHAMBER DESIGN



BAFFLES ON UPPER PORTS WITH TYPE 3 CHAMBER DESIGN



BAFFLES ON LOWER PORTS WITH TYPE 6 CHAMBER DESIGN

DIMENSIONS ARE IN FT

PARTIAL DETAILS
TYPES 2, 3, AND 6 CHAMBER DESIGNS

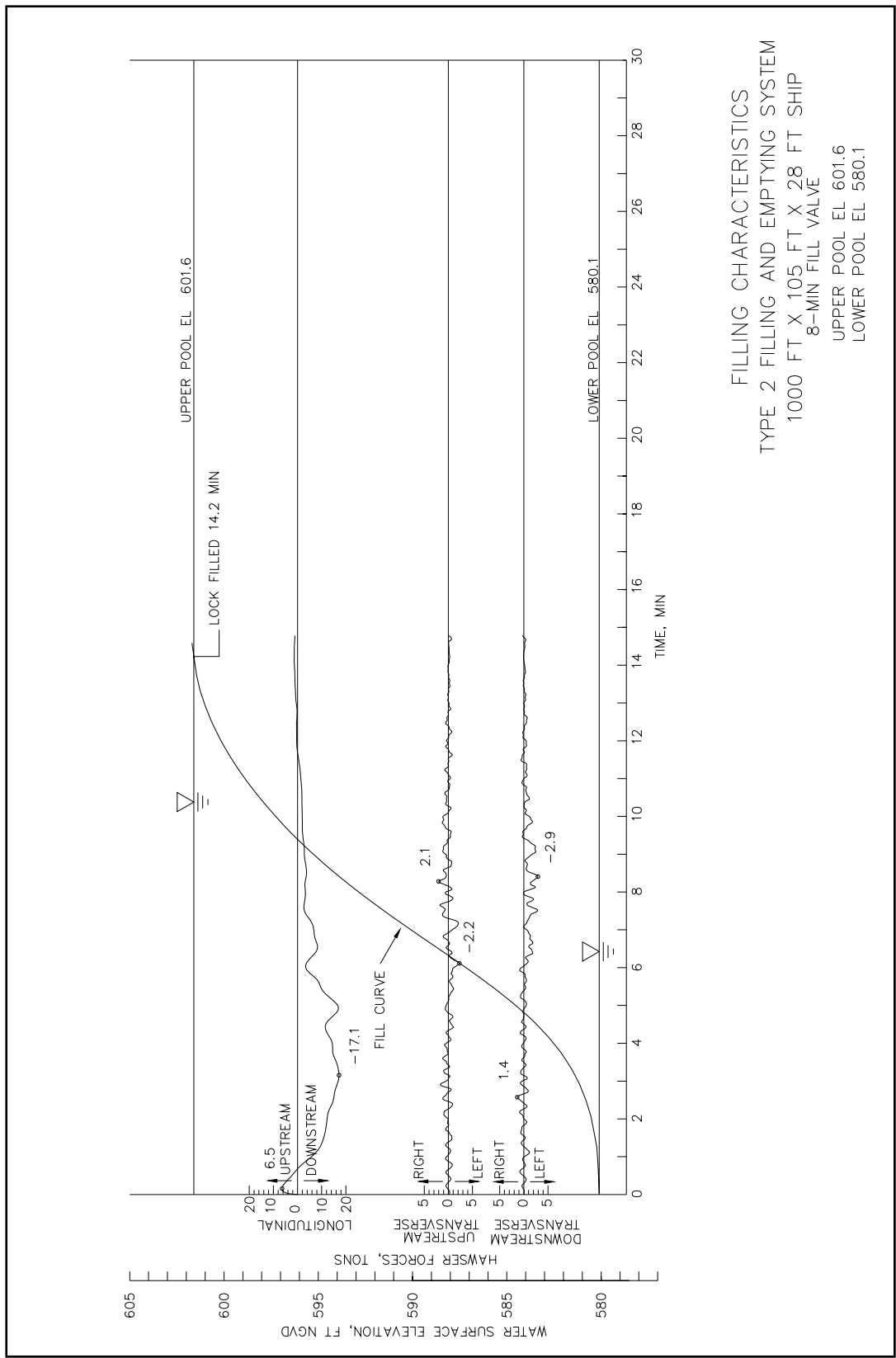
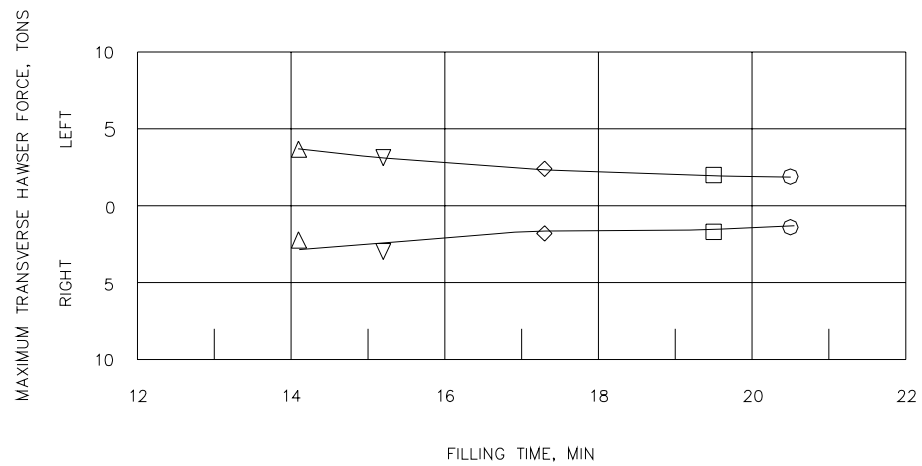
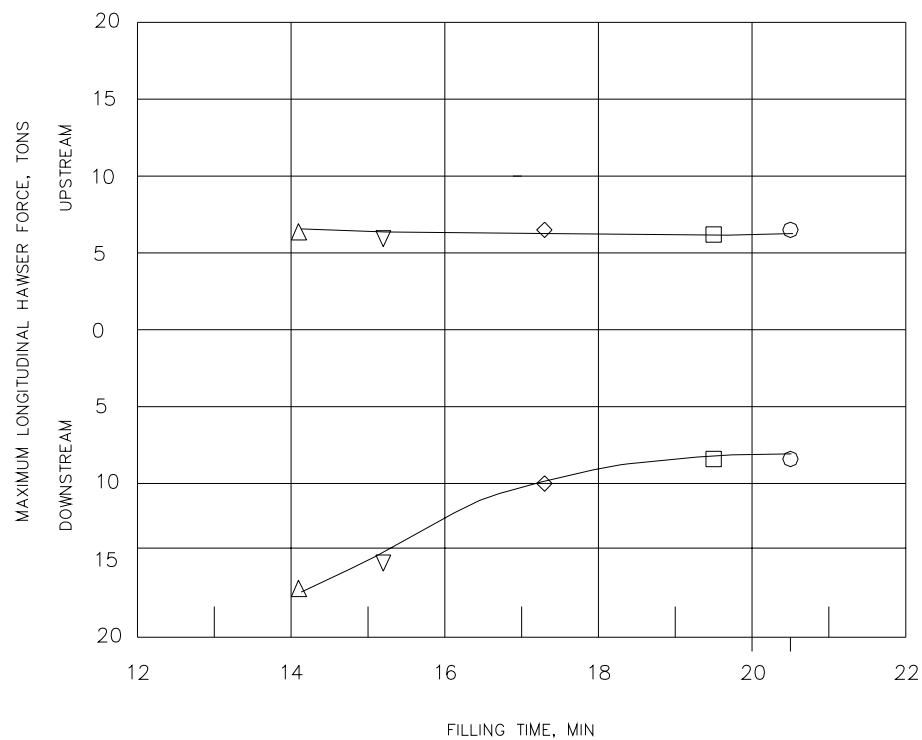
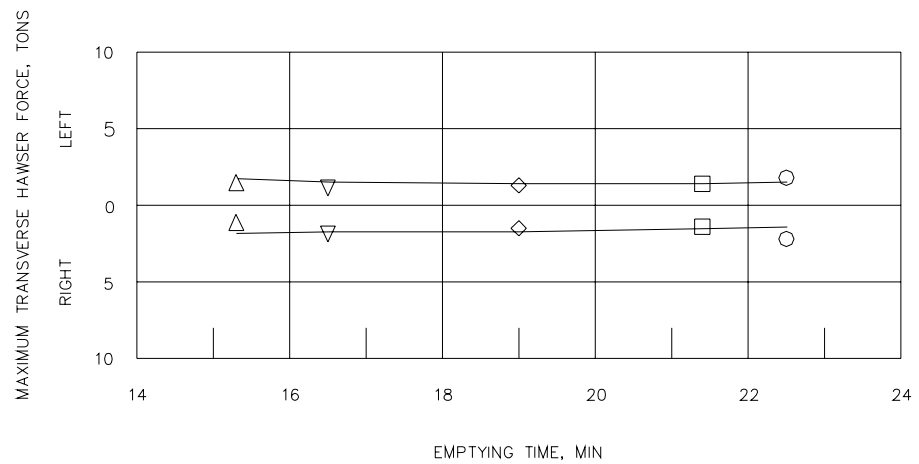
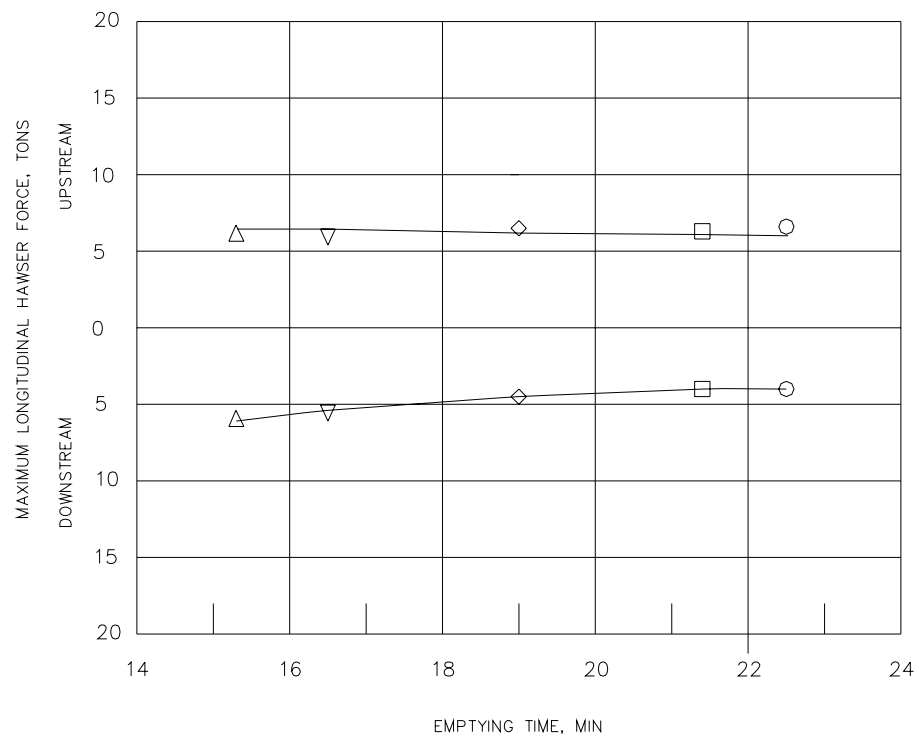


Plate 28



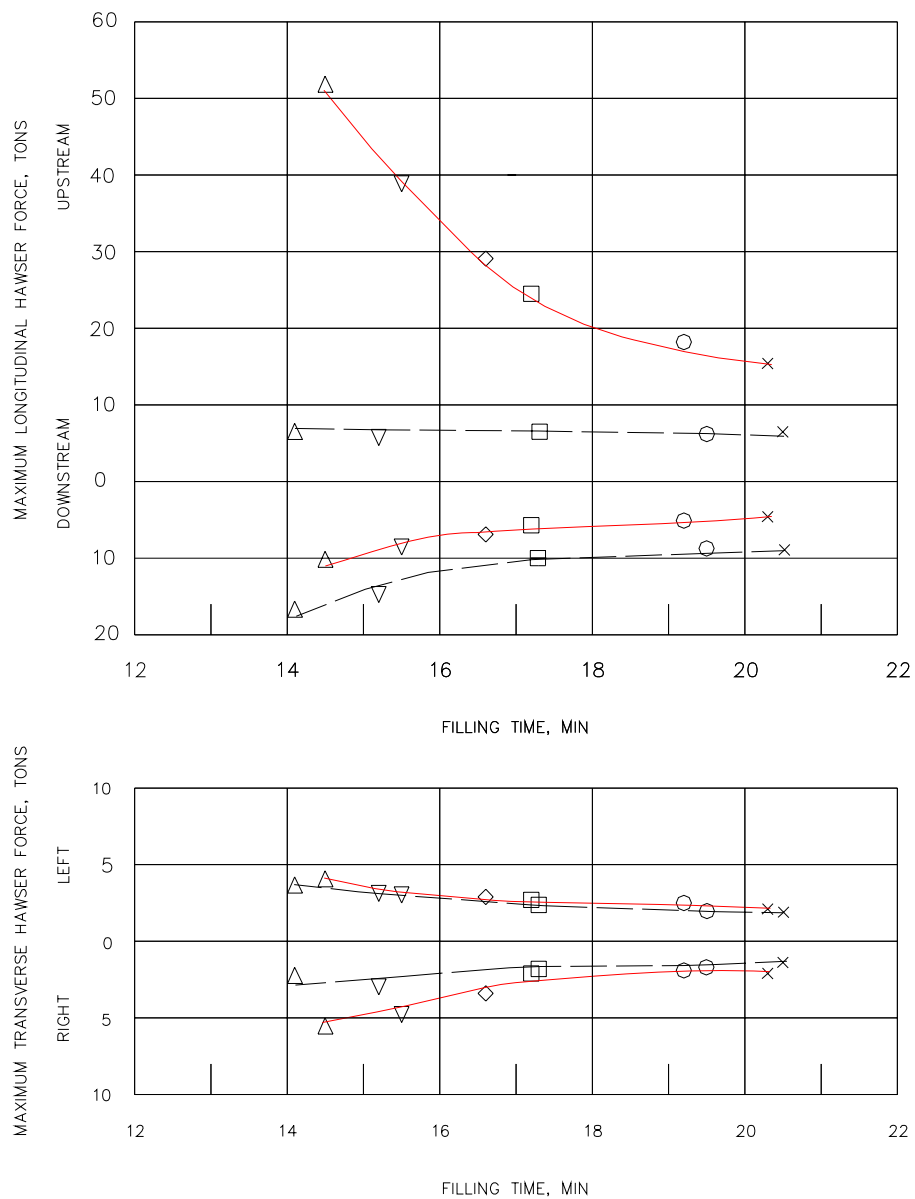
LEGEND	
SYMBOL	VALVE SCHEDULE, MIN
△	8
▽	10
◇	14
□	18
○	20

HAWSER FORCES
 DURING FILLING
 TYPE 2 DESIGN
 FILLING AND EMPTYING SYSTEM
 UPPER POOL EL 601.6
 LOWER POOL EL 580.1
 21.5-ft. LIFT



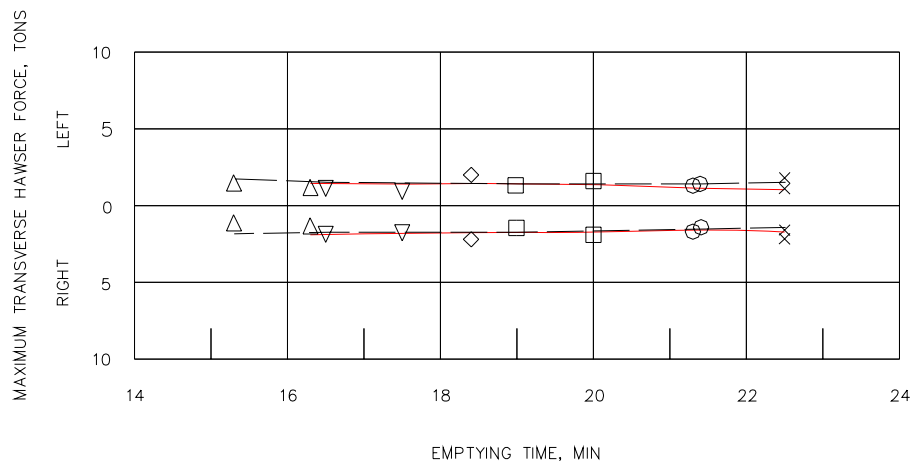
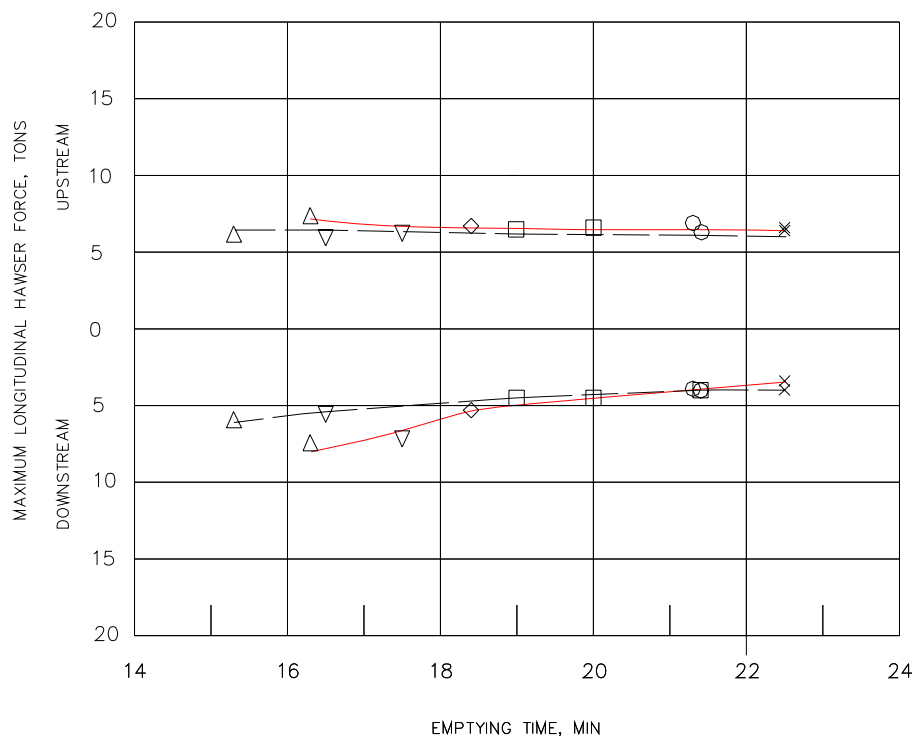
LEGEND	
SYMBOL	VALVE SCHEDULE, MIN
△	8
▽	10
◇	14
□	18
○	20

HAWSER FORCES
DURING EMPTYING
TYPE 2 DESIGN
FILLING AND EMPTYING SYSTEM
UPPER POOL EL 601.6
LOWER POOL EL 580.1
21.5-ft. LIFT



LEGEND	
SYMBOL	VALVE SCHEDULE, MIN
△	8
▽	10
◇	12
□	14
○	18
×	20
—	PLAN A
- -	TYPE 2

HAWSER FORCES
DURING FILLING
PLAN A AND TYPE 2 DESIGN
FILLING AND EMPTYING SYSTEM
UPPER POOL EL 601.6
LOWER POOL EL 580.1
21.5-FT LIFT



LEGEND	
SYMBOL	VALVE SCHEDULE, MIN
△	8
▽	10
◇	12
□	14
○	18
×	20
—	PLAN A
- -	TYPE 2

HAWSER FORCES
 DURING EMPTYING
 PLAN A AND TYPE 2 DESIGN
 FILLING AND EMPTYING SYSTEM
 UPPER POOL EL 601.6
 LOWER POOL EL 580.1
 21.5-FT LIFT

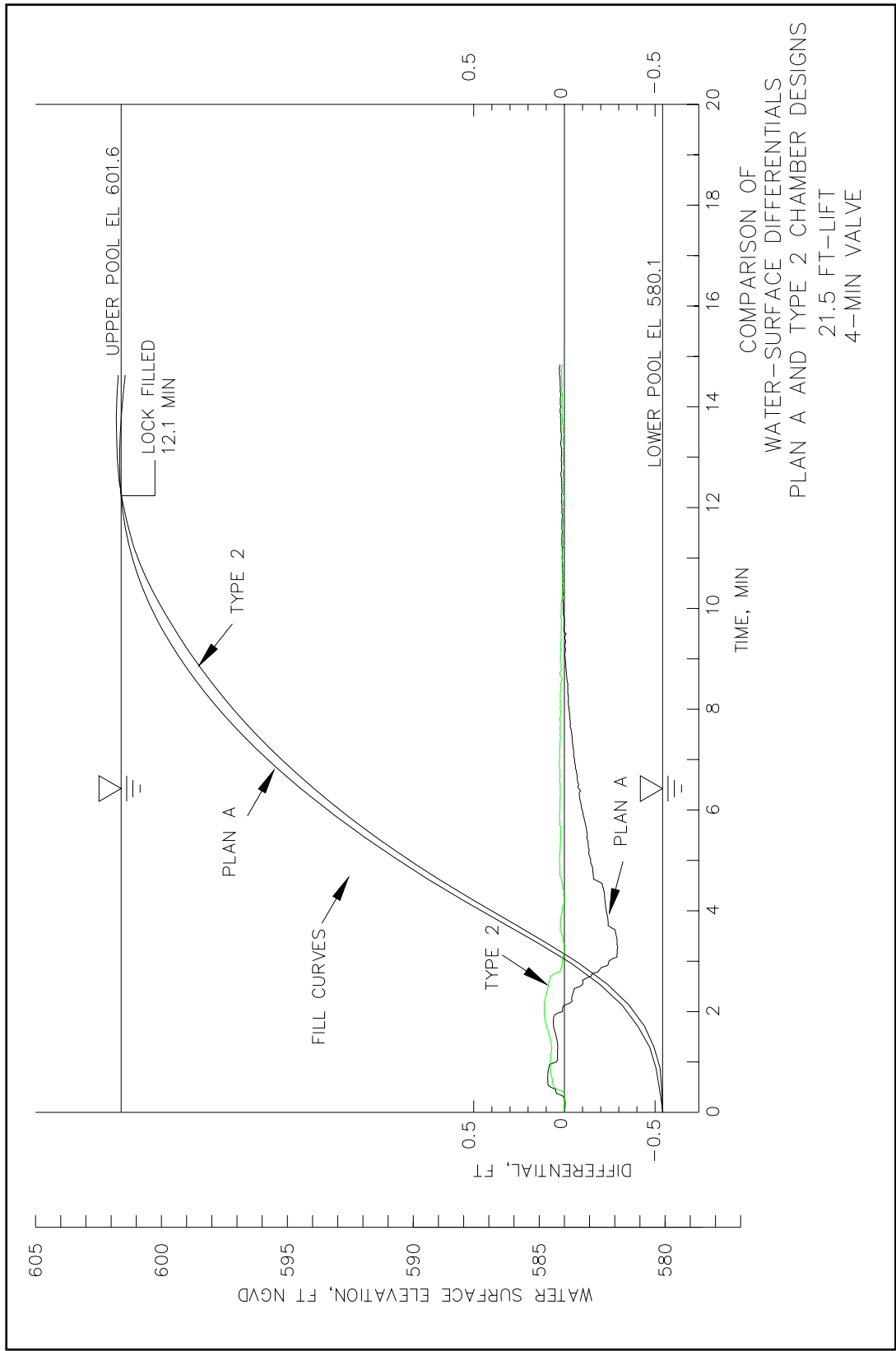
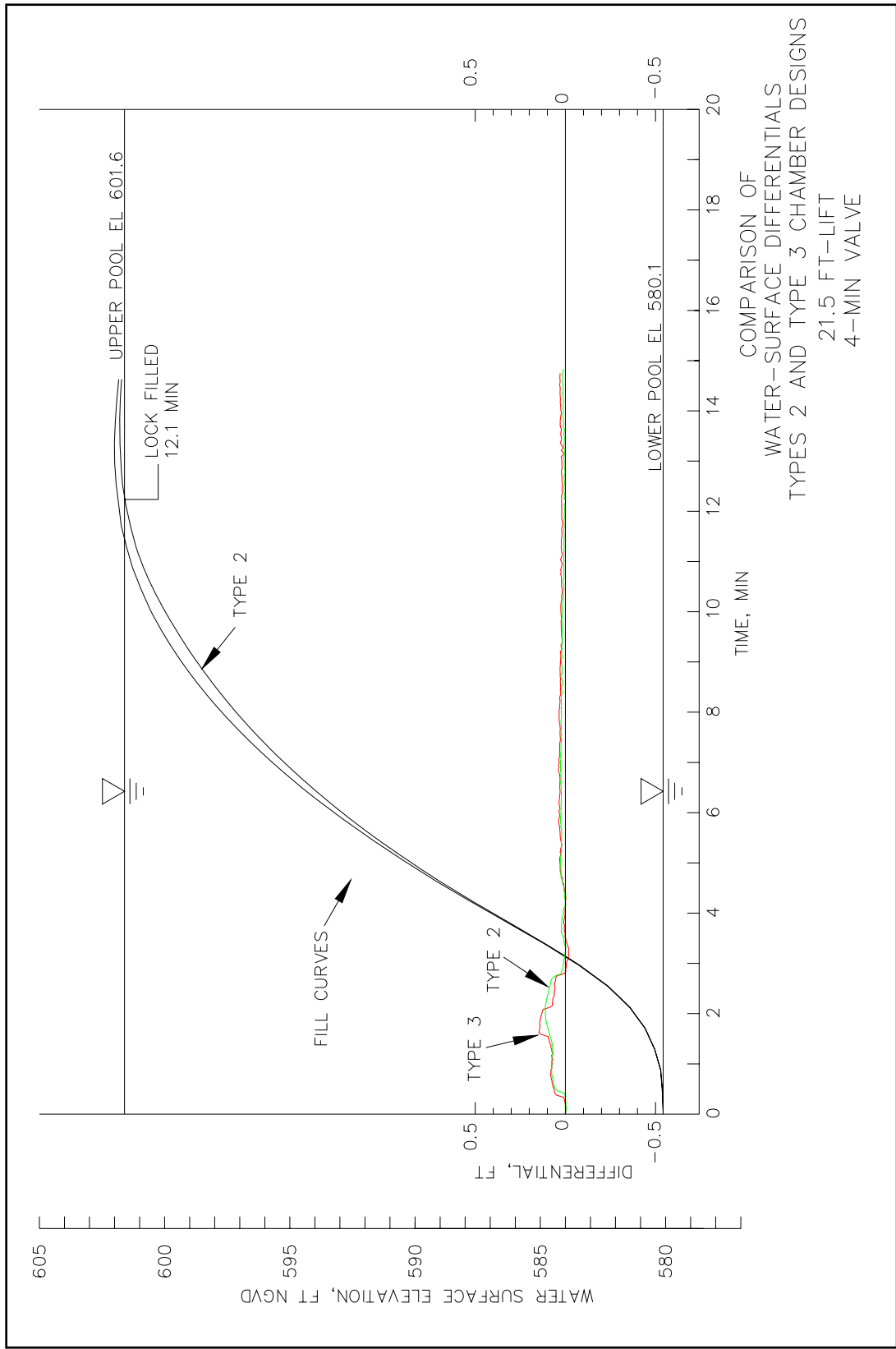


Plate 34



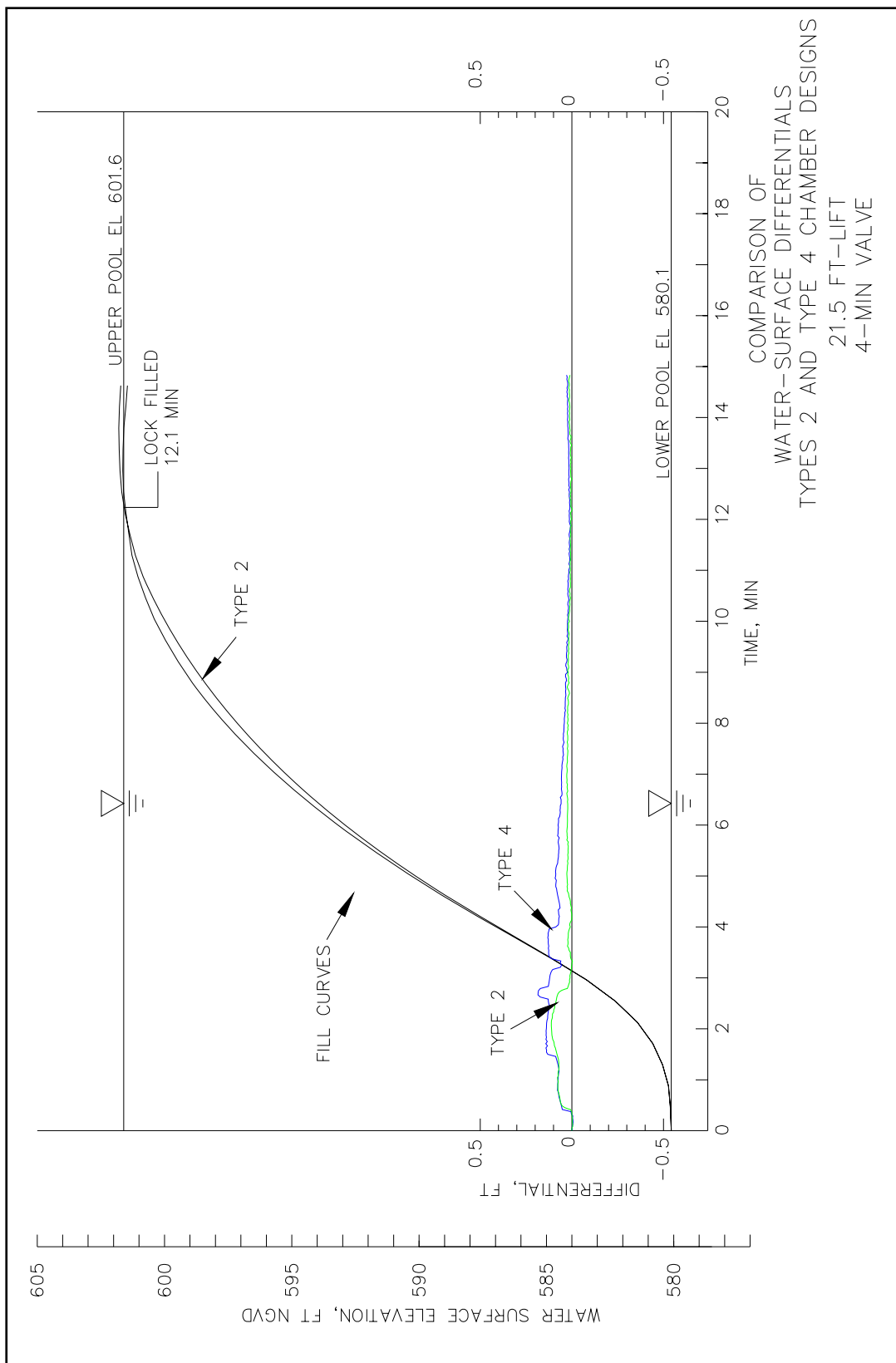
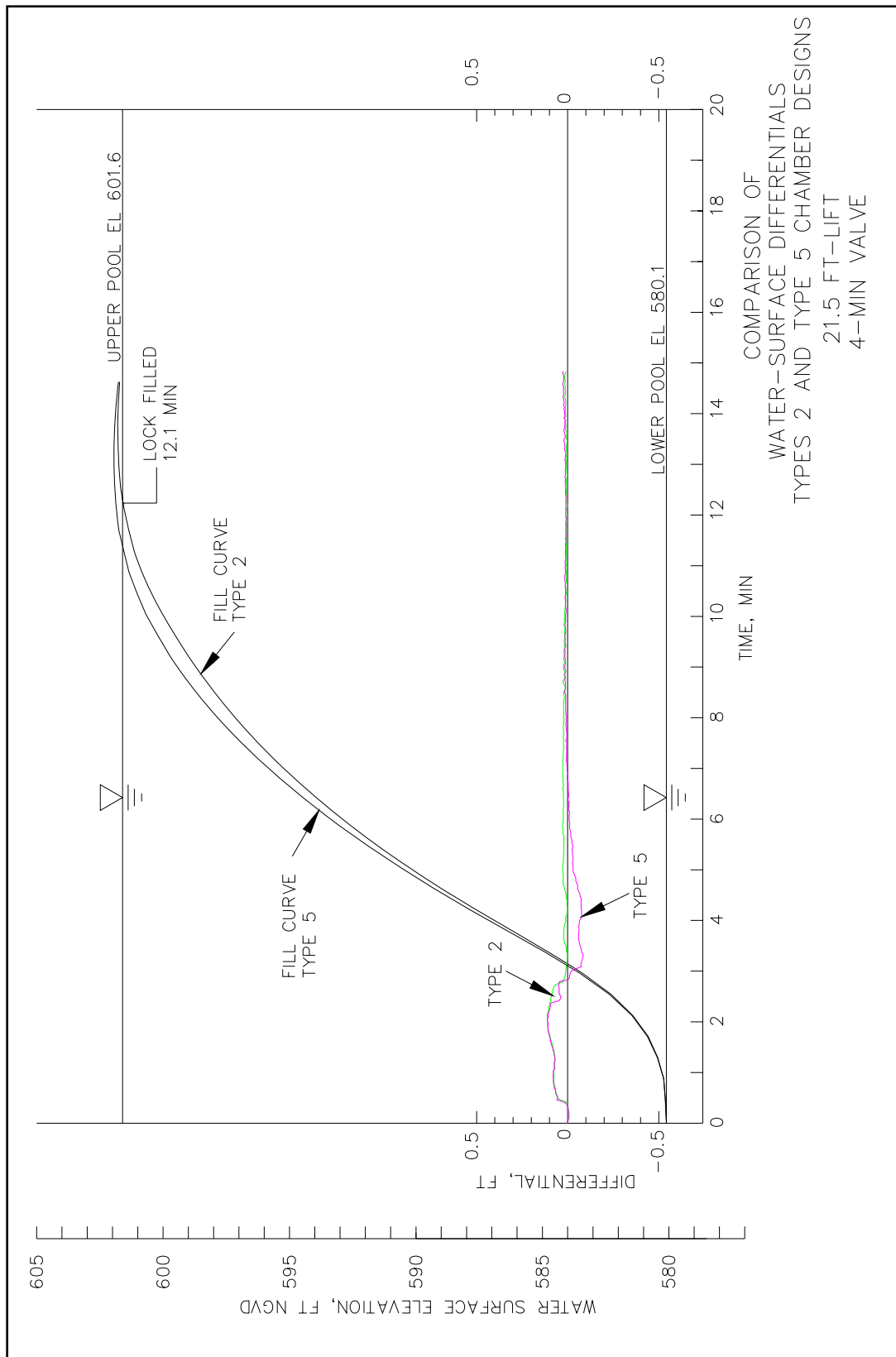


Plate 36



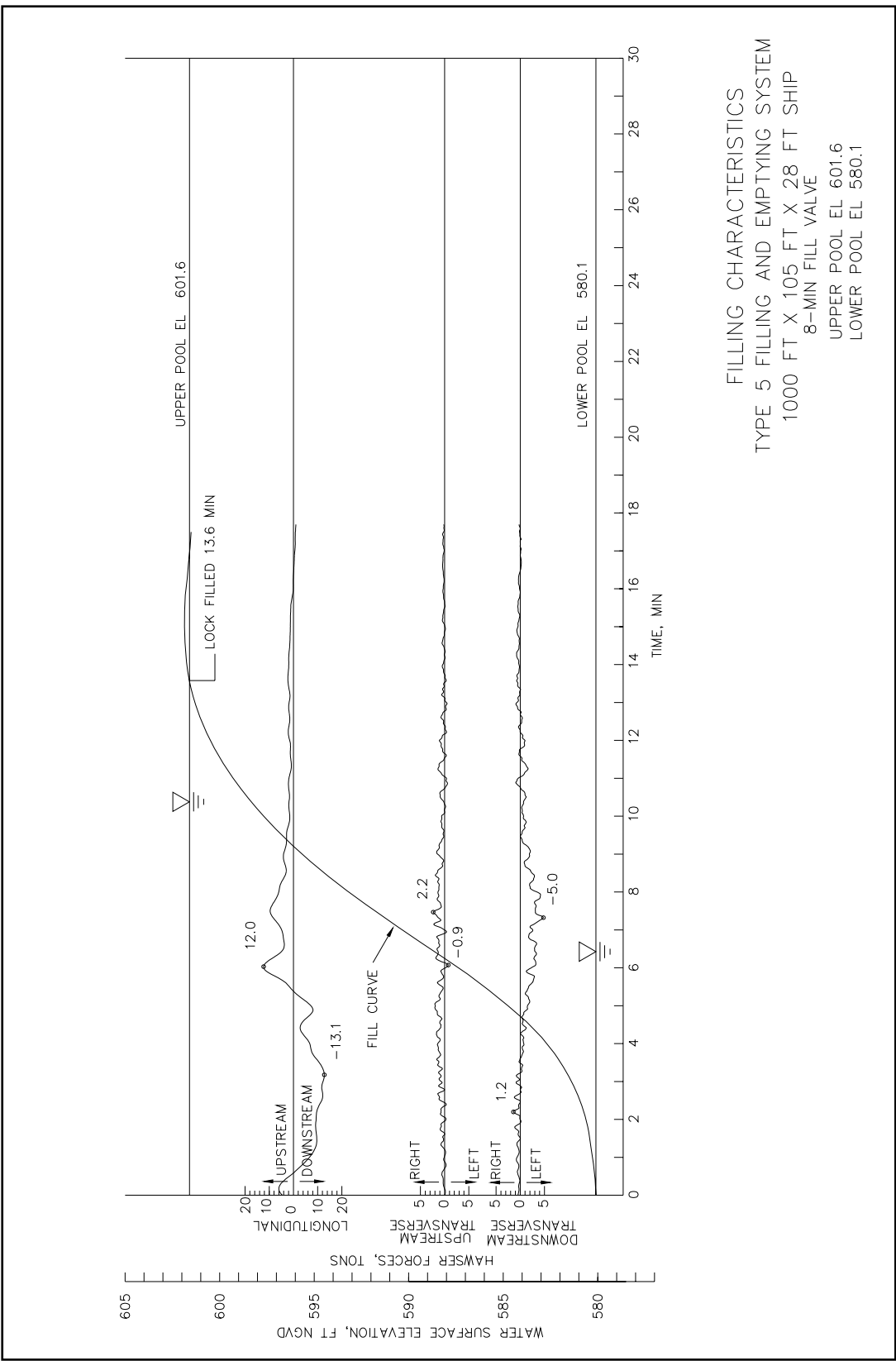
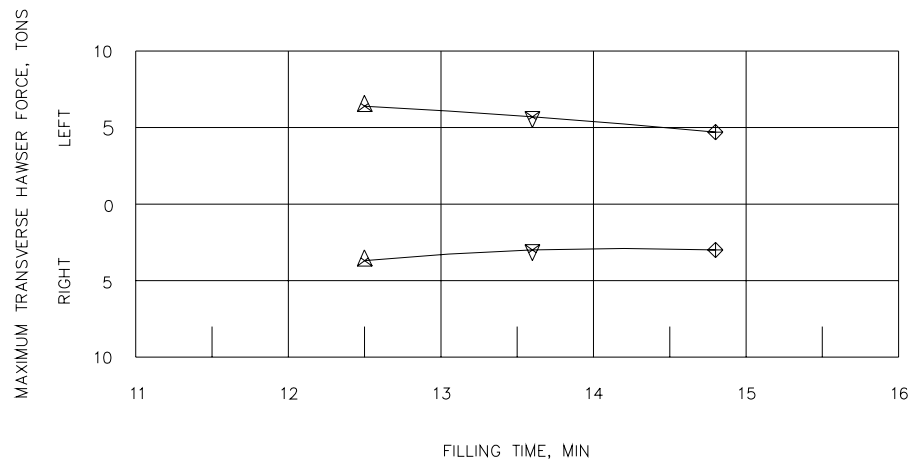
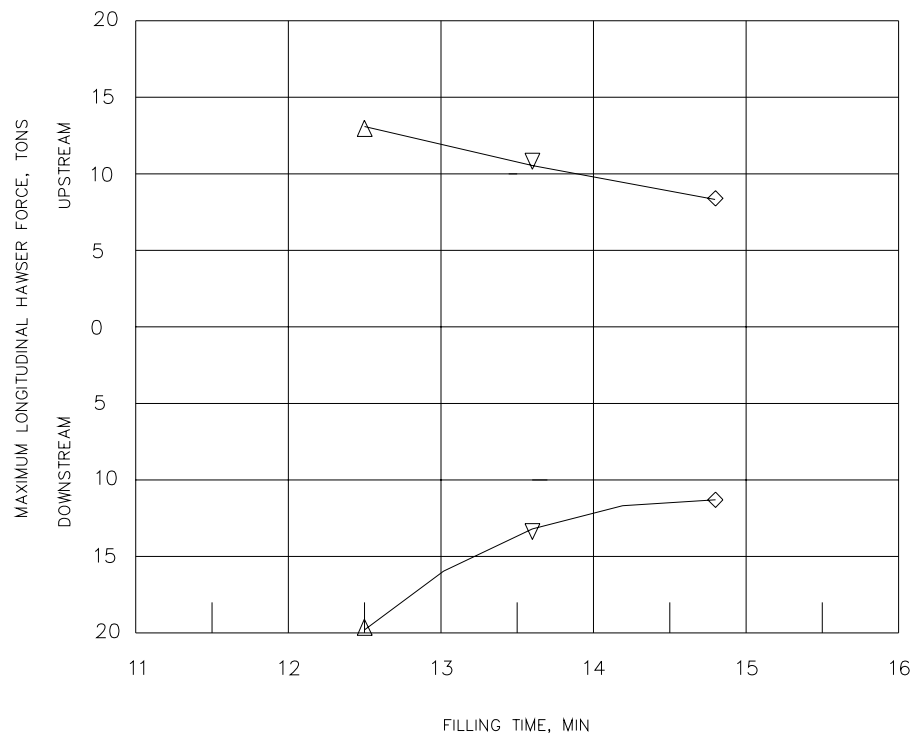
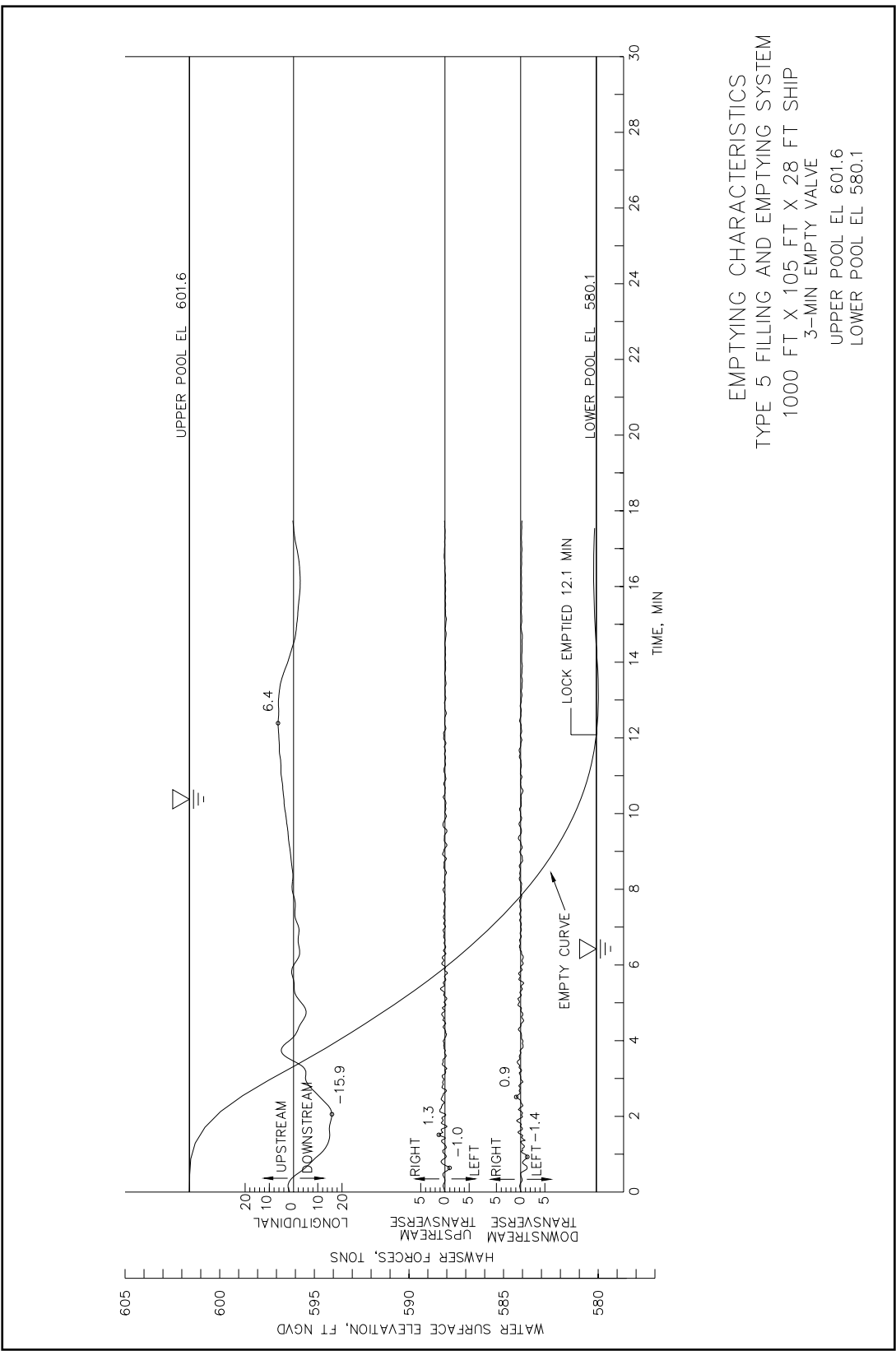


Plate 38

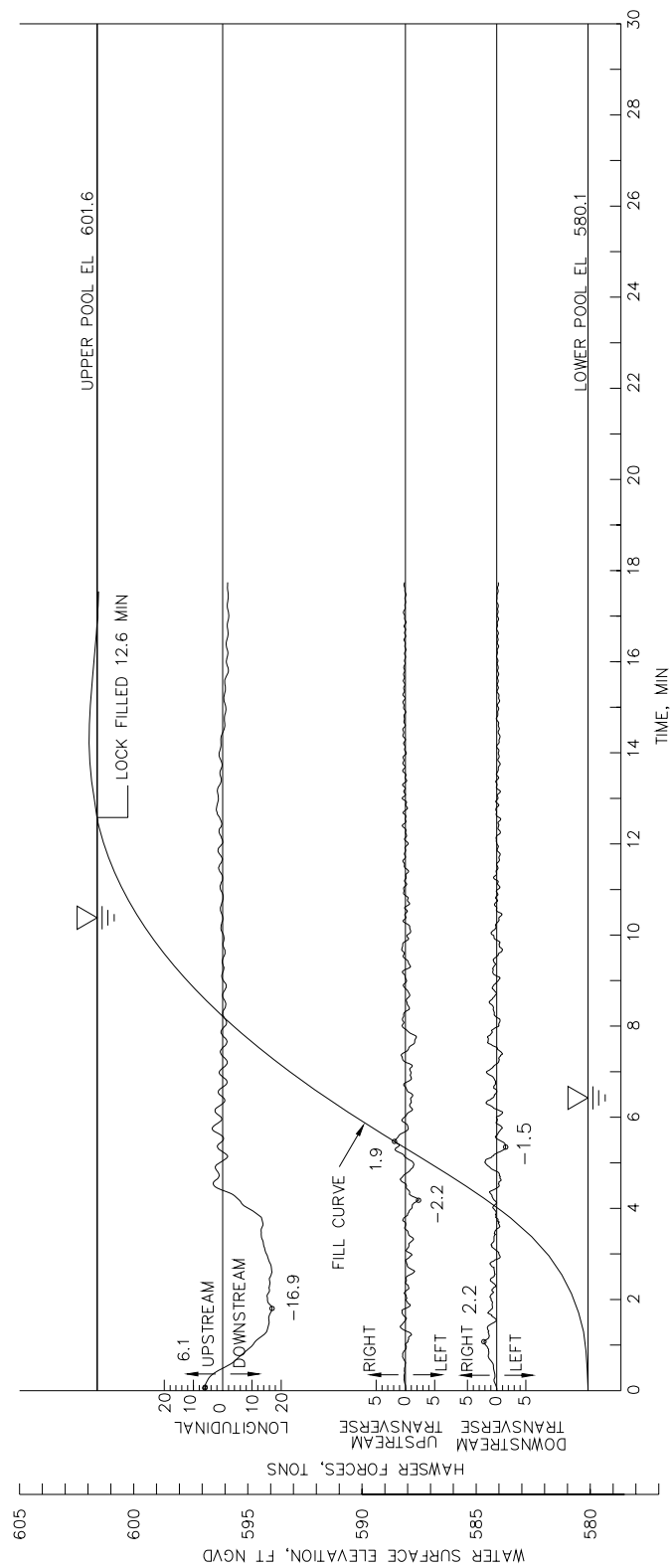


LEGEND	
SYMBOL	VALVE SCHEDULE, MIN
Δ	6
▽	8
◇	10

HAWSER FORCES
DURING FILLING
TYPE 5 DESIGN
FILLING AND EMPTYING SYSTEM
UPPER POOL EL 601.6
LOWER POOL EL 580.1
21.5-ft. LIFT



EMPTYING CHARACTERISTICS
TYPE 5 FILLING AND EMPTYING SYSTEM
1000 FT X 105 FT X 28 FT SHIP
3-MIN EMPTY VALVE
UPPER POOL EL 601.6
LOWER POOL EL 580.1



FILLING CHARACTERISTICS
 TYPE 12 FILLING AND EMPTYING SYSTEM
 1000 FT X 105 FT X 28 FT SHIP
 TEST NO. 87
 6-MIN FILL VALVE
 UPPER POOL EL 601.6
 LOWER POOL EL 580.1

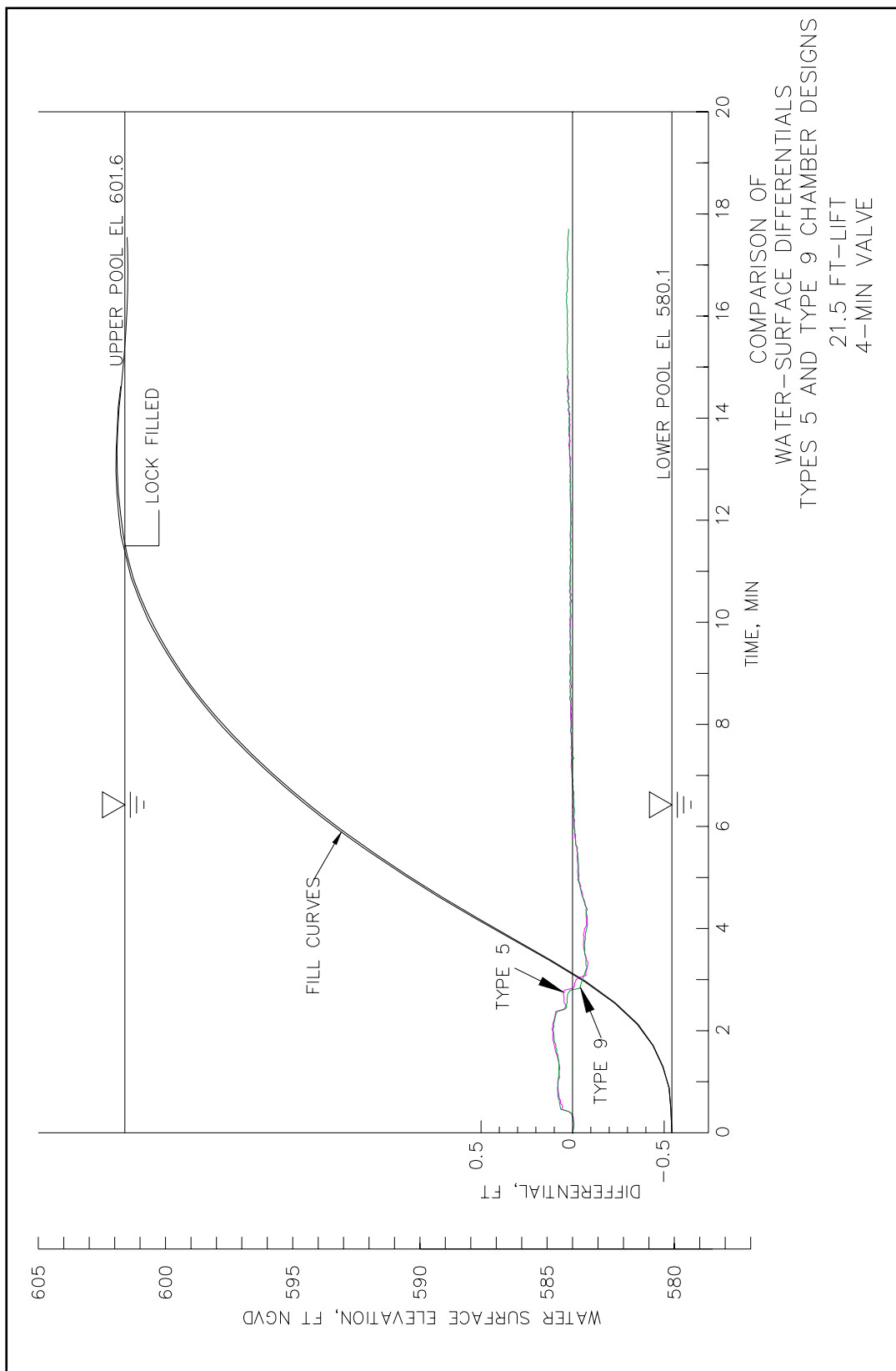
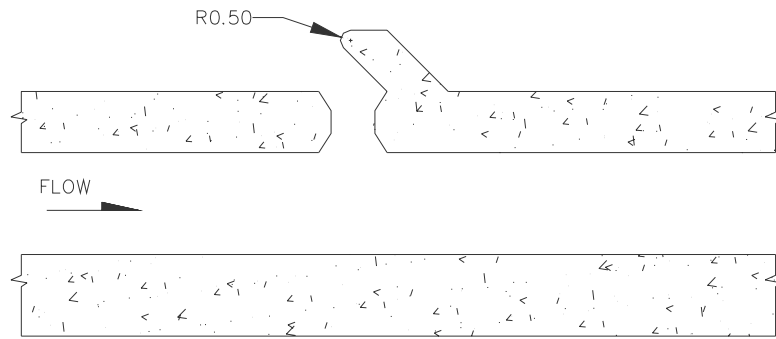
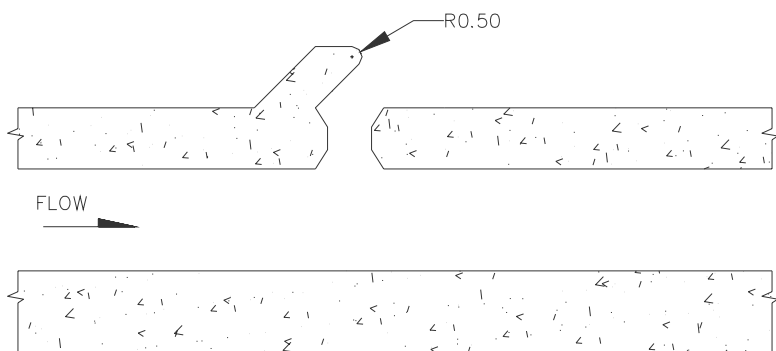


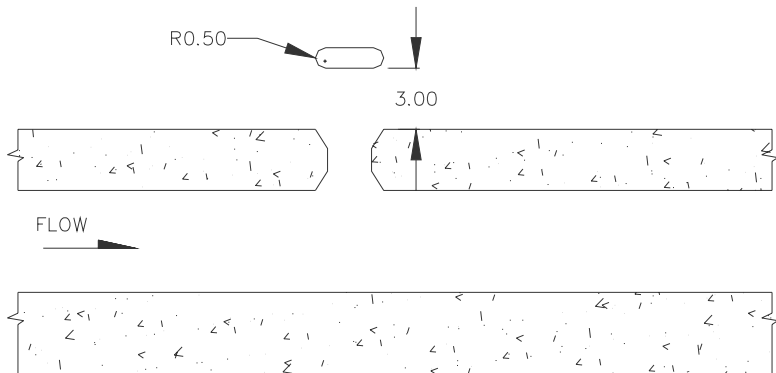
Plate 42



BAFFLE DESIGN FOR ROWS 1-7 UPPER PORTS



BAFFLE DESIGN FOR ROWS 8-10 UPPER PORTS



BAFFLE DESIGN FOR LOWER PORTS

DIMENSIONS ARE IN FT

TYPE 10 CHAMBER DESIGN

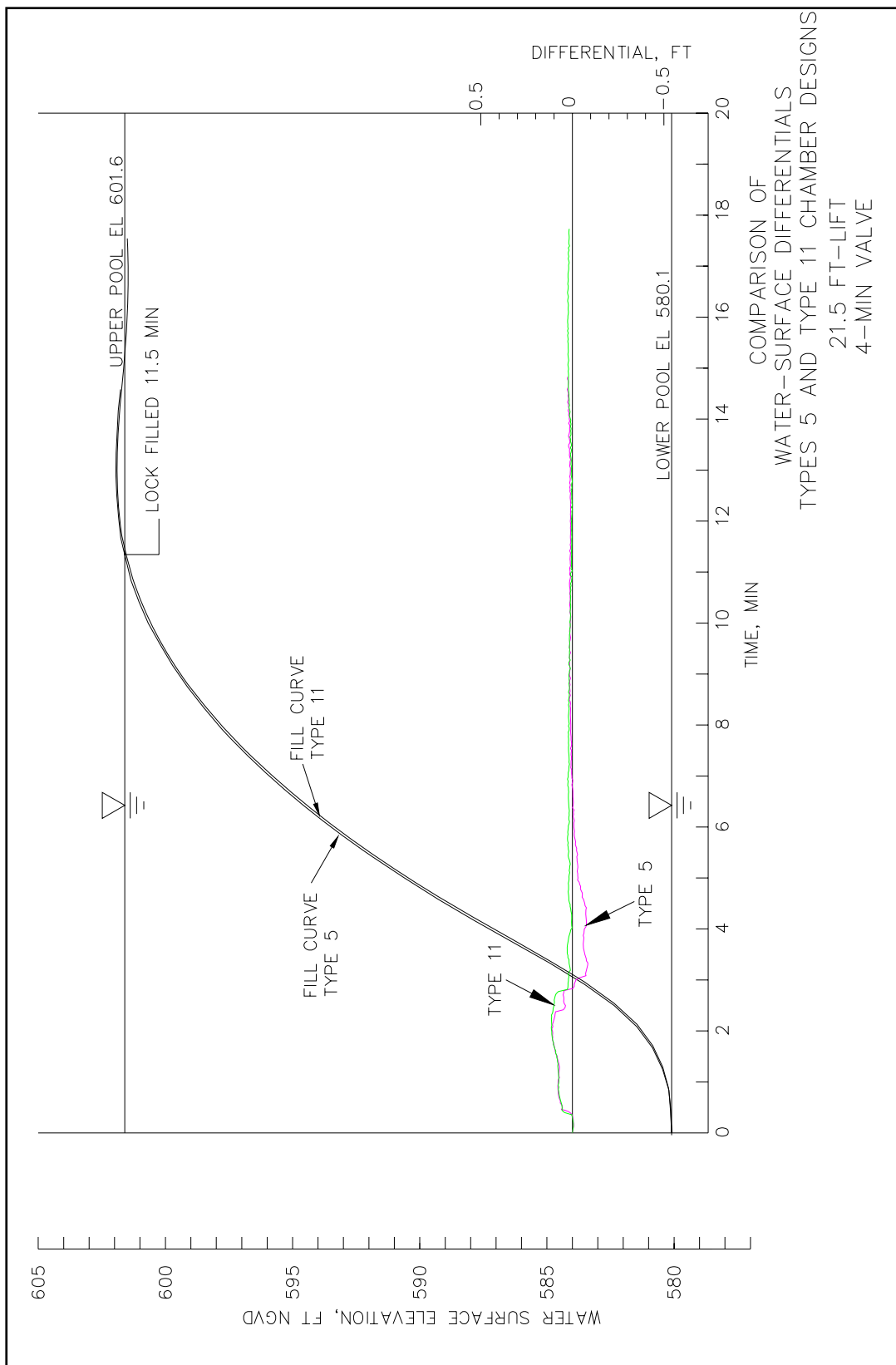
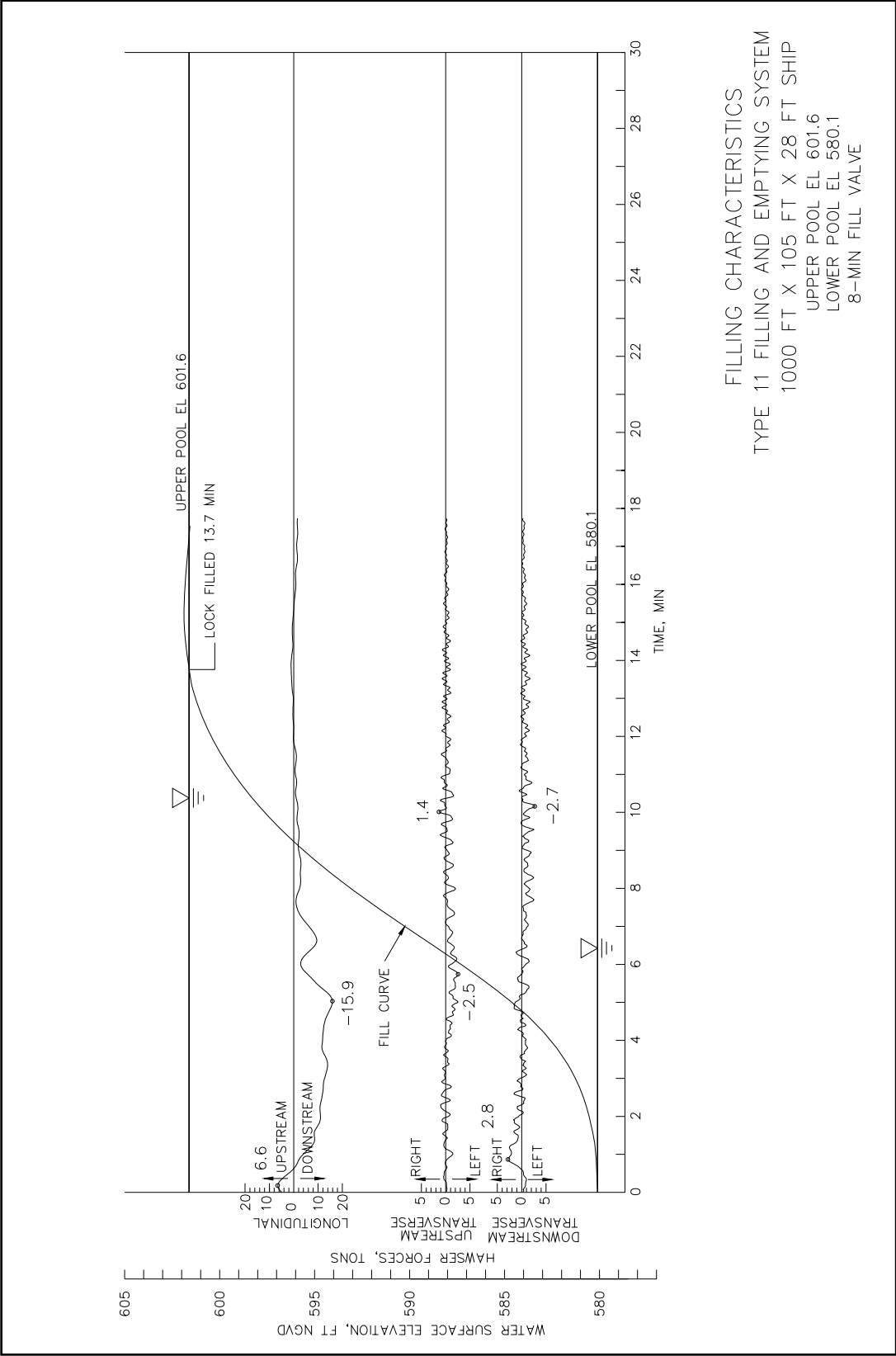
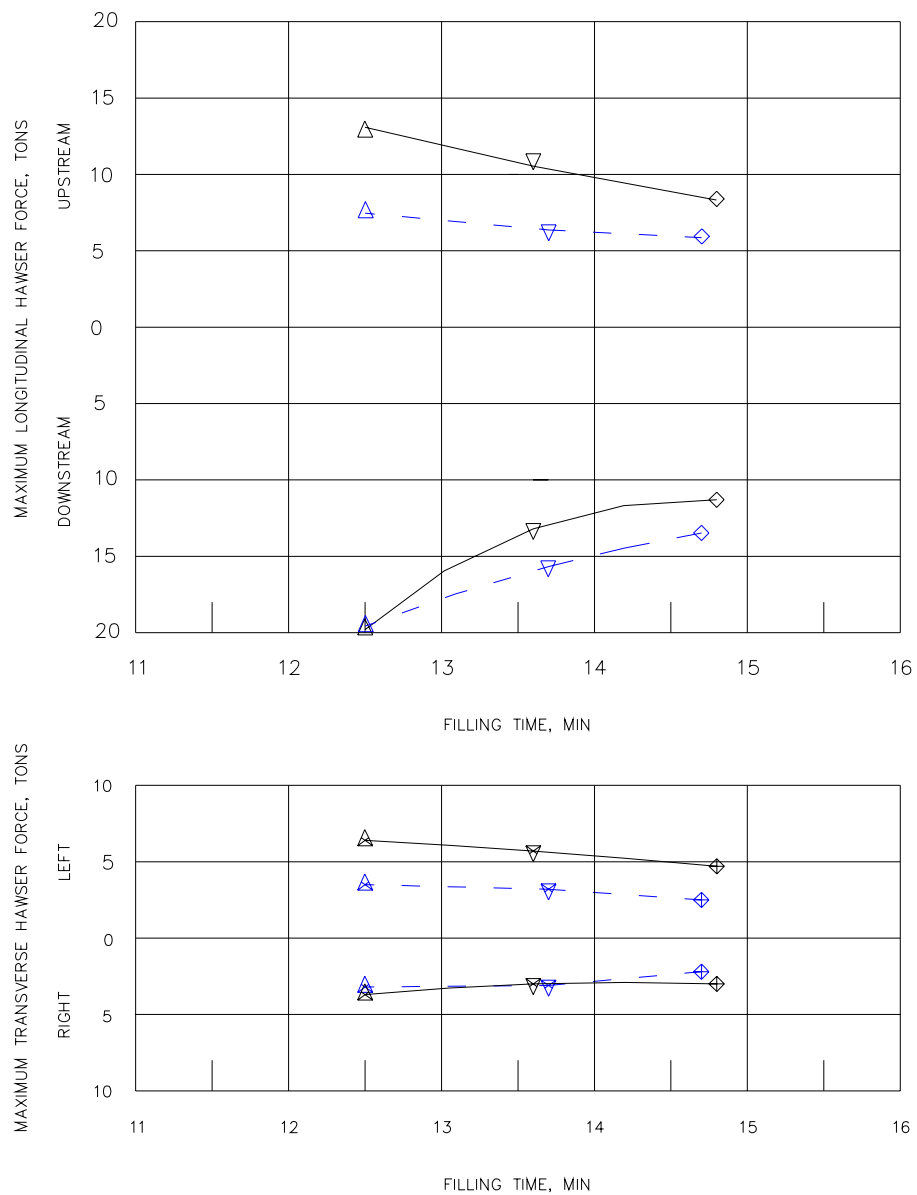
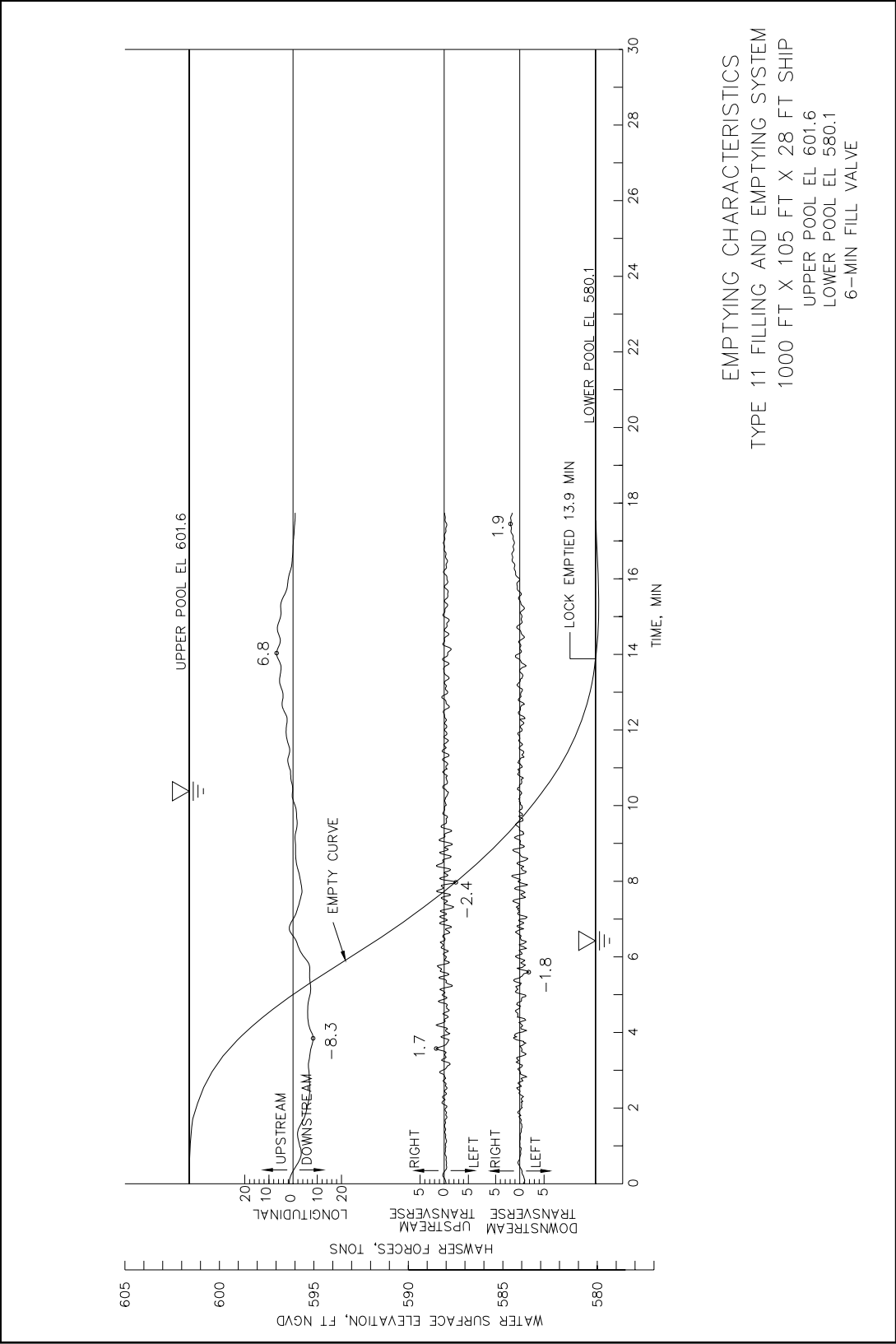


Plate 44

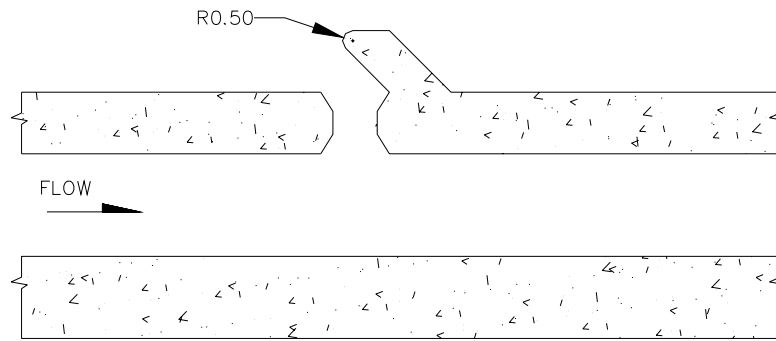




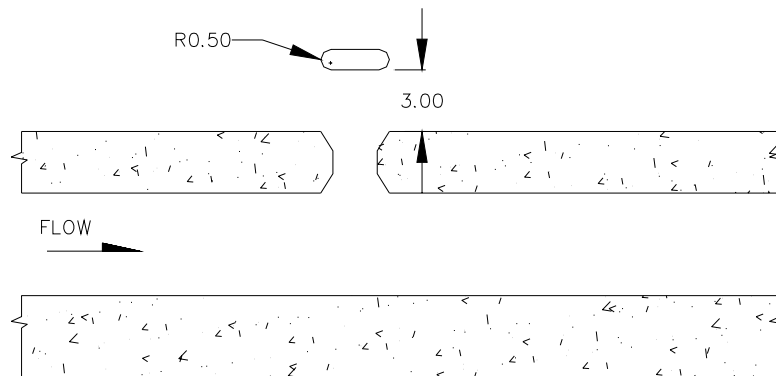
COMPARISON OF
HAWSER FORCES
DURING FILLING
TYPES 5 AND 11 DESIGN
FILLING AND EMPTYING SYSTEMS
UPPER POOL EL 601.6
LOWER POOL EL 580.1
21.5-ft. LIFT



EMPTYING CHARACTERISTICS
TYPE 11 FILLING AND EMPTYING SYSTEM
1000 FT X 105 FT X 28 FT SHIP
UPPER POOL EL 601.6
LOWER POOL EL 580.1
6-MIN FILL VALVE



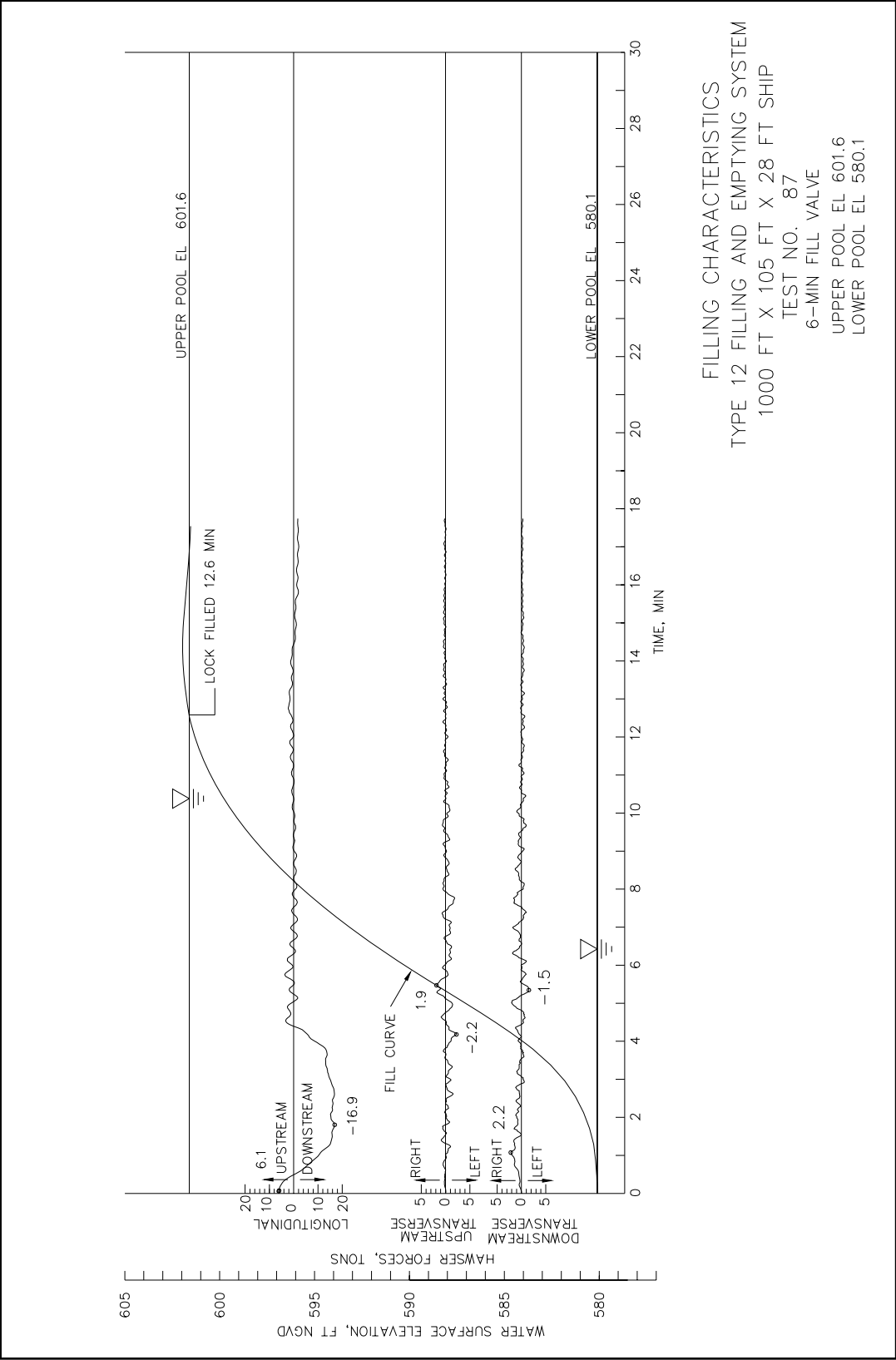
BAFFLE DESIGN FOR ROWS 1, 2, 4, 6, 8, and 10 UPPER PORTS
PORTS IN ROWS 3, 5, 7, AND 9 WERE BLOCKED OFF

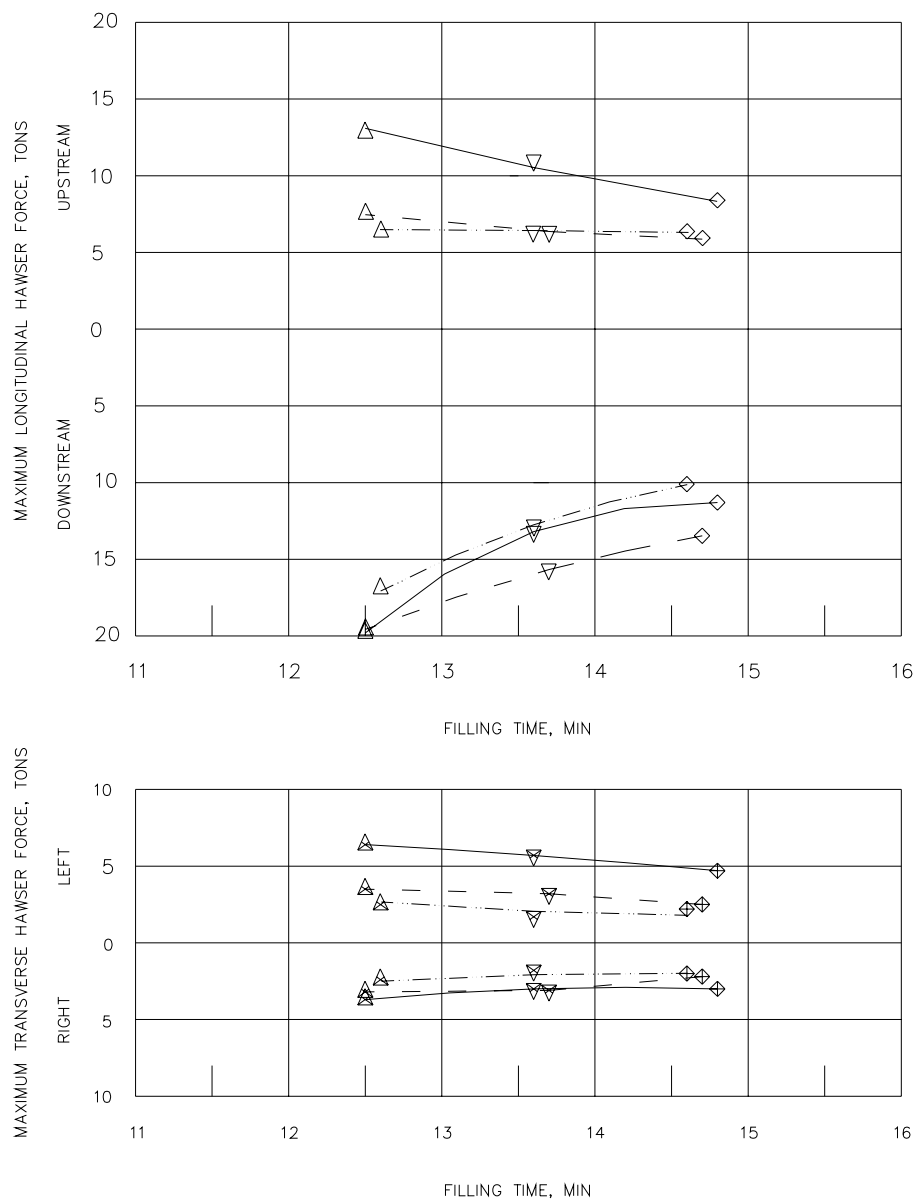


BAFFLE DESIGN FOR ROWS 11, 13, 15, 17, 19, AND 20 LOWER PORTS
PORTS IN ROWS 12, 14, 16, AND 18 WERE BLOCKED OFF

DIMENSIONS ARE IN FT

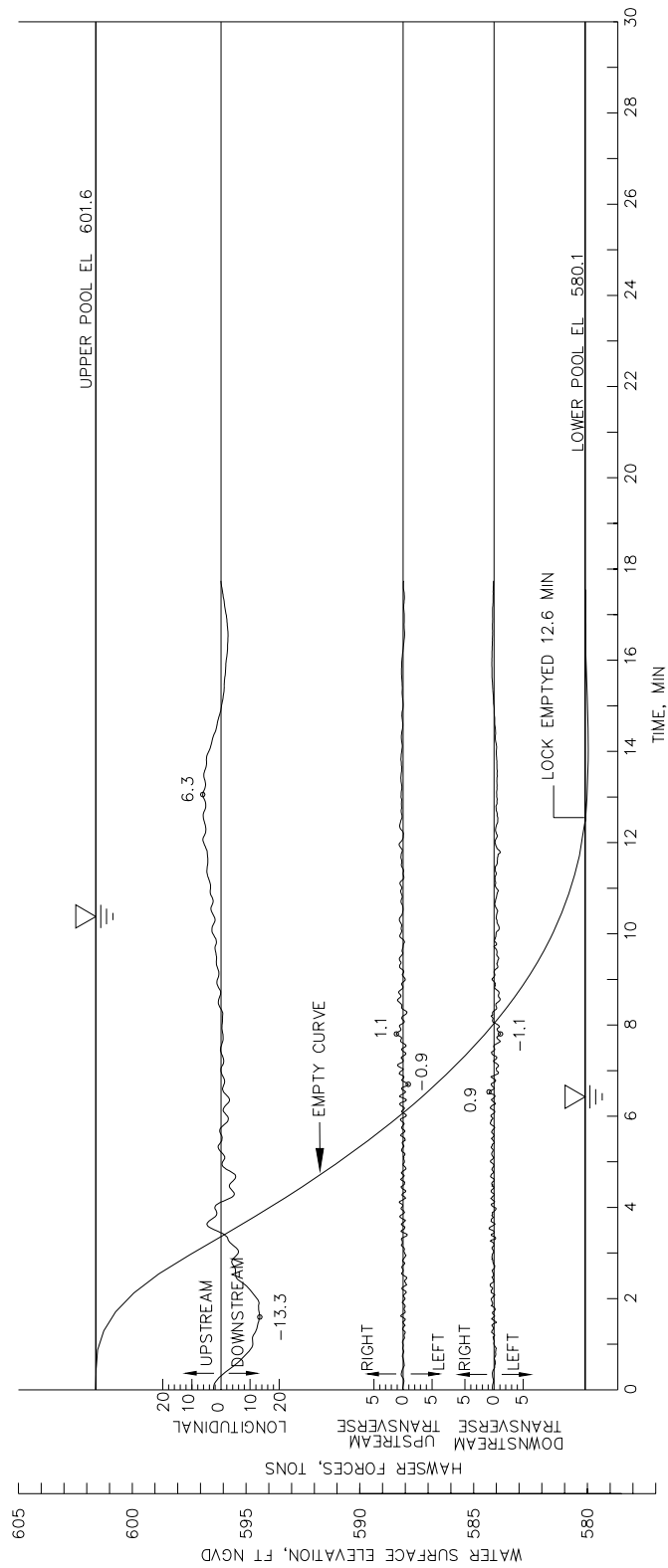
TYPE 12 CHAMBER DESIGN



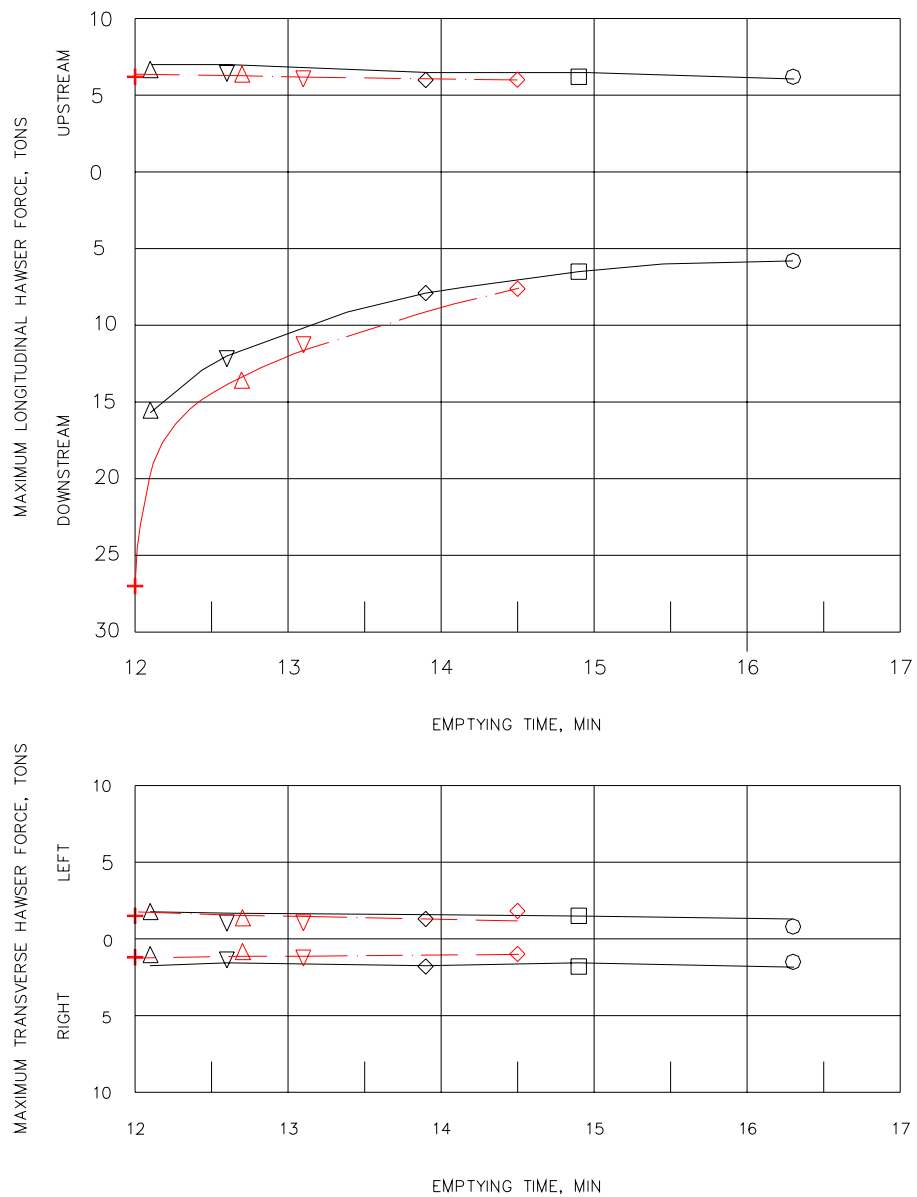


LEGEND	
SYMBOL	VALVE SCHEDULE, MIN
△	6
▽	8
◇	10
—	TYPE 5
- - -	TYPE 11
- · - · -	TYPE 12

COMPARISON OF
 HAWSER FORCES
 DURING FILLING
 TYPES 5, 11, AND 12 DESIGNS
 UPPER POOL EL 601.6
 LOWER POOL EL 580.1
 21.5-ft. LIFT



FILLING CHARACTERISTICS
 TYPE 12 FILLING AND EMPTYING SYSTEM
 1000 FT X 105 FT X 28 FT SHIP
 TEST NO. 86
 3-MIN EMPTY VALVE
 UPPER POOL EL 601.6
 LOWER POOL EL 580.1

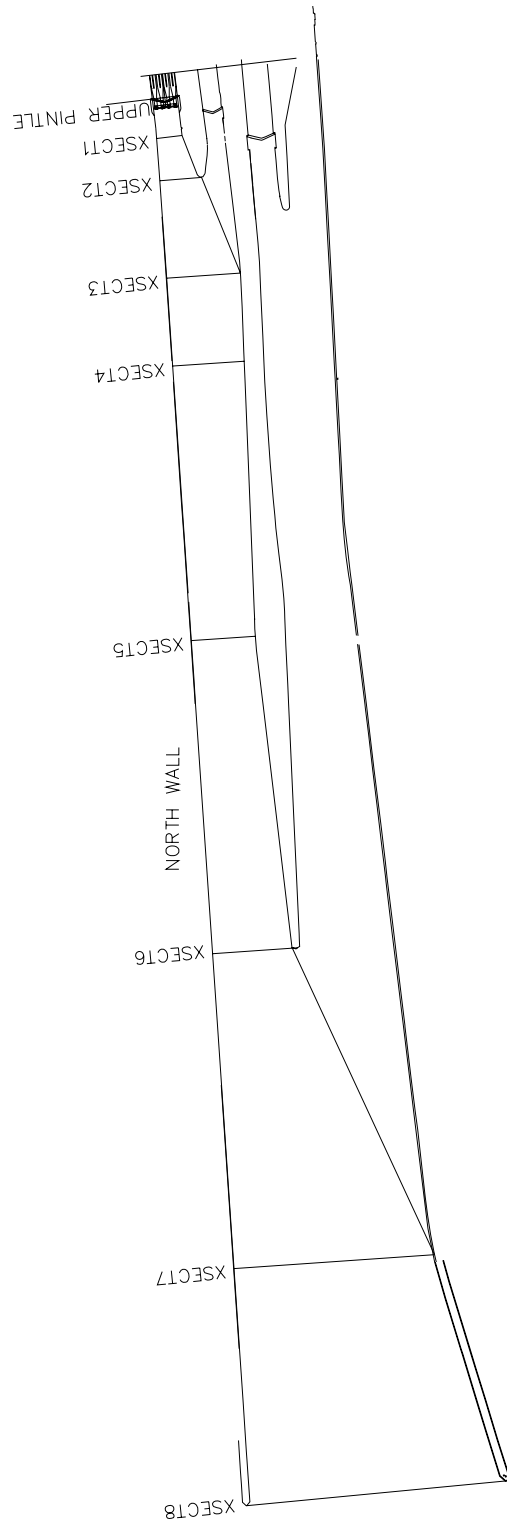


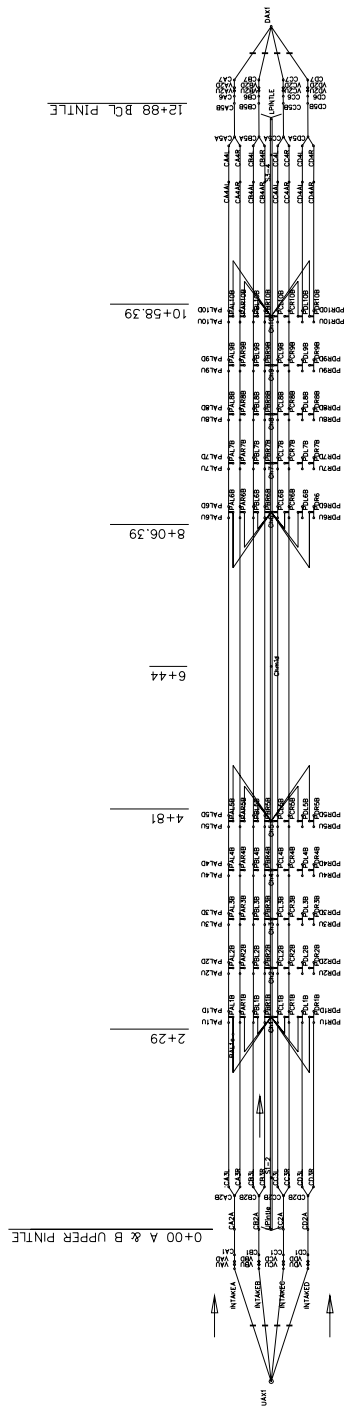
LEGEND			
SYMBOL	VALVE SCHEDULE, MIN	DESIGN	LINETYPE
+	2	5	—
△	3	12	- - -
▽	4		
◇	6		
□	8		
○	10		

COMPARISON OF
HAWSER FORCES
DURING EMPTYING
TYPES 5 AND 12 DESIGN
FILLING AND EMPTYING SYSTEMS
UPPER POOL EL 601.6
LOWER POOL EL 580.1
21.5-ft. LIFT

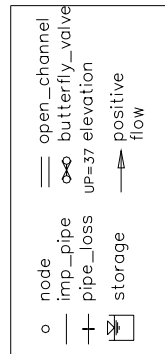


LOCATION OF CROSS SECTIONS
IN UPPER APPROACH



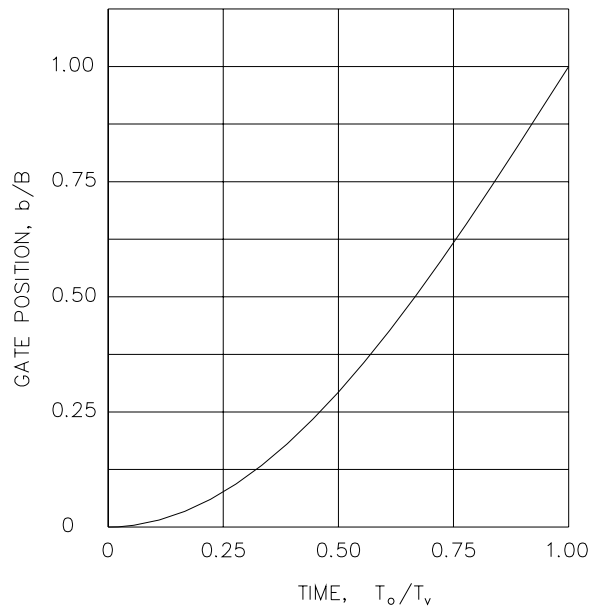


PLAN - FILLING AND EMPTYING SYSTEM



SOO ILCS PLAN A
FILLING AND EMPTYING SYSTEM
LOCKSIM SCHEMATIC

WES CURVE



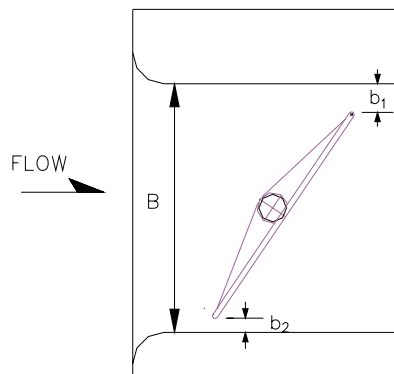
b/B	T_o/T_v
0	0
0.001	0.022
0.004	0.056
0.015	0.111
0.034	0.167
0.060	0.222
0.094	0.278
0.134	0.333
0.181	0.389
0.234	0.444
0.293	0.500
0.357	0.555
0.426	0.611
0.500	0.667
0.577	0.722
0.658	0.778
0.741	0.833
0.826	0.889
0.913	0.944
1.000	1.000

T_o = TIME SINCE OPENING BEGAN

T_v = TIME TO OPEN FULL

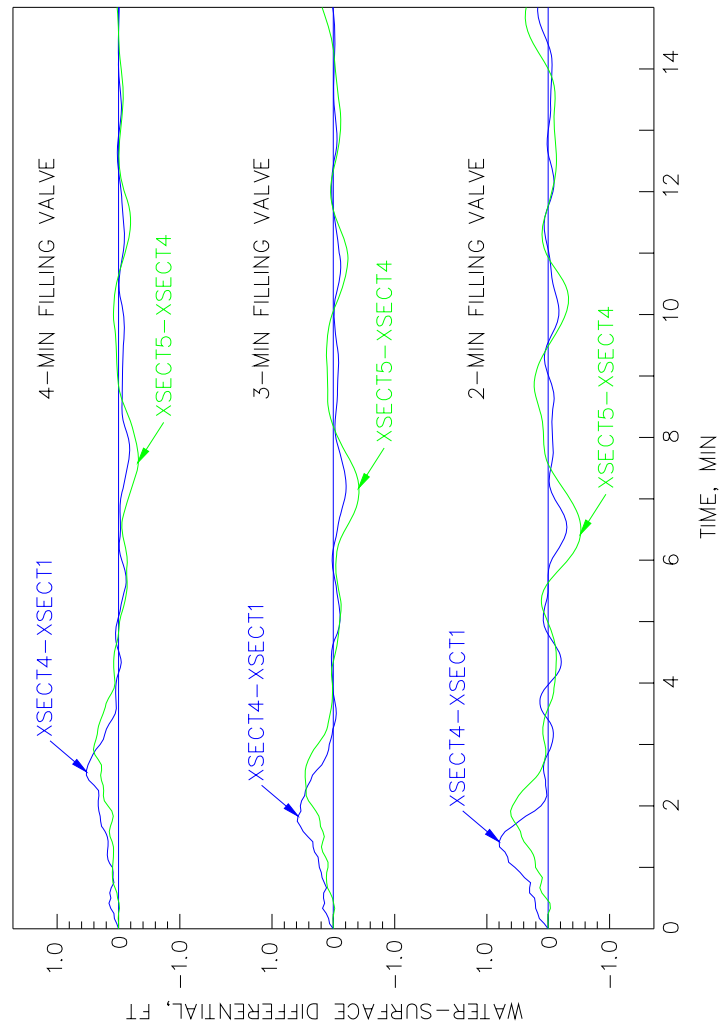
B = 12 FT

b = VERTICAL DIST. FROM LIP TO ROOF +
VERTICAL DIST. FROM LIP TO FLOOR
($b_1 + b_2$)

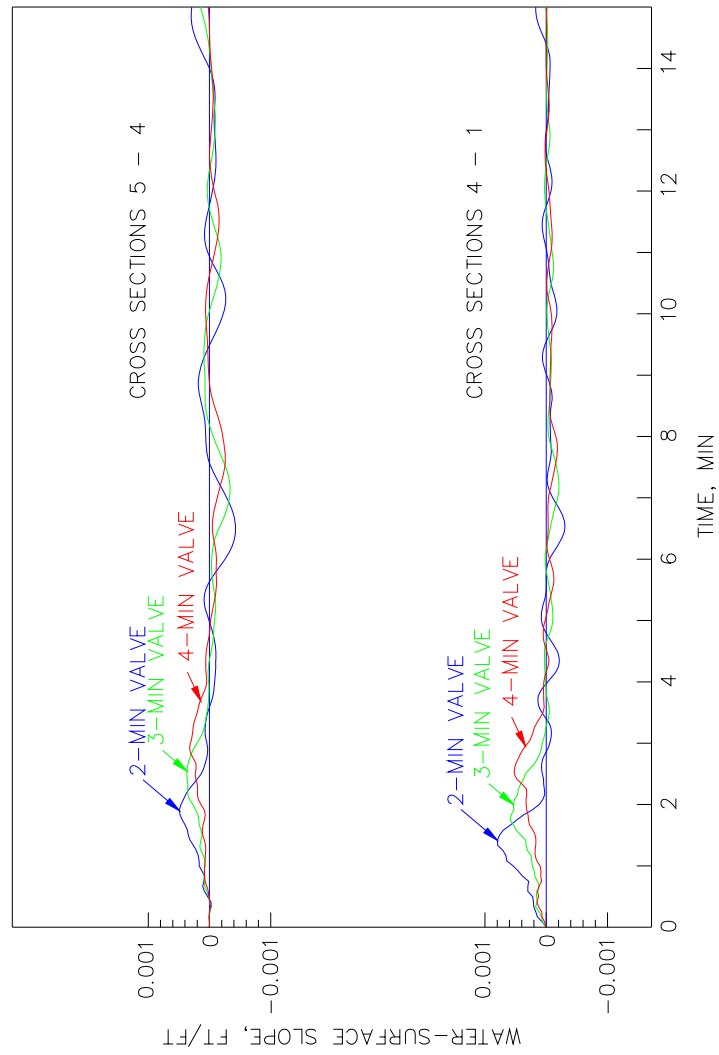


SECTION

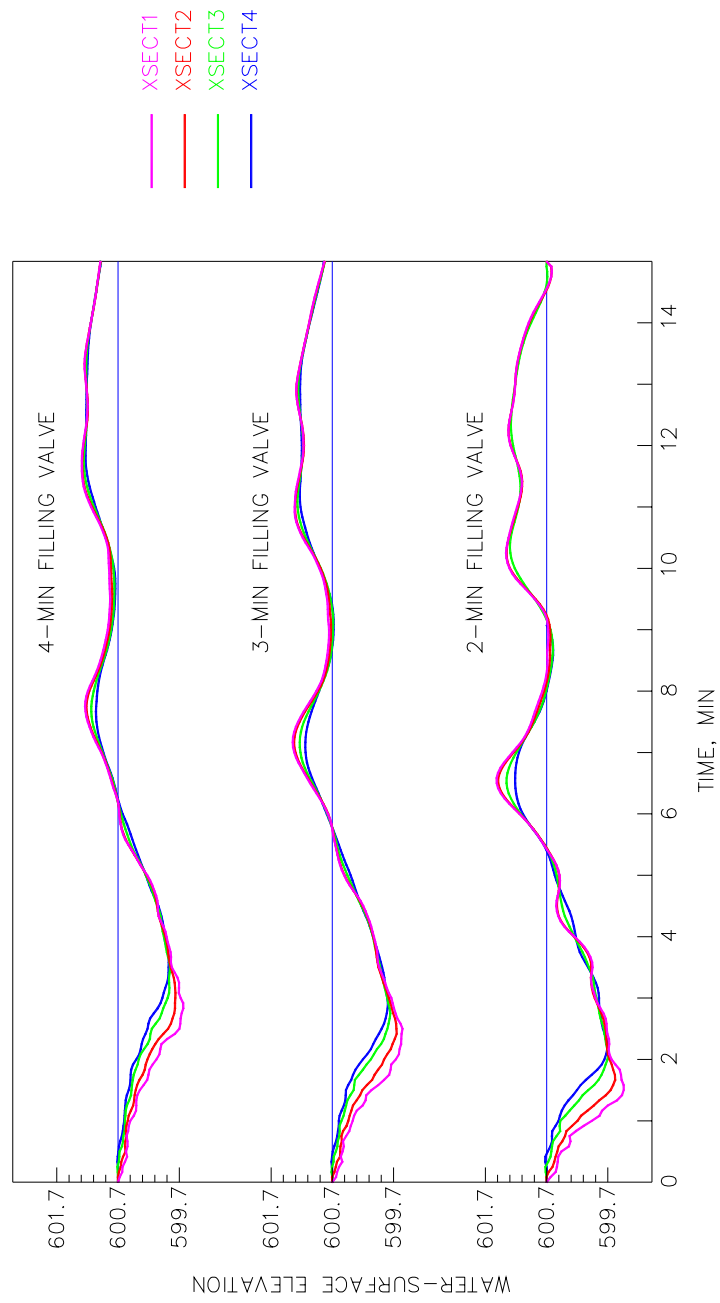
VALVE CURVE



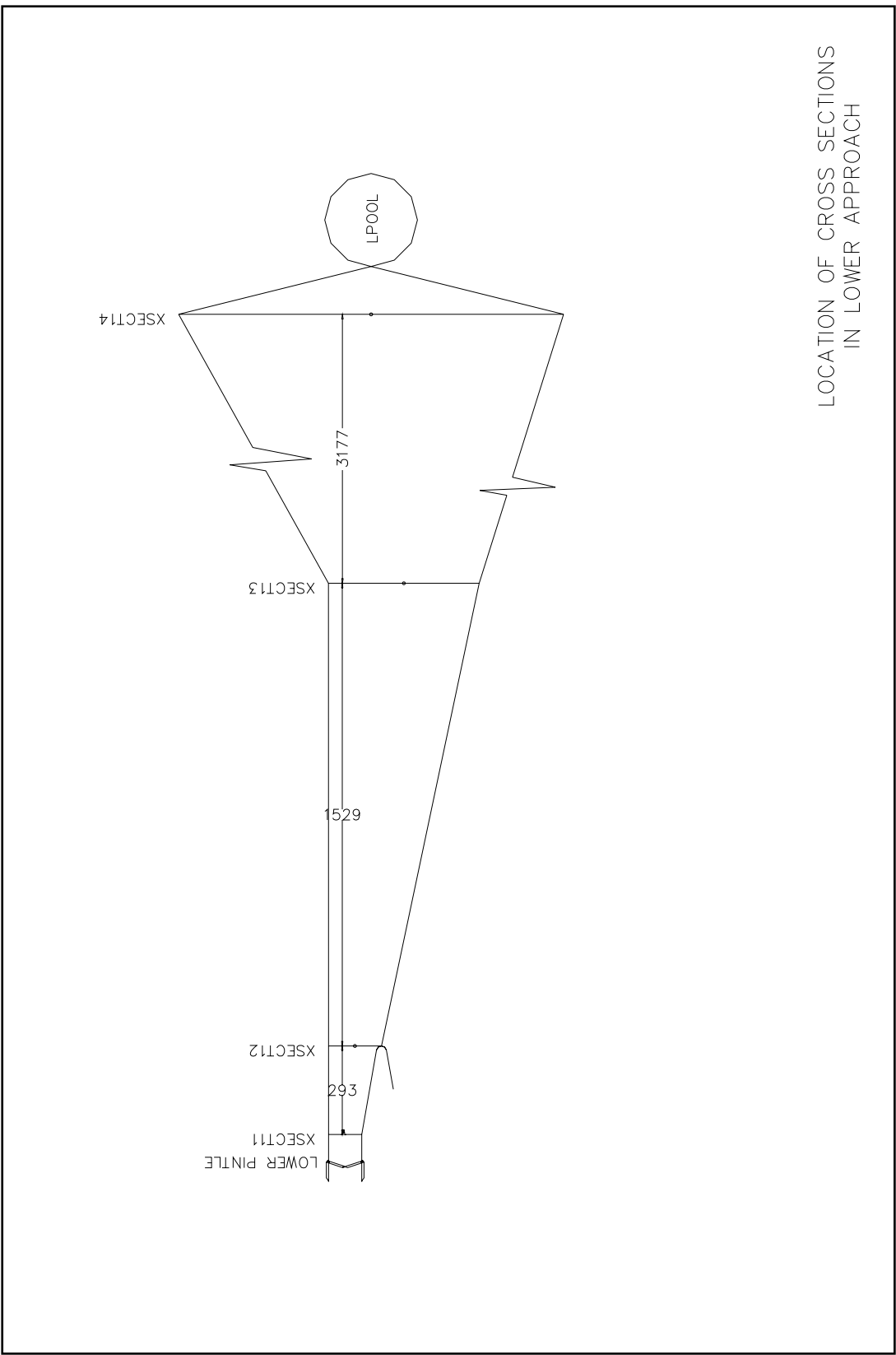
COMPARISON OF
WATER-SURFACE DIFFERENTIALS
UPPER APPROACH
21.5 FT-LIFT



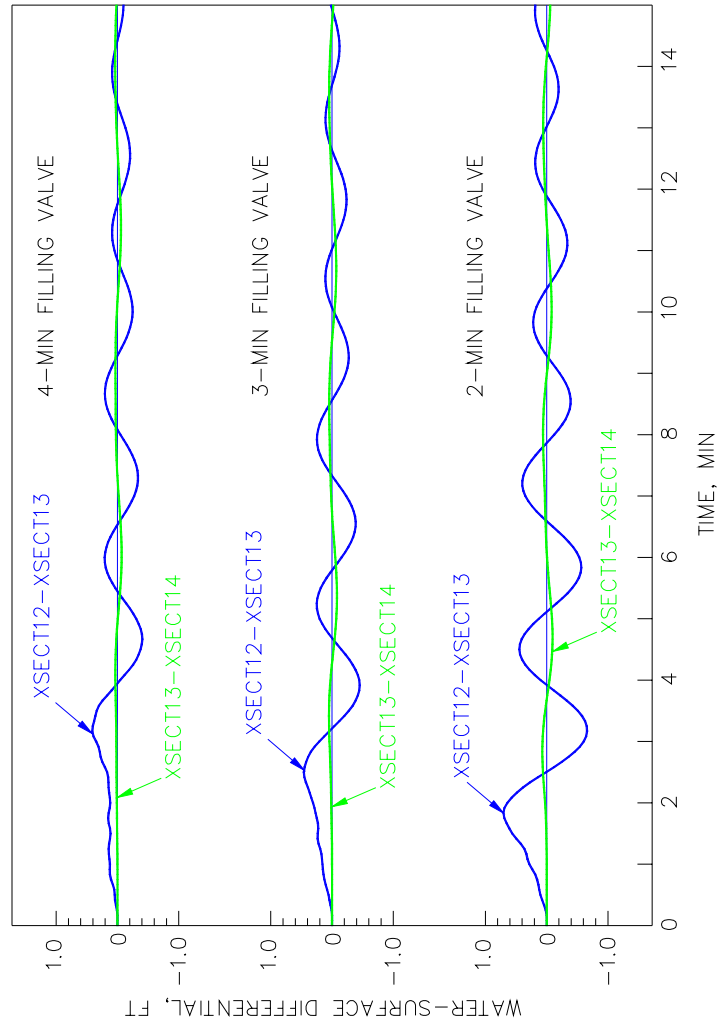
COMPARISON OF
WATER-SURFACE SLOPES
UPPER APPROACH
21.5 FT-LIFT



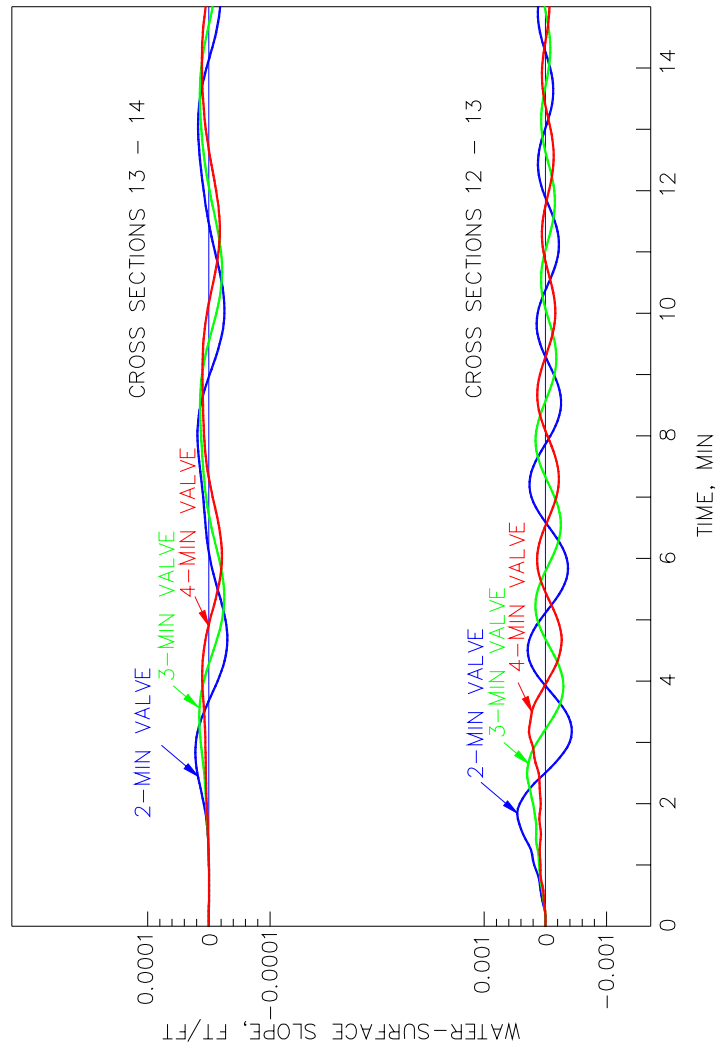
WATER-SURFACE ELEVATIONS
UPPER APPROACH
CROSS SECTIONS 1-4
21.5 FT-LIFT



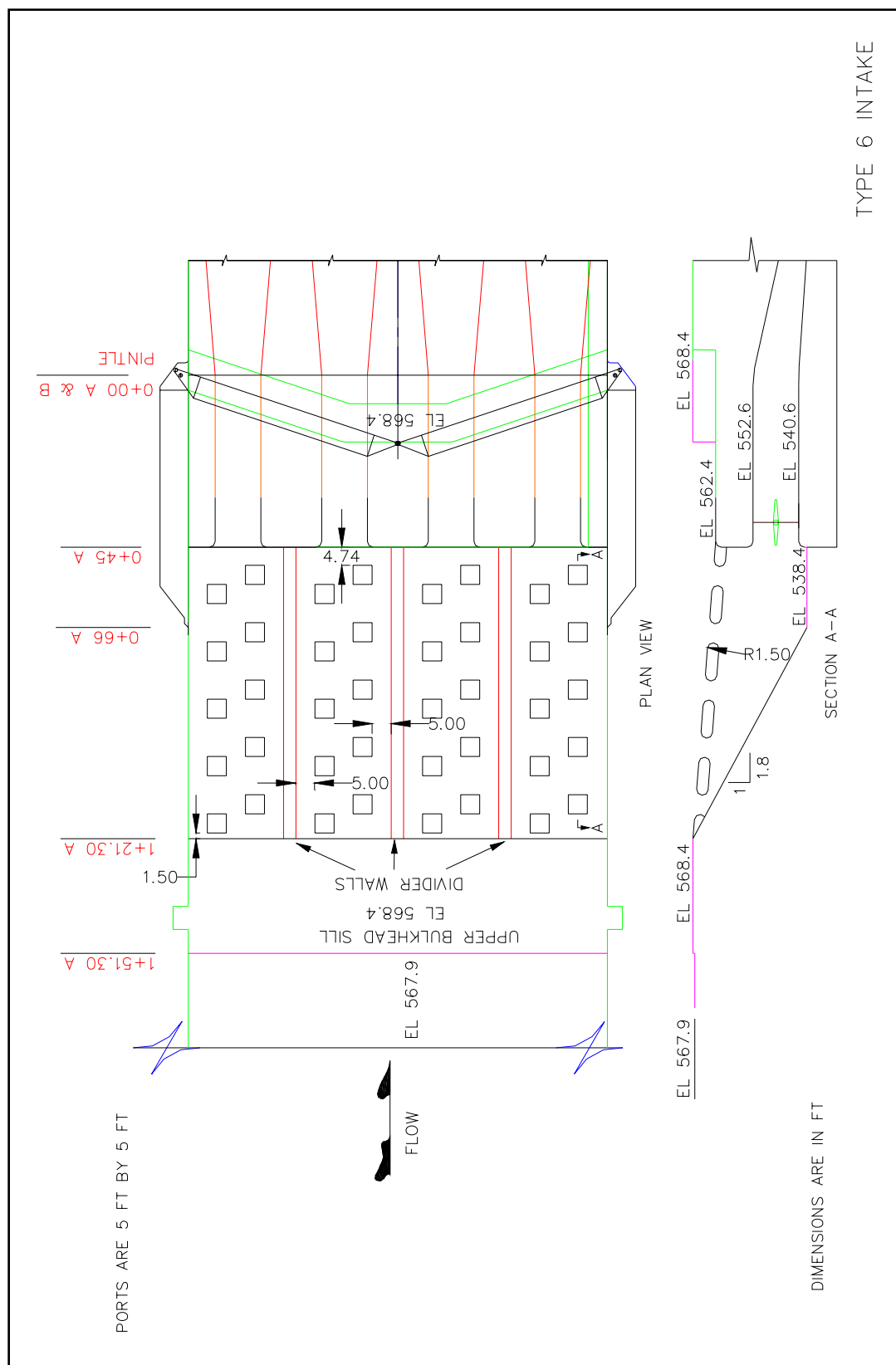
LOCATION OF CROSS SECTIONS
IN LOWER APPROACH

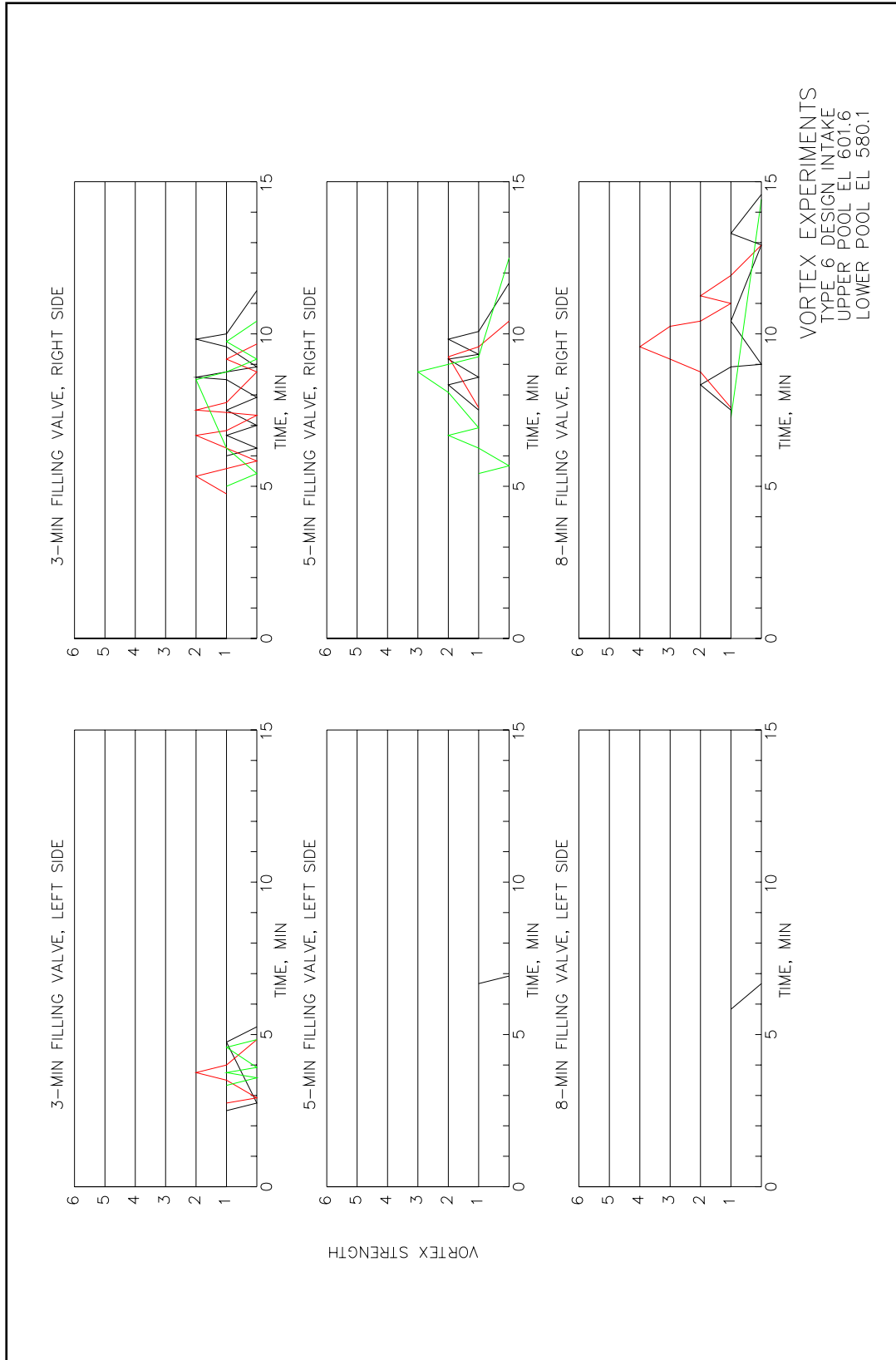


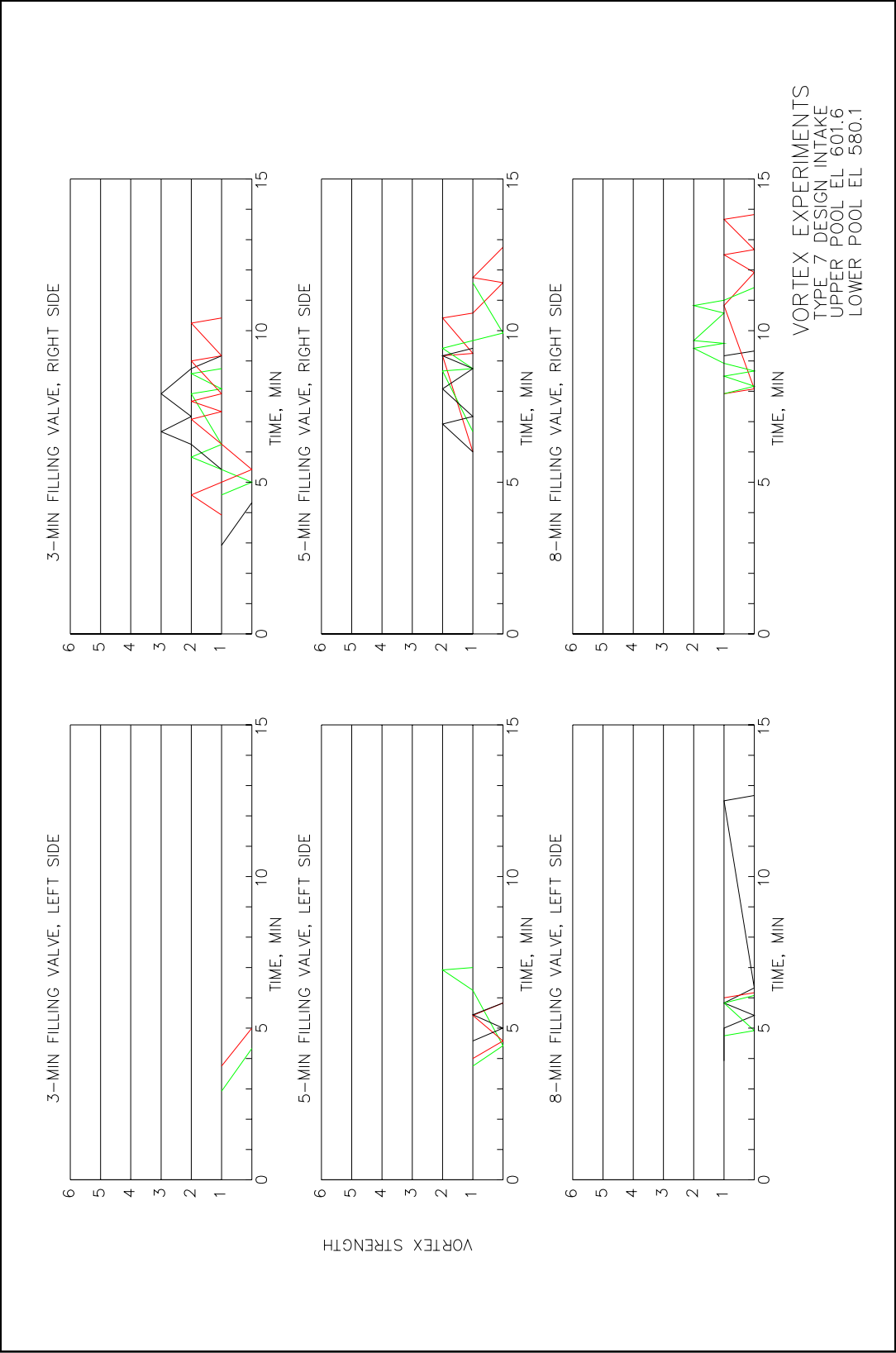
COMPARISON OF
WATER-SURFACE DIFFERENTIALS
LOWER APPROACH
21.5 FT-LIFT

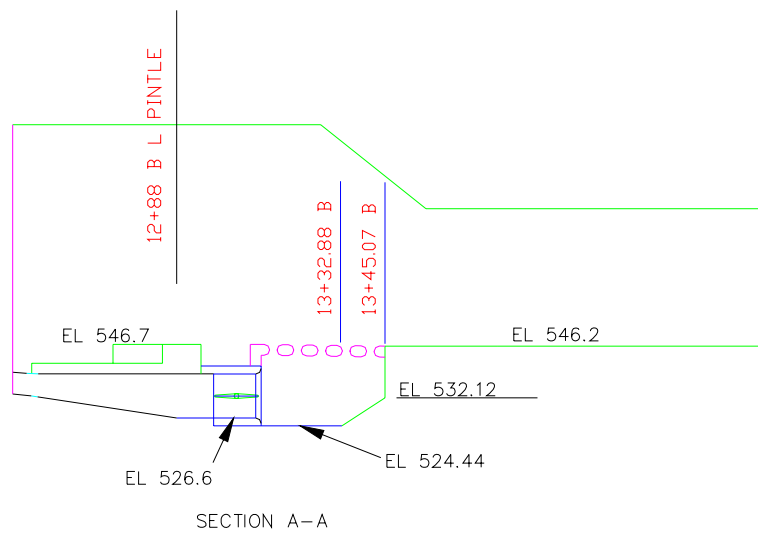
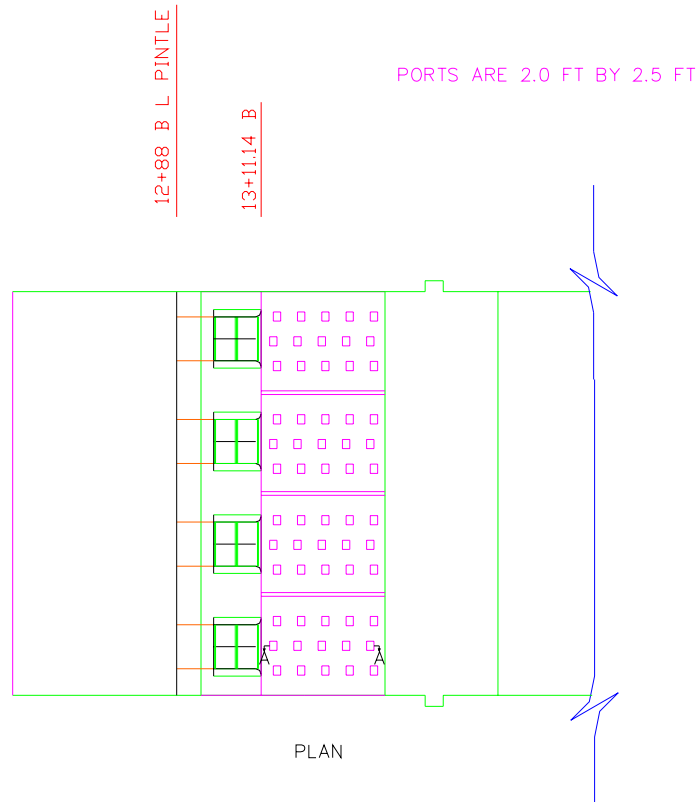


COMPARISON OF
WATER-SURFACE SLOPES
LOWER APPROACH
21.5 FT-LIFT



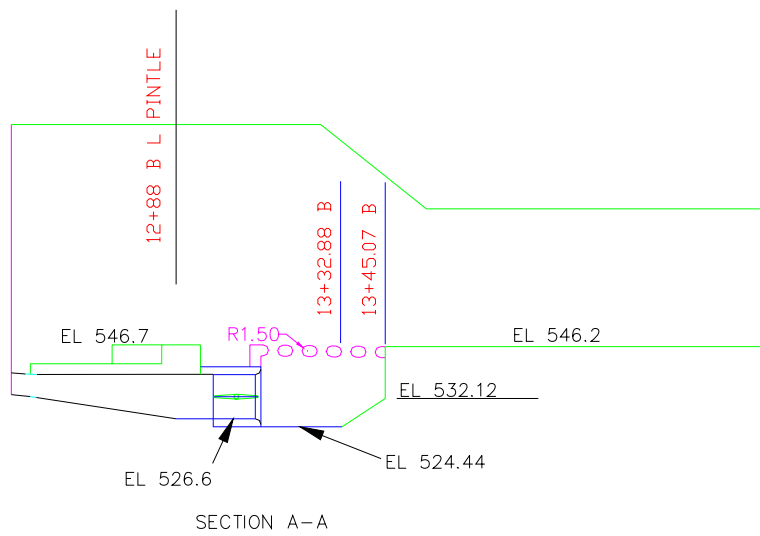
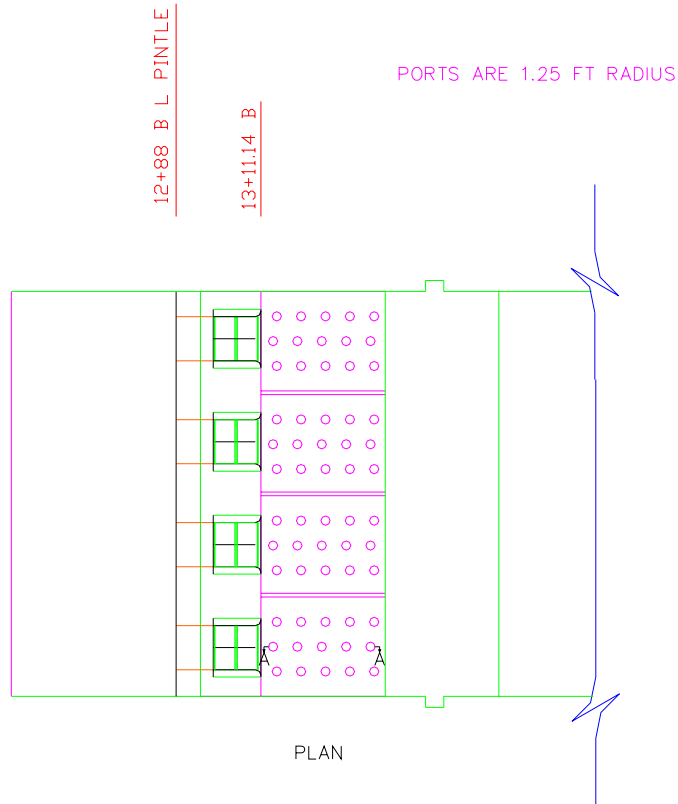






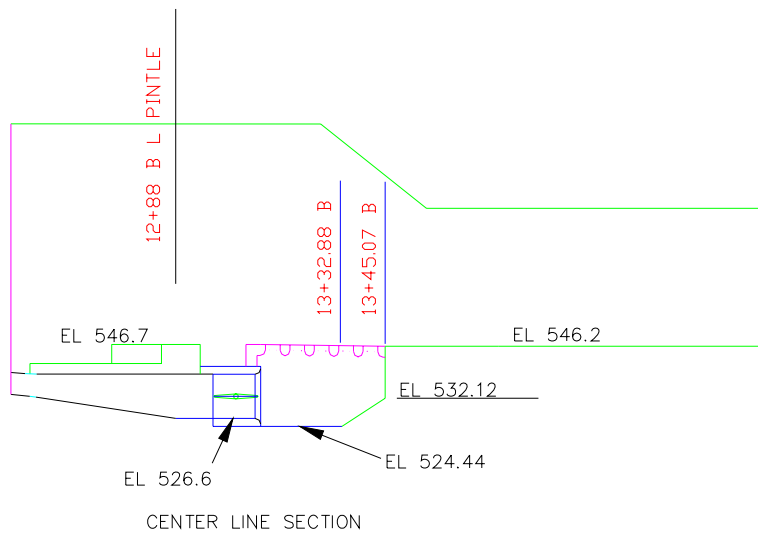
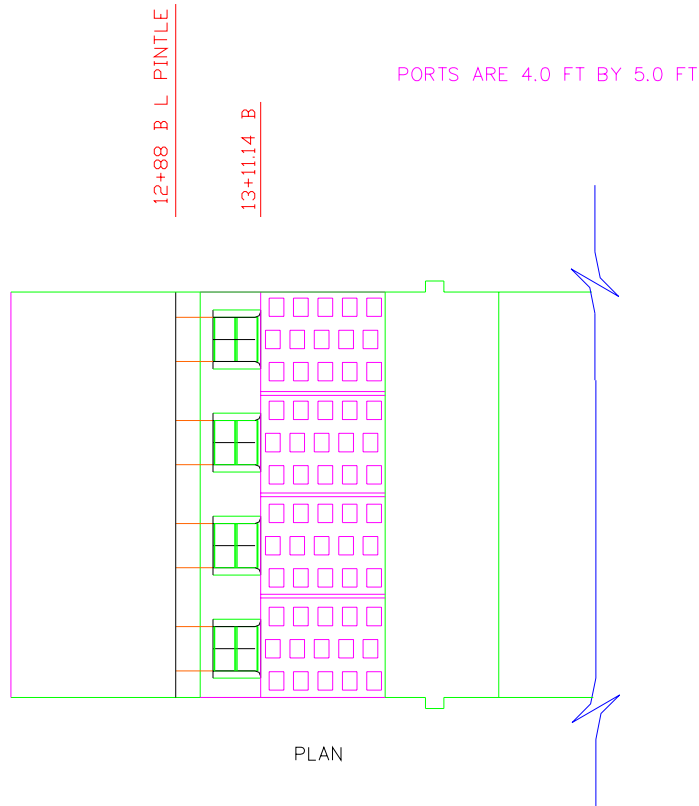
DIMENSIONS ARE IN FT

TYPE 2 DESIGN
OUTLET AREA



DIMENSIONS ARE IN FT

TYPE 3 DESIGN
OUTLET AREA



DIMENSIONS ARE IN FT

TYPE 4 OUTLET
DESIGN

REPORT DOCUMENTATION PAGE				Form Approved OMB No. 0704-0188	
Public reporting burden for this collection of information is estimated to average 1 hour per response, including the time for reviewing instructions, searching existing data sources, gathering and maintaining the data needed, and completing and reviewing this collection of information. Send comments regarding this burden estimate or any other aspect of this collection of information, including suggestions for reducing this burden to Department of Defense, Washington Headquarters Services, Directorate for Information Operations and Reports (0704-0188), 1215 Jefferson Davis Highway, Suite 1204, Arlington, VA 22202-4302. Respondents should be aware that notwithstanding any other provision of law, no person shall be subject to any penalty for failing to comply with a collection of information if it does not display a currently valid OMB control number. PLEASE DO NOT RETURN YOUR FORM TO THE ABOVE ADDRESS.					
1. REPORT DATE (DD-MM-YYYY) September 2005		2. REPORT TYPE Final report		3. DATES COVERED (From - To)	
4. TITLE AND SUBTITLE New Lock for Soo Locks and Dam, Sault Ste. Marie, Michigan, St. Mary's River				5a. CONTRACT NUMBER	
				5b. GRANT NUMBER	
				5c. PROGRAM ELEMENT NUMBER	
6. AUTHOR(S) John E. Hite, Jr., and Andrew M. Tuthill				5d. PROJECT NUMBER	
				5e. TASK NUMBER	
				5f. WORK UNIT NUMBER	
7. PERFORMING ORGANIZATION NAME(S) AND ADDRESS(ES) Coastal and Hydraulics Laboratory, U.S. Army Engineer Research and Development Center, 3909 Halls Ferry Road, Vicksburg, MS 39180-6199 Cold Regions Research Engineering Laboratory, U.S. Army Engineer Research and Development Center, 72 Lyme Road, Hanover, NH 03755-1290				8. PERFORMING ORGANIZATION REPORT NUMBER ERDC TR-05-8	
9. SPONSORING / MONITORING AGENCY NAME(S) AND ADDRESS(ES) U.S. Army Engineer District, Detroit, 477 Michigan Ave., Detroit, MI 48226 U.S. Army Engineer District, Huntington, 502 8th Street, Huntington, WV 25701-2070				10. SPONSOR/MONITOR'S ACRONYM(S)	
				11. SPONSOR/MONITOR'S REPORT NUMBER(S)	
12. DISTRIBUTION / AVAILABILITY STATEMENT Approved for public release; distribution is unlimited.					
13. SUPPLEMENTARY NOTES					
14. ABSTRACT The U.S. Army Engineer District, Detroit (LRE) proposes construction of a new lock at the Soo Locks on the St. Mary's River near Sault Ste. Marie, Michigan. The lock will replace the existing Davis and Sabin locks in the North Canal. Currently, the Poe Lock is the only facility at Soo Locks capable of handling the Great Lakes system's largest vessels. These large vessels account for more than half of the potential carrying capacity of the Great Lakes fleet. A laboratory model study was performed to evaluate the lock filling and emptying system and ice lockage procedures. It is expected that the new lock will have upper approach ice congestion problems similar to those experienced at the existing Soo Locks. A major objective of the ice tests in the physical model was to maximize ice lockage performance. The original design filling and emptying system was modified to achieve acceptable filling and emptying times. The total no of ports was reduced and structural baffles were installed on the upper and lower ports of the system to provide an even distribution of flow into and out of the chamber during filling and emptying. The permissible filling and emptying times based on maximum allowable hawser forces were 13.0 and 12.4 min, respectively. The lower ice valves brought the ice farther into the lock during ice drawing experiments although having the ice in direct contact with the lower miter gates would interfere with their operation. The upper ice valves were about equal to the combined use of filling valves and the manifolds in the upper miter gates in terms of ice flushing performance.					
15. SUBJECT TERMS Hawser forces Ice drawing		Ice flushing Lock filling and emptying system Lock intake		Lock outlet Soo locks St. Mary's River	
16. SECURITY CLASSIFICATION OF:			17. LIMITATION OF ABSTRACT	18. NUMBER OF PAGES 136	19a. NAME OF RESPONSIBLE PERSON
a. REPORT UNCLASSIFIED	b. ABSTRACT UNCLASSIFIED	c. THIS PAGE UNCLASSIFIED			19b. TELEPHONE NUMBER (include area code)